THESIS

LONGITUDINAL ANALYSIS OF CYTOKINE PROFILES DURING PRION INFECTION

Submitted by

Dana Hill

Department of Microbiology, Immunology, and Pathology

In partial fulfillment of the requirements

For the Degree of Master of Science

Colorado State University

Fort Collins, Colorado

Summer 2015

Master's Committee:

Advisor: Mark Zabel

Terry Spraker
Robert Callan
Tracy Nichols

ABSTRACT

LONGITUDINAL ANALYSIS OF CYTOKINE PROFILES DURING PRION INFECTION

Prion diseases, or transmissible spongiform encephalopathies (TSEs), are invariably fatal, typically species-specific neurodegenerative disorders affecting a number of mammalian species, including felids, caprids, cervids, mustelids, and humans. Propagated by a misfolded cellular protein that is ubiquitously expressed among all mammals, prion diseases are unique in that the infectious agent lacks nucleic acid and is able to persist in the environment for many years, maintaining infectivity through multiple routes of transmission. The role of the immune system during the acute and chronic phases of TSE infection is not well understood and is complicated by the fact that the infectious prion protein (PrP^{Sc}) shares the same primary structure as the normal cellular PrP protein (PrP^{C}). Neuropathological lesions associated with prion disease have no apparent inflammatory infiltrate, although extensive gliosis and neuronal loss are hallmark observations. Additionally, the adaptive immune response does not appear to recognize PrP^{Sc} prions as foreign due to primary biochemical structure homology with PrP^{C}. However, a number of recent findings have revealed a strong association between PrP and the immune system.

While the physiological function of PrP^{C} remains unclear, it has been shown to play a role in binding and transporting copper, and it also provides neuroprotection by inhibiting pro-apoptotic pathways. PrP^{C} is most abundant in the central nervous system (CNS), with the second highest level of expression on the surface of various immune cells, including follicular dendritic cells (FDCs) and B cells. Expression of PrP^{C} in the lymphoreticular system (LRS) has been linked to

PrP^{Sc} trafficking and replication in the periphery, perhaps by sequestering PrP^{Sc}-containing aggregates on the surface of immune cells and perpetuating the conversion of PrP^{C} into the pathogenic form. Fibril depositions accumulate in the brain later in the course of disease and correspond to astrogliosis in affected neuronal tissue, implicating CNS immune involvement. Central nervous system immune responses likely play a role in prion neurodegenerative disease, potentially by contributing to neuronal cell death and spongiosis, or by initiating neuroprotective mechanisms.

Identifying cytokines present throughout prion disease pathogenesis will help determine if immunopathology is initiated and may tease out other information about PrP-expressing immune cells and cytokine expression levels. In a pilot study, cytokine profiles were measured longitudinally in transgenic mice infected with prions as compared to control animals inoculated with normal brain homogenate (NBH). Serum cytokine levels were measured in cervidPrP-expressing mice infected with chronic wasting disease (CWD) prions and control mice inoculated with NBH using the BioPlex suspension array system. We analyzed IL-1β, TNF-α, IFN-γ, GM-CSF, IL-2, IL-6, IL-10, IL-4, and IL-5 at baseline levels, day one post-inoculation, and at two-week intervals through terminal disease (data not shown). At the time of sacrifice, mouse serum and brain homogenate cytokine levels were also analyzed. As a distinct continuation of this study, TgA20 mice over-expressing murine PrP^{C} 4- to 10-fold were infected with Rocky Mountain Laboratories (RML) mouse-adapted prions and serum cytokines analyzed in a similar longitudinal fashion. Additional sacrifices were made at 40, 60, and 80 days post-inoculation for cross-sectional comparison of cytokine profiles present in brain homogenate, where prion-induced lesions are most concentrated. We aimed to account for age- and sex-related cytokine variations, and, in

addition to the cytokines listed above, IL-12p70, IL-13, and IL-18 were also analyzed. This study represents the first longitudinal experiment analyzing systemic and neuro-inflammation in the same prion-infected animals throughout their entire disease course.

Based on literature from other protein-misfolding diseases, we hypothesized a small increase in serum pro-inflammatory cytokines, specifically IL-1β, IL-6, IL-13, IL-18, TNF-α, and IFN-γ, present at 1 day post-inoculation (dpi), immediately following neuroinvasion around roughly 60dpi, and prior to terminal disease. As with any inflammatory response, we anticipated a counter-immune response through activation of immune regulatory pathways, represented by expression of the anti-inflammatory cytokine IL-10. Eventually, near terminal disease, severe neurodegeneration and chronic gliosis would exhaust central immune responses and presumptively cause any existing neuroprotective pathways to shut down. This loss of a chronic inflammatory state in the brain was projected to be represented by a decrease in—or absence of—pro- and anti-inflammatory cytokines.

Oxidative stress from a chronic pro-inflammatory state has been identified in a number of neurodegenerative diseases as a mechanism leading to neuronal vacuolation and apoptosis, but remains to be distinctly identified in prion disease models and is complicated by propagation of PrP^{Sc} in the LRS prior to neuroinvasion. The aims of the current study are to unveil significant pro- and anti-inflammatory responses as represented by cytokine profiles in the brain and periphery throughout the course of disease following intraperitoneal (IP) inoculation in a murine scrapie animal model.

Our findings show IL-2 and IL-5 had the most significant and consistent expression throughout the disease course. As both treatment groups were affected similarly, cytokine data is suggested to reflect over-expression of PrP^C in TgA20 mice or relate to transgene insertion of *Prnp* gene copies within the transgenic model. Intermittent cytokine spikes among individual and grouped animals from both treatment groups were observed occasionally throughout the range of time points that were sampled and correlate to non-specific transient inflammatory responses unrelated to prion infection. Cross-sectional analysis of cytokines in brain homogenate showed a profile distinct of that observed in the periphery, with a single male RML-infected mouse showing a pro-inflammatory response comparable to LPS-induced controls.

The observed cytokine profiles provide insight into the alterations of immune cellular pathways resulting from PrP^C overexpression and reinforce the physiologic role of PrP in T lymphocyte activation and subsequent B lymphocyte activation by T helper subsets. The role of mononuclear cell involvement was investigated through quantitation of MCP-1 via ELISA, and revealed expression levels well below LPS-induced controls in mouse serum but significantly increased expression levels in pooled brain homogenate of RML-male TgA20s. Unexpected cytokine profile expression, taken together with the survival curve and neuropathology from this study, reveal unique relationships and patterns of PrP^C in the immune system and prion disease progression to terminal disease.

Our findings support those of others, such as the involvement of cofilin-actin rods disrupting neuronal transport and contributing to synaptic loss prior to neuronal vacuolation and cell death.

Amyloid fibrils participate in interactions with PrP^C to induce neuroinflammation via NOX activity. Similarly, Aβ and pro-inflammatory cytokines signal through similar, PrP^C-dependent pathways to form axonal rods and contribute to synaptic loss. Additionally, metal cations (Cu, Mn, Mg, Fe) with unknown implications in prion pathogenesis were investigated in cervidized mice to determine their role in cervid disease progression. These results show that increased [Cu] resulted in decreased survival times and confirmed alterations in pro-inflammatory gene mRNA transcripts as well as protein expression in these same mice, further reinforcing the involvement of the immune system in neurodegenerative diseases.

TABLE OF CONTENTS

LIST OF TABLES

LIST OF FIGURES

CHAPTER 1:

Introduction

Prion diseases are described as invariably fatal neurodegenerative disorders caused by disseminated deposition of misfolded protein plaques throughout the central nervous system (CNS), resulting in vacuolation and eventually neuronal loss. Once believed to be a chronic infection induced by a slow virus, overwhelming evidence indicates infectious agent, PrP^{Sc}, is a misfolded version of the cellular prion protein (PrP^{C}), lacking informative genetic material while retaining transmissibility (Prusiner, 1982). This "protein-only" hypothesis paved the way for research on transmissible spongiform encephalopathies (TSE) and led to the coined term "prion."

Scrapie was first described in 1732 and is the oldest known prion disease affecting captive sheep and goats. While scrapie is classified as a naturally occurring prion disease, Kuru and Bovine Spongiform Encephalopthy (BSE, aka mad cow disease) occur "unnaturally" as a result of ritualistic cannibalism and consumption of prion-contaminated bone meal product, respectively. Other factors tie into the infectivity of prions, with evidence of sporadic disease (Hsiao et al., 1989), genetic susceptibilities (Hsiao et al., 1989; Collinge, 1997), and important biochemical properties of the prion protein itself (Rogers et al., 1993; Silveira et al., 2005).

The exact structure of PrP^{Sc} and how it causes neurotoxicity is not known, however, once misfolded it has the ability to convert cellular, alpha-helical PrP^{C} into the infectious, beta-pleated form which contains a resilient protease-resistant core (McKinley, Bolton, & Prusiner, 1983). PrP^{Sc} oligomers and fibrils persist in the environment for extremely long periods of time due to

their resistance to high temperatures, ultraviolet irradiation, proteinase K degradation, as well as other decontamination methods and denaturing conditions commonly used against bacteria and viruses (Prusiner, 1982, Weissmann et al., 1996). This begs the questions of how a protein that is ubiquitously expressed among all mammalian species: 1. Misfolds to become infectious? 2. Causes irreversible, chronic neurodegenerative disease? 3. Gains resistance to common decontamination practices? 4. Achieves strain properties among certain like-species, while other species appear to be resistant to infection? 5. Accomplishes all of this without eliciting a response from the body's primary defenses—the immune system?

Humans suffer from a number of distinct prion diseases including Creutzfeldt-Jakob Disease (CJD), Gerstmann-Straussler-Scheinker (GSS) syndrome, and fatal familial insomnia (FFI) - all of which can be inherited through extremely rare, autosomal dominant mutations of the *Prnp* gene encoding PrP^{C} (Doh-ura et al., 1989; Goldfarb et al., 1991; Hsiao et al., 1989; Hsiao et al., 1990a/b; Owen, 1989), or can arise sporadically (Palmer et al., 1991). In addition, variant CJD (vCJD) is a new CJD-like syndrome that appears to be linked to consumption of prion-contaminated meat distributed from the UK following the emergence of bovine spongiform encephalopathy in the early 1990s (Aguzzi & Weissmann, 1996b; Bruce et al., 1997; Chazot et al., 1996; Collinge et al., 1996; Hill et al., 1997a). Clinical presentation of certain human prion diseases can be strikingly similar to other human neurodegenerative disorders, but differences in the time to terminal disease and lesion profiles within the CNS typically sets them apart (Aguzzi & Weissmann, 1996b; Lasmezas et al., 1996). Despite this, and without a reliable ante-mortem diagnostic assay, it is estimated that a large number of prion-infected people are misdiagnosed as having frontotemporal dementia or Alzheimer's Disease (AD), creating a legitimate public health concern (Doran &

Larner, 2004; Roberson et al., 2005; Tsivgoulis et al., 2014). Confirmed cases of prion diseases being acquired iatrogenically or from sub-clinically infected blood and tissue (dura graft) donors (Houston et al., 2000; Kobayashi et al., 2015; Llewelyn et al., 2004) add to this concern.

Chronic wasting disease (CWD) is a prion disease affecting wild and captive populations of deer, elk, and moose in North America, Canada, and, as of 2001, South Korea. Classified as the only naturally-occurring prion disease of free-ranging animals, CWD was first described just 48 years ago, and the origin remains unclear. Multiple hypotheses exist to explain the sudden appearance of CWD - the most plausible involves horizontal or environmental transmission from scrapie-infected sheep housed at an outdoor facility in Fort Collins, CO, in 1967, where it was first reported by Colorado Parks and Wildlife. However, scrapie was first described in 1732, and without nucleic acid or any previous evidence of prions crossing a species barrier, the emergence of CWD still eludes us. Little evidence exists supporting the hypothesis that consumption of CWD-infected meat puts humans at risk of developing prion disease. Although, the spike of vCJD cases in the UK, presumptively from the BSE outbreak, suggests that we exercise caution.

Bovine Spongiform Encephalopathy (BSE) tells a different story than CWD. Prions from BSE-infected animals have crossed multiple species barriers, including humans, felines, and ungulates. It is unknown how BSE prions gained the ability to cross multiple species barriers, and, while all potential vCJD cases cannot definitively be traced back to the BSE outbreak in the UK, evidence strongly suggests a correlation (Aguzzi and Weissmann, 1996b, Bruce et al., 1997; Collinge et al., 1996; Ziedler et al., 1997). In order to understand the phenomena being observed with BSE, we

must gain a stronger understanding for the physiological role of PrP^{C} and how it behaves once converted to PrP^{Sc}.

The cellular prion protein is a 36 kDa glycoprotein that is rich in alpha helices and linked to the cellular membrane through a glycophosphatidylinositol (GPI) anchor (Stahl et al., 1992). The primary protein consists of roughly 200 amino acids - give or take for different species – with a structured C-terminal domain and a non-structured N-terminal domain (AA 23-120). One of three glycosylation sites is present on the N-terminus, as well as an octapeptide repeat region and two histidines which bind copper with high affinity (Brown et al., 1997a). The protein's GPI anchor and remaining glycosylation sites compose the C-terminal domain, in addition to a single disulfide bond connecting helices two and three. Cellular PrP is typically concentrated to lipid rafts of the plasma membrane and has a number of proposed, redundant functions, due to the fact that PrP knockout ($PrP^{0/0}$) mice do not exhibit any overt dysfunctions and live relatively normal lives (Bueler, 1992; Bueler, 1993 Hsiao et al., 1989).

Interestingly, PrP^{C} itself appears to be an essential factor for fatal prion infection, ultimately elicited by PrP^{Sc} (Bueler et al., 1993). $PrP^{0/0}$ mice inoculated with prions are completely resistant to prion-induced neurodegeneration but may display altered behavior or physiology (Bueler et al., 1993; Prusiner et al., 1993; Tobler et al., 1996). Mouse models where PrP^{C} is anchorless (i.e. lacking the GPI-portion of PrP) rather than attached to the cell membrane show a decreased infectivity of PrP^{Sc}, as well as distinct, minimal clinical disease, more similar to that of AD than scrapie (Chesebro et al., 2005). This suggests that PrP^{C} being "used up" by autoconversion to PrP^{Sc} is not sufficient enough to cause disease (i.e. loss of function of PrP^{C} alone cannot account for

prion neurodegeneration). If animal models can live relatively normal lives without expression of PrP in its normal form, then it suffices to say that formation of PrP^{Sc} must induce pathologic alterations to result in terminal disease. Since both forms of the prion protein are required (Bueler et al., 1993), however, it implies that PrP^{C}-PrP^{Sc} interaction initiates an intracellular signal through GPI-linked PrP^{C}, inducing neurotoxicity (Chesebro et al., 2005; Mallucci et al., 2003).

Interestingly, new paradigms of prion formation have been found in mammalian innate immune systems. Analogs of PrP^{C} that display conformational changes and *reversible* fibril formation have been found to be crucial cytoprotective immune mechanisms (Hou et al., 2011). Viral infection of murine cells activates RIG-I-like pathways, which, in turn activate mitochondrial antiviral signaling proteins (MAVS) to fibrilize like prions and causes activation of the transcription factors IRF-3 and NFκB. Type I interferons are then produced in order to establish an antiviral state. One can see how reversible fibril formation—with similar structure to prion fibrils—as an essential factor for important antiviral immune pathways, is an incredibly valuable finding. It has since been proposed that PrP^{C} may be cytoprotective under stress (Flechsig and Weissmann, 2004; Roucou and LeBlanc, 2005; Westergard et al., 2007) as seen in other prion models, and a physiological change in the fibril somehow makes fibril formation irreversible, and, over time, failure to clear these structures becomes pathogenic.

PrP^{C} is translated from *Prnp* gene transcripts, some polymorphisms of which are linked to a variety of inherited human prion disorders, as mentioned above. The prion protein proceeds through the endoplasmic reticulum and Golgi apparatus for post-translational modifications and glycosylation before being transported to the cell surface. Once there, it is thought that PrP^{C} plays a role in cell

adhesion, cell signaling, and/or binding copper in a pH dependent manner to cause PrP^{C} internalization into the cell (Kiachopoulos et al., 2004; Pauly & Harris, 1998; Perera & Hooper, 2001). While it is known in other neurodegenerative diseases such as AD, PD, and ALS that the cellular toxicity is mediated by oxidative stress in apoptotic pathways, the cellular mechanisms underlying neurotoxic prion diseases are less clearly defined (Giese et al., 1995; Williams et al., 1997).

If $PrP^{C} \rightarrow PrP^{Sc}$ conversion is causing oxidative stress or activating certain cellular pathways to cause neurotoxicity, analyzing cell signaling molecules such as pro- and anti-inflammatory cytokines may reveal clues about the pathological processes taking place and the cellular players involved. Indeed, neuropathological lesions associated with prion disease do not recruit immune cells, as shown by a complete lack of inflammatory infiltrate near PrP^{Sc} deposits or spongiform lesions (Aucouturier et al., 2000; Berg, 1994). Additionally, prions do not appear to induce an adaptive antibody response, possibly due to the identical primary amino acid sequence of PrP^{C} and PrP^{Sc} (Porter, Porter, & Cox, 1973). Instead, once in the brain, prions hide undetected, silently disturbing neuronal homeostasis until PrP^{Sc} deposition and neuronal vacuolation become apparent histologically along with extensive astrogliosis and microgliosis. Eventually, synaptic loss and spongiosis is so great that clinical symptoms arise and disease progresses uninhibited to complete paralysis and/or multi-organ shutdown.

But what is happening during these long incubation periods, prior to neuroinvasion? How do prions enter the body, make their way to the brain, and what takes them so long to do so? Multiple routes of transmission have been proposed for acquired prion diseases, including horizontal transmission

via contact/ingestion of contaminated bodily fluids, environmental transmission via ingestion or inhalation of prion-contaminated fomites (soil, water, etc.), and transfusion or transplantation of blood and/or various medical devices. The potential of vertical transmission is currently being investigated. Once ingested, prions are found in tonsils (Hill et al., 1997), survive the acidic environment of the stomach, and proceed to the small intestine, where they are sampled by M cells and taken up into mucosal associated lymphoid tissues, such as the Peyer's patches (Donaldson et al., 2012). This process is expedited in the presence of inflammation/epithelial damage (Sigurdson et al., 2009). Conversely, prions have also been shown to efficiently transmit disease via intranasal inoculation with shorter incubation times, possibly by entering the olfactory epithelium and bypassing peripheral replication (DeJoia et al., 2006; Kincaid & Bartz, 2007).

Surprisingly, the hallmark neuropathological profile seen in prion disease is not observed in the periphery. Prion diseases are characterized by species tropism, pathological profiles in the brain, clinical presentation, and time course of disease, but that doesn't mean that infectious PrP^{Sc} deposits are exclusively neurotropic. Following central or peripheral inoculation, in the end-stages of disease PrP^{Sc} depositions are found in many areas throughout the body with no apparent pathological changes in the parenchyma of peripheral organs. Numerous secondary lymphoid organs, muscle tissue, and other areas of chronic inflammation are shown to have high titers of PrP^{Sc} at terminal disease (Heikenwalder et al., 2005), but with no interruption of the physiological function of that organ (Fraser et al., 1996). Only when PrP^{Sc} contacts a GPI-anchored, PrP^{C}-expressing cell within the central nervous system is the result pathologic (Baldwin et al., 1992; Brown, Schmidt, & Kretzschmar, 1995; Gellman & Gibson, 1996). If we understand which cells are harboring, transporting, and aiding replication of prions in the periphery during the

months/years of incubation period, we could potentially intervene prior to neuroinvasion and stop the progression of disease.

Involvement of the LRS during prion disease is intriguing because of an apparent failure to induce an inflammatory or adaptive immune response yet clear association with PrP, suggesting a role in sequestration, replication, and/or transport of the prion protein. Prion replication in peripheral lymphoid tissues prior to neuroinvasion is a key component in a number of prion diseases, including scrapie (Fraser et al., 1996), CWD, vCJD, and BSE. By looking closely at the cellular signals present throughout prion infection, we hope to tease out more information about which cells are involved and how/or when certain events related to prion propagation and neuroinvasion are taking place. The normal linear progression of activation of the immune system in response to pathogen-associated molecular patterns involves positive feedback mechanisms and cell-specific signaling pathways for initial stimulation and continued activation. It is no wonder then, that immune components and cellular players involved in prion disease pathogenesis also display a certain degree of cellular interdependence, with monocytes and dendritic cells bridging the gap between innate and adaptive immunity.

A number of these immune cell types have already been identified, and not surprisingly they involve a variety of immune cells which express PrP^{C} at levels second highest to the CNS (Cashman et al., 1990; DeArmond et al., 1986). Amongst these are B lymphocytes, T lymphocytes, natural killer (NK) cells, platelets, erythrocytes, monocytes, dendritic cells (DCs), and, most importantly, follicular dendritic cells (FDCs) (Cashman et al., 1990; Clarke & Kimberlin, 1984; Dodelet & Cashman, 1998; Fraser & Farquhar, 1987). Dürig et al. (2000) further characterized

PrP^C expression patterns on peripheral cells in circulation and discovered similar expression levels among T lymphocytes, NK cells, and monocytes, while B cells displayed significantly lower levels of PrP^C, contrasting the findings of Cashman et al. (1990).

The complement cascade has also been verified in prion and AD pathogenesis, shown by direct binding of C3, C1q, and Factor H to abnormal prion protein (Blanquet-Grossard et al., 2005; Mitchell et al., 2007; Sim et al., 2007) and amyloid (Jiang et al., 1994). Accelerated peripheral prion pathogenesis is correlated with complement factors C3, C1q, and CD21/CD35 receptors on the surface of FDCs (Aucouturier, 2001; Beringue et al., 2000; Zabel et al., 2007), and inhibition of neuroinvasion was observed following low-dose prion inoculation into C1q- and/or Bf/C2-KO mice (Klein et al., 2001). Previous researchers within our lab also demonstrated that CD21/CD35-/- mice do not develop terminal disease (Michel et a., 2012) and C3 expression in murine CWD models accelerates disease (Michel et al., 2013).

It is well known that FDCs play a key role in peripheral prion propagation (Brown et al., 1999; Fraser & Farquhar 1987; Montrasio et al., 2000), however, DCs, monocytes, and macrophages show conflicting results (Aucouturier et al., 2001; Beringue et al., 2000; Beringue et al., 2002; Wathne & Mabbott, 2012). Indeed, PrP^C expression on myeloid cells is important for their maturation, and PrP-/- models display compromised stimulation of T cells by DCs (Ballerini et al., 2006; Dürig et al., 2000).

Evaluation of prion disease progression during the time between inoculation and terminal stages of disease has largely been neglected. This is partly due to the exceptionally long incubation

periods observed in chronic neurodegenerative diseases and is exacerbated by the fact that prion protein species barriers have limited the development of animal models. Various experimental methods have now been established to overcome these issues, such as transgenic rodent models over-expressing the prion protein, mouse-adapted scrapie prion strains, cervidized mice, and alternative routes of inoculation (i.e. intracerebral, or IC) which expedite disease progression. Different prion disease strains, animal models, and routes of inoculation all result in variable clinical and pathological prion disease manifestations. While one experimental model might not necessarily be better than another, certain disease models are preferable in studies of prion pathogenesis and immune involvement.

A few investigators have looked at cytokine and chemokine gene transcript levels during prion infection through RT-PCR, and found these results to be non-representative of the actual functional protein levels being translated. The majority of experimental models investigating prion immunopathogenesis choose to employ IC inoculation, as opposed to peripheral routes. While this may reduce incubation period, IC inoculation bypasses peripheral lymphotropic prion replication and induces a level of traumatic injury to the brain which is undesirable when analyzing immune cellular pathways. An ideal—but unrealistic—model would closely resemble the natural host and natural route of inoculation, express a normal level of prion protein and have an intact immune cell phenotype, but have a reasonable incubation period and retain pathologic lesions characteristic of that particular prion disease/strain. For this study, a mouse-adapted scrapie inoculum (RML) was injected intraperitoneally (IP) in TgA20 mice overexpressing the murine prion protein 4- to 10-fold (Chandler, 1961; Fischer et al., 1996). This transgenic model and inoculum combo have

been used in prion research by other groups also investigating prion immunopathogenesis, making for more relevant data comparison.

In order to analyze functional protein levels of immune cell signaling molecules, we chose to employ the BioPlex suspension array system to quantitate serum cytokine levels. This relatively new multiplex immunoassay combines the sample preparation of an ELISA with the technology of flow cytometry for sensitive measurement of multiple analytes from a single, minute sample size (~25µl). Magnetic beads conjugated to antibody specific for different analytes (via kits from eBioscience) are distinctly colored using ratios of internal red and infrared dyes, allowing the BioPlex machine to differentiate between analytes (Figure 1). An antibody mixture is incubated with a small sample of serum and cytokine levels are determined using a secondary biotinylated detection antibody (Figure 2). A streptavidin-PE reporter dye is excited by lasers and quantitated based on the standard curve generated. This assay allows for the measurement of multiple cytokines from a small sample size, and, for our study, was easily optimized for analysis of mouse brain homogenate supernatant as well. The variety of eBioscience magnetic bead kits also provided a somewhat customized cytokine array, with a comprehensive Th1/Th2 cytokine 11-plex kit combined with an IL-10 simplex kit to include anti-inflammatory responses.

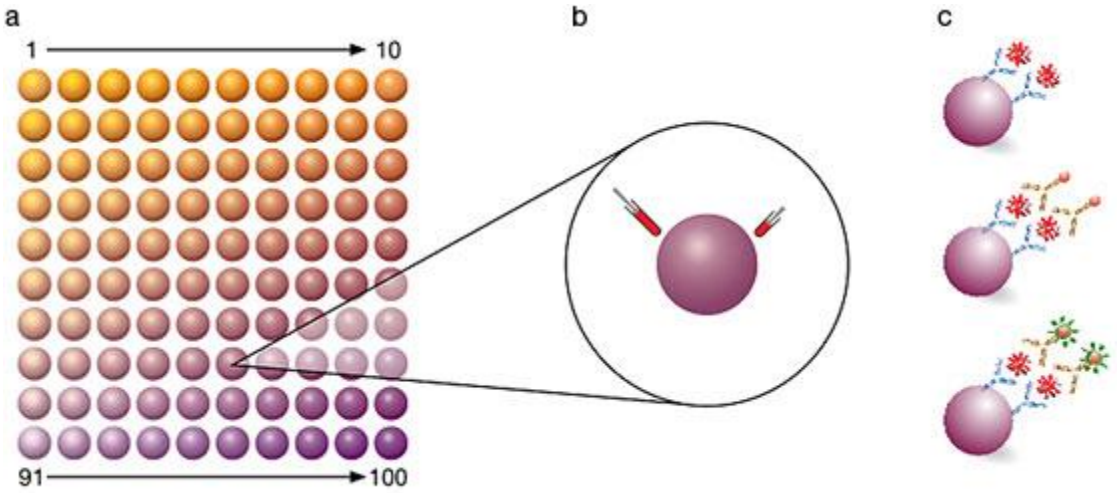

Figure 1 (a-c): BioPlex Suspension Array System-Beads
Magnetic beads are impregnated with different ratios of red and infrared dyes, making them distinctly recognizable by the red classification laser (a & b). Bead region ratios are assigned to a particular analyte depending on the detection antibody conjugated to that bead and entered into the BioPlex machine. Sample is incubated with a customized bead mixture, similar to an ELISA (c).

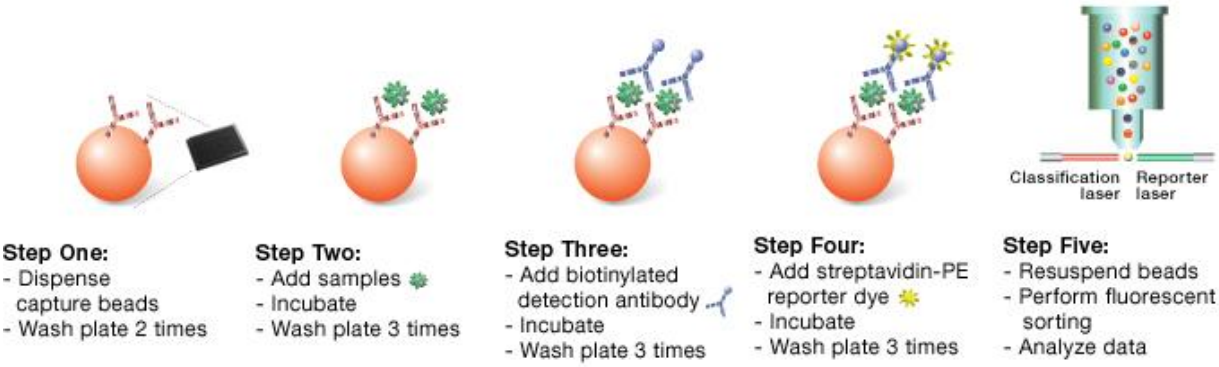

Figure 2: BioPlex Suspension Array Overview
Samples are prepared similar to an ELISA, except detection antibodies are conjugated to magnetic beads rather than the plate bottom to allow for multiple analyte detection from a single sample. Flow Cytometry is then used to quantitate protein expression through detection of biotinylated antibody with streptavidin-PE.

Specifically, we wanted to investigate the presence of inflammatory mediators and regulators that may play a role in prion pathogenesis, including certain analytes (IL-1B, IL-6, TNF-a) which have been previously reported in the literature for playing a role in neurodegeneration or neuroprotection (Blum-Degena et al., 1995; Campbell et al., 1994; Lindholm et al., 1987; Mogi et

al., 1994, Mogi et al., 1996; Tribouillard-Tanvier et al., 2009). Cytokines not only play a role in cell signaling and recruitment, but also function in cell proliferation and differentiation. In the periphery, the LRS and complement are known to play a role in prion pathogenesis through propagation of PrP^{Sc}, however, immune responses within the CNS, are much more tightly regulated for the obvious reason of limited space to accommodate inflammatory cells. The blood-brain-barrier (BBB) and additional regulatory mechanisms may cause immune responses in the periphery to vary greatly from what is observed in the CNS, therefore separate analysis of these immune responses is necessary.

Histopathological findings associated with scrapie infection include spongiosis, neuronal and neuropil vacuolation, PrPres, gliosis (Fraser et al., 1988; Jendroska et al., 1991), as well as synaptic loss (Budka, 2003). A lack of inflammatory infiltrate of peripheral immune cells during TSE infection make studying central immune responses important. Astrocytes and microglia make up the two most important cell types contributing to neuroinflammation, as they are stimulated to undergo proliferation early on during prion disease (Betmouni, Perry, & Gordon, 1996; Block, Zecca & Hong, 2007; Campbell et al., 1994; DeArmond, Kristensson, & Bowler, 1992; Giese et al., 1998; Williams et al., 1994; Williams et al, 1997), and both cell types have been shown to produce cytokines and have an impact on neuronal survivability (Williams et al., 1994; Kim et al., 1999; Campbell et al., 1994).

NF-κB is a ubiquitously expressed transcription factor shown to be involved in a number of inflammatory processes and stimulated by many different ligands. Within the CNS, these include TNF-α, Fas ligand, nerve growth factor (NGF), and secreted amyloid-β (Aβ) precursor protein,

resulting in neurotoxic, neuroprotective, and anti-apoptotic effects depending on the stimulus and cell type (Mattson & Camandola, 2001). Its involvement in neurodegenerative disorders has been studied extensively, and also linked with prion disease pathogenesis (Bacot et al., 2003; Fabrizi et al., 2001; Zhou et al., 2008). Stimulation of NF-κB through PrP^{C}-dependent signaling pathways and by PrP106-126 has been shown to upregulate pro-inflammatory cytokine gene expression and inducible nitric oxide synthase (iNOS) (Lu et al., 2012; Sonati et al., 2013). iNOS is involved in immunity acting as a catalyst in the formation of reactive oxygen (ROS) and nitrogen intermediate species, such as nitric oxide (NO), through reaction with NADPH oxidase (Barth et al., 2009).

This study represents the first and only to assess cytokine profiles in the serum of the same prion-infected mice from baseline levels, chronically throughout the delayed onset of disease following IP inoculation, until terminal morbidity score warrants euthanasia. Additional sacrifices were made at time points leading up to terminal disease (40, 60, and 80dpi) for cross-sectional comparison of cytokine profiles present in the brain homogenate of mice prior to prion neuroinvasion (40dpi), and afterwards (60dpi—based on previous observations), and were compared with cytokines present in brain homogenate of terminally-ill mice.

Bioassay:

Mice:

TgA20 mice (n=31) overexpressing murine PrP^C 4- to 10-fold over wild type were genotyped by H. Bender and housed at Colorado State University Laboratory Animal Resources (LAR) facility. Animals were inoculated IP with 1% brain homogenate of either normal brain homogenate (NBH) or Rocky Mountain Laboratories (RML) mouse-adapted scrapie prions, with 1% pen strep in sucrose solution. Due to colony breeding problems, mice from this study were inoculated in two separate groups but followed identical study design and sample collection procedures. Mice were euthanized at 40 (n=6), 60 (n=6), or 80 (n=7) days post inoculation, or once terminal disease was apparent (n=12) for cross-sectional brain homogenate cytokine analysis (Figure 3). Morbidity scoring was used for impaired extensor reflex, tail rigidity, akinesia, tremors, ataxia, and weight loss, with the presence of any three of these symptoms indicating terminal illness.

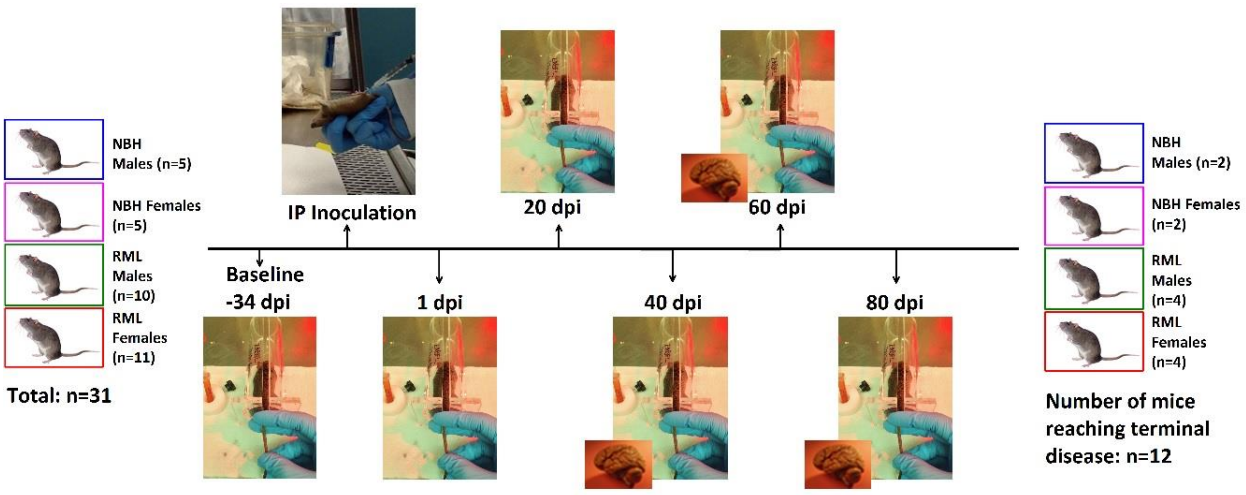

Figure 3: Timeline of Longitudinal Cytokine Study
Schematic of longitudinal cytokine study showing the overall timeline of events as well as the numbers of mice starting out and ending the study. Photos show actual IP inoculation of TgA20

mice as well as tail bleeding set-up. Additional sacrifices were made at 40, 60, and 80dpi, shown by a small brain picture overlapping tail-bleed photos to represent cross-sectional brain homogenate cytokine analysis. Mice that were carried out to terminal disease were analyzed for serum and brain homogenate cytokine levels as well.

Euthanasia and Tissue Harvest:

At the time of sacrifice, CO2 euthanasia was carried out and the following tissues were harvested and immediately frozen at -80°C: mediastinal lymph node; mesenteric lymph node; half spleen; and small half of brain (brains cut just off-center). The other half of the spleen and larger half of the brain were placed in 10mls of 4% buffered formalin together for 24 hours then transferred to 70% ethanol until cut into cassettes for histopathology. After allowing 20-30 min for clotting, whole blood samples from post-euthanasia heart-stick were centrifuged at 3000rpm for 10 min and serum transferred to Eppendorf tubes for immediate freezing with other tissues.

Longitudinal Serum Collection:

Serum was obtained via tail bleeding per LAR's mouse bleeding guidelines. One hundred microliters of whole blood was collected in BD Microtainer serum separator tubes (ref# 365959) and allowed to clot for 20-30 min. Samples were spun down at 3000rpm for 10 min on Micromax benchtop centrifuge and serum placed in new eppendorf tubes and stored at -80°C until analysis on BioPlex.

LPS-Induction Experiment:

Two TgA20 mice (1 male, 1 female) negative for PrP^{res} were intraperitoneally injected with 100ul of 1μg/ml of LPS (generously provided by Ron Tjalkens' lab) in PBS. After three hours, both mice were euthanized and tissues were collected per above euthanasia protocol. Serum and brain

homogenate from LPS-induced mice were analyzed on the BioPlex Suspension Array system as a positive control/visual comparison for cytokines observed in prion-infected mice.

Histopathology:

Brains and spleens were cut in coronal sections and GFAP and H&E staining were performed by Todd Bass at the CSU Diagnostic Medicine Center.

IHC was done in-house using unconjugated BAR224 for PrP^{res}. Prepared slides were deparafinized by heating in an incubator for 45 minutes then exposed to xylene, twice, for 10 minutes each. Tissues were rehydrated then digested via a 30 minute, 88% formic acid treatment. Antigen retrieval was carried out using 1X Dako Antigen retrieval solution then washed in 1X PBS. Quenching was achieved using 3% hydrogen peroxide in MeOH for 30 minutes and were subsequently washed and blocked in FACS buffer (5% BSA mixed 1:1 with superblock) for 30 minutes. Tissues were incubated with unconjugated BAR224 mAb (Cat# 10009035) at 1:500 overnight and then developed using AEC (3-amino-9-ethylcarbazole) until signal was visualized. After another wash, slides were counterstained with hematoxylin, rinsed with tap water, and then incubated with bluing reagent for 5 minutes. After a final wash, slides were cover-slipped, visualized, and photographed on the Olympus BX41 microscope equipped with Olympus DP72 camera with Colorado State University pathologist, Dr. Terry Spraker, at the Diagnostic Medicine Center.

Western Blot:

Ten percent brain homogenate from all TgA20 mice in the cytokine study (including LPS mice) were Proteinase K-digested at 200µg/ml of recombinant, PCR grade PK (Roche, ref# 03 115 887 001) for 30 minutes at 37°C at 800rpm on heat block (Eppendorf Thermomixer R). One sample (136539-1 RML_M) was left undigested as a control. TgA20 NBH (PK -), the above PK-digested samples, and TgA20 RML (used for inoculum—PK+) were loaded onto 12% NuPage 12-well gels (10µl undigested, 15µl PK-digested loaded). Ten microliters of 3X loading buffer (Novex NuPage LDS 4X sample buffer, ref# NP0007; and 10X reducing agent, ref# NP0009) were added to undigested samples (diluted 1:5 in PBS) and to 20µl of digested samples (18ul sample, 2ul PK). All samples were then placed on heat block at 95°C for 5min at 800rpm before being loaded onto the gels. Samples were run at 110V for 10 minutes, then 150V for 60 min with a Coomassie gel marker with BSA to confirm transfer of protein onto membrane. Protein was completely transferred onto membrane after 30 minutes at 110V.

Blots were allowed to block for 1 hour in 5% nonfat dry milk + PBS and 0.1% tween before being probed with BAR 224 antibody at 1:20,0000 in superblock (Thermo Scientific ref# 37517), in the fridge on a rocker overnight. Blots were washed 6X with PBST for 10min each and then developed using Millipore HRP Substrate (Immobilon Western, Cat# WBKLS0500). Blots were exposed and bands visualized on Luminescent Image Analyzer, ImageQuant LAS 4000 gel dock.

BioPlex:

Sample and Standard Preparation:

Serum samples were thawed on ice, vortexed for 3-5 seconds, and re-centrifuged at 3000rpm for 10min. Mouse serum was placed in separate Eppendorf tubes and diluted 1:6—brain homogenate 1:10—in Universal Assay Buffer (UAB). Serum and brain homogenate dilutions were determined via optimization experiments using eBioscience 11-plex kits combined with IL-10 simplex to accurately quantitate protein expression in both sample types as well as kit standards. During sample centrifugation, cytokine standards (S1-S8) were prepared as 4-fold serial dilution in UAB, according to eBioscience protocol. Control wells were comprised of extra reconstituted standard, diluted 1:64 to equate S4 and placed at the end of the plate to ensure the assay worked throughout entire plate reading.

96-Well Bead Plate Preparation:

Two U-bottom, untreated, 96-well plates were labeled for either beads or samples (in duplicate). Sixty microliters of UAB, S1-S8, samples (up to n=37) and controls were loaded into sample plate, for blank, standard, sample (diluted serum/brain homogenate) and control wells, respectively—this plate was kept on ice until bead plate was prepped. Antibody magnetic bead mixture (11-plex) and IL-10 beads were vortexed for 30 sec each prior to being loaded. Fifty microliters of the 11-plex bead mixture was loaded into all blank, standard, sample, and control wells (in order of bead plate reading). The bead plate was secured onto magnetic plate and beads were allowed to settle for two min. Bead plate + magnet apparatus was inverted over sink to decant excess fluid, quickly dabbed on paper towel, then returned to benchtop where plate was removed from magnet and freshly-vortexed IL-10 beads were added and gently mixed by pipetting. The bead plate was re-

secured to magnetic plate, allowed two minutes for bead-settling, then washed two times, as follows:

Washing Protocol:

The bead plate + magnet apparatus was inverted over sink to decant excess fluid and then quickly dabbed onto paper towel to dry plate surface. Wash buffer (100µl—previously diluted to 1X solution) was quickly added to all wells using multi-channel pipette to prevent bead drying. Beads were allowed to settle for another 30 sec to 1 min, then the plate was decanted over sink again. Wells were washed with 100µl UAB a total of two to three times using the same method as above.

Magnetic Antibody Bead-Sample Incubation:

Using a multi-channel pipette, 50µl of well contents from sample plate were transferred to bead plate, and mixed gently by pipetting. Once all samples were transferred, the bead plate was removed from magnet, wells covered with plate cover, wrapped in foil to protect beads from light and placed on a plate shaker at room temp for 90 min at 600rpm.

BioPlex Machine, Protocol Setup:

Protocol details saved for each BioPlex run. Bead regions entered for 11-plex (IFN-g, GM-CSF, IL-1β, IL-2, IL-4, IL-5, IL-6, IL-12p70, IL-13, IL-18, TNF-a) and IL-10 simplex, per eBioscience manual. Standard concentrations calculated using S1 concentration (provided by eBioscience) and 4-fold serial dilution through S8. Controls matched to S4 concentration (S1 diluted 1:64 for each analyte). Details for specific protocol and samples described, and associated dilutions entered (1:6

for serum, 1:10 for brain homogenate). One hundred beads per region specified, run at low RP1 target value settings, with a sample size of 100µl. Gates set at 5000-25,000.

Detection Antibody:

Following 90 min sample incubation, plate was returned to magnet and left for 2 min prior to three plate washes (see washing protocol above). Detection antibody 50X concentrate, for 11-plex and IL-10 simplex, each diluted to 1X working solution based off 25µl/well calculation, plus extra to account for pipetting error. Detection antibody 1X solution vortexed gently then added in 25µl increments to each row using multi-channel pipette. A new plate sealer was placed over wells and beads protected from light during 30 min, room-temp incubation on plate shaker at 600rpm.

Streptavidin-PE:

Plate returned to magnet and washed a total of three times. Total volume of strep-PE estimated using 50µl/well calculation. Once plate removed from magnet, 50µl of Strep-PE added to each well using multi-channel pipette. Plate re-sealed, protected from light and incubated on plate shaker at room temp for 30 min at 600 rpm.

Preparation for BioPlex:

Plate returned to magnet and washed an additional three times. Once the plate was removed from magnet, beads resuspended in 120µl of reading buffer (provided in eBioscience 11-plex kit) and plate covered and placed on plate shaker for 1 min at 800rpm. BioPlex machine (warmed-up and calibrated prior to plate-reading) ejects calibration plate, and bead plate inserted into BioPlex machine for analysis.

Statistical analysis:

A repeated-measure analysis between treatment (TX) groups and over time for IL-2 and IL-5 performed by Ann Hess in SAS. Adjusted raw and Tukey p-values were obtained to show significant differences over the time course of the study for IL-2 and IL-5. Additional GraphPad Prism (version 5.0d) statistical analysis was also performed.

ELISA:

Monocyte Chemoattractant Protein-1 (MCP-1) expression was quantitated in pooled mouse sera via R&D mouse MCP-1 duoset sandwich ELISA (catalog # DY479, Lot# 1320396) performed by Dr. Valerie Johnson of Dr. Steven Dow's laboratory. Due to a limited amount of remaining sample volume following BioPlex protein array analysis, mouse sera and brain homogenates from each treatment group (NBH males, NBH females, RML males, and RML females) were pooled and analyzed.

CLARITY:

CLARITY protocol:

This novel 3-dimensional brain imaging technique was originally developed by Chung et al. (2013) at Stanford University. The CLARITY protocol was carried out as described by Chung et al. and adapted by our group to incorporate our immunohistochemistry and other histological staining techniques. Briefly, hydrogel monomers (acrylamide and bisacrylamide), formaldehyde, and thermally triggered initiators were infused into mouse tissues at 4°C and held at this temperature for 1-3 days, allowing for tissue crosslinking and covalent linking between hydrogel monomers

and mouse biomolecules (proteins, nucleic acids, etc.). Polymerization of biomolecule-conjugated monomers into hydrogel meshwork was thermally-initiated by incubating infused tissue at 37°C for 3 hours. Lipids and other molecules lacking functional groups remain unbound, and the following electrophoresis step (4 days) allows for tissue clearance of all unbound material. The end result is a full or large section brain tissue that is transparent and able to be stained and unstained as desired, allowing for visualization of 3-dimensional stain uptake within intact cellular architecture (except lipids).

The availability of NFκB-GFP mice, along with development of a new lab protocol for CLARITY prompted us to investigate NFκB activation in a RML-infected mouse sacrificed at 60dpi (mouse provided by Dr. Val Johnson). For this experiment, we used a 1mm section of brain tissue (to expedite the tissue-clearing process) and assessed brain regions expressing GFP using confocal microscopy.

CLARITY Imaging- Zeiss Confocal Inverted Scope:

Argon laser (λ 488) used to visualize a 1mm section of brain from GFP/NFκB mice. DIC channel as well as Ch3 LP505 (GFP=530) were turned on for Z-stack. Z-settings: Start:0.300μm; Interval 10 (Optimal 9.89μm); Pixels 512 X 512; Scan speed 3; DIC scan 5μm. Image of GFP expression within the caudal medulla and cerebellum obtained at 10X magnification.

Flow Cytometry:

Four TgA20 mice were euthanized and brains and spleens harvested then placed in 5mls of FACS buffer (recipe from Coldspring Harbor: 1 X PBS, 2% FBS, and 1mM EDTA). Organs were mashed through cell strainer screen (BD Falcon) and resulting homogenates were placed in Eppendorf tubes (500µl for spleens, 200µl for brains). Samples were spun at 3000rpm in IEC Micromax benchtop centrifuge for 5 minutes. Supernatant was removed and pellet was washed in 1ml FACS buffer. Samples were then subjected to a soft centrifugation at 1000rpm for 5 minutes. Wash and soft spin (1000rpm for 5 min) was repeated two times.

Cells were FC blocked at 1:100 FC block in FACS buffer for 30 minutes. Cells were washed twice then incubated with BAR224 antibody at 1:100 with 7% mouse serum in FACS buffer for 20 minutes in the dark at room temp. Excess antibody was washed away using 1ml FACS buffer, followed by a soft spin. Lysis buffer (155mM NH_4Cl, 12mM $NaHCO_3$, and 0.1mM EDTA) was used in place of FACS buffer for the final wash. Cells were centrifuged one final time, supernatant disposed of, resuspended in 1ml FACS buffer, transferred to library tubes, and kept in the dark until analysis on the Cyan Flow Cytometer at the Colorado State University, Veterinary Teaching Hospital. PE-Texas red channel, Brain 700V, Spleen 600V.

Results

Bioassay:

Mice were euthanized at 40dpi, 60dpi, 80dpi, or when prion disease morbidity scores indicated terminal illness (Table 1). RML-female mice reached terminal illness and were euthanized prior to the first RML-male who showed any clinical symptoms (Figure 4). NBH control mice were allowed to survive out to 158dpi for the terminal time point and no clinical signs of prion disease were apparent at the time of euthanasia (see appendix for supplementary URL link to YouTube videos).

Table 1: Cytokine Study TgA20 Information Table
TgA20 mice from the longitudinal cytokine study are separated by euthanasia time point to show the division of treatment groups and genders of mice, as well as ages at the time of inoculation and euthanasia. Mice were euthanized at 40dpi (average age of 154 days old), 60dpi (averaging 160 days old), 80dpi (averaging 178 days old), or when terminal illness became apparent. NBH control mice for the terminal time point were allowed to live 14 days past the euthanasia of the RML-inoculated mouse, 134097-3, which had the longest incubation period for the RML treatment group.

Cytokine Study TgA20 Information Table						
Animal ID	**TX Group**	**Gender**	**Age at Inoculation (days)**	**Age at euth (days)**	**DPI @ euth**	**Incubation Period (days to terminal illness)**
133157-5	NBH	M	103	145	40	n/a
136540-1	NBH	F	117	159	40	n/a
136539-2	RML	M	117	159	40	n/a
136539-3	RML	M	117	159	40	n/a
136550-3	RML	F	110	152	40	n/a
136550-4	RML	F	110	152	40	n/a
133157-4	NBH	M	103	163	60	n/a
136540-2	NBH	F	117	177	60	n/a

133707-4	RML	M	92	152	60	n/a
134097-1	RML	M	77	137	60	n/a
135588-2	RML	F	103	163	60	n/a
136550-1	RML	F	110	170	60	n/a
133157-3	NBH	M	103	183	80	n/a
133158-5	NBH	F	103	183	80	n/a
133707-1	RML	M	92	172	80	n/a
133707-2	RML	M	92	172	80	n/a
134098-1	RML	F	77	157	80	n/a
135588-4	RML	F	103	183	80	n/a
136550-2	RML	F	110	193	80	n/a
134098-3	RML	F	77	177	100	100
134098-5	RML	F	77	177	100	100
134098-4	RML	F	77	188	111	111
134098-2	RML	F	77	193	117	117
134097-2	RML	M	77	197	120	120
136539-1	RML	M	117	238	121	121
134097-4	RML	M	77	205	128	128
134097-3	RML	M	77	220	144	144
133157-1	NBH	M	103	260	158	n/a
133157-2	NBH	M	103	260	158	n/a
133158-1	NBH	F	103	260	158	n/a
133158-3	NBH	F	103	260	158	n/a
141158-1	LPS	M	n/a	114	n/a	n/a
140726-1	LPS	F	n/a	114	n/a	n/a

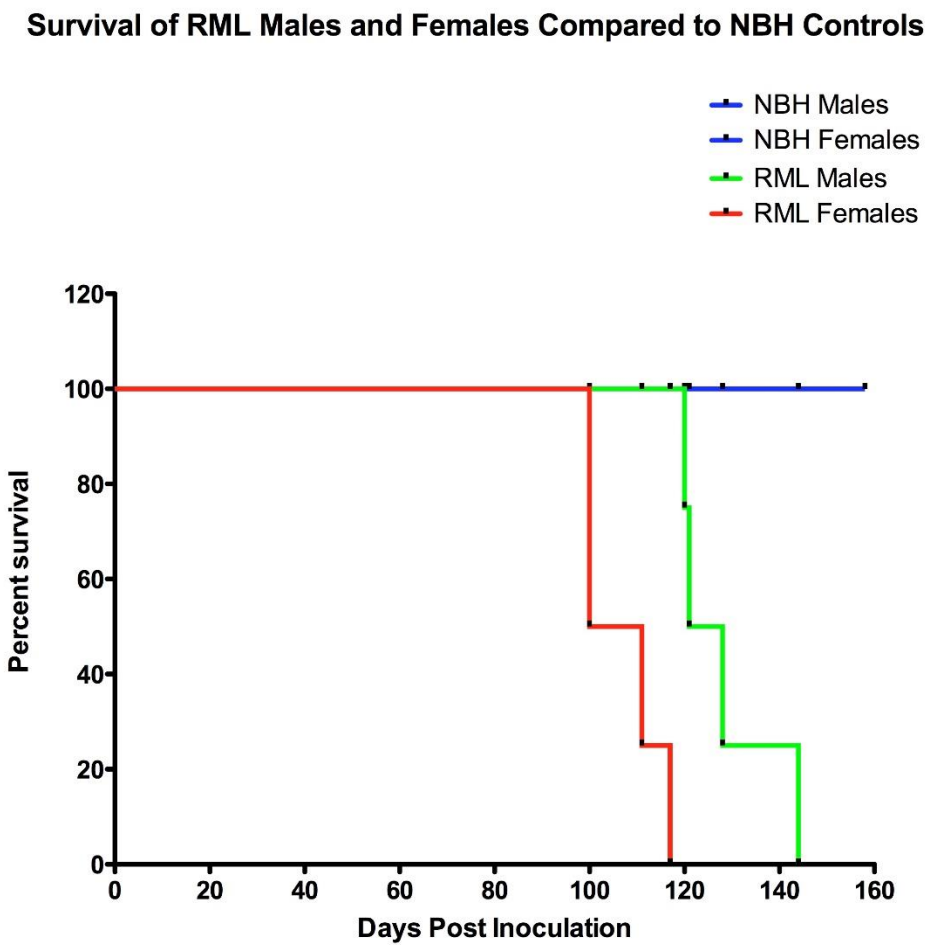

Figure 4: Kaplan-Meier Survival Curve of Cytokine Study TgA20 Mice
Kaplan-Meier survival curve generated using Prism software (version 5.0d). RML-Males and RML-females were euthanized when prion disease morbidity score indicated terminal illness. NBH animals were euthanized at 158dpi with no outward signs of prion disease. RML-females were euthanized an average of 107dpi, whereas RML-male mice averaged 128dpi with no overlap between the two groups.

Western Blot:

Western blot confirmed the presence of PK-resistant material in brain homogenate from RML-inoculated mice at 60dpi, 80dpi and at terminal disease (Figure 5, A&B). The absence of PrP^{res} at 40dpi confirms our hypothesis that RML-prions, when inoculated IP, do not enter the brain until

after 40 days post inoculation. NBH-inoculated animals from all time points were negative for PrP^{res}.

5A.

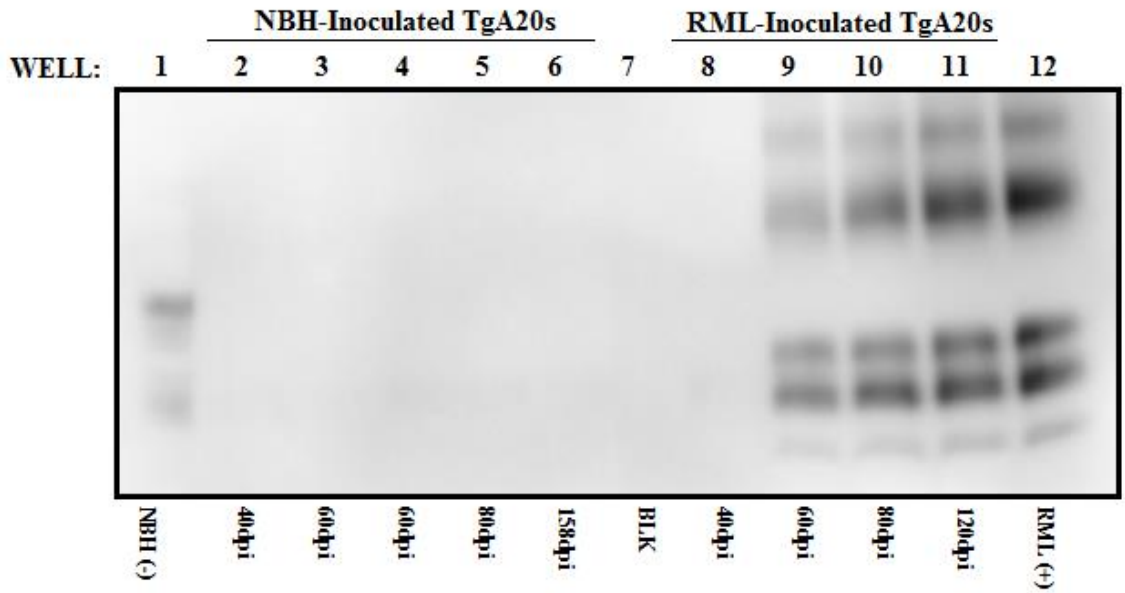

5B.

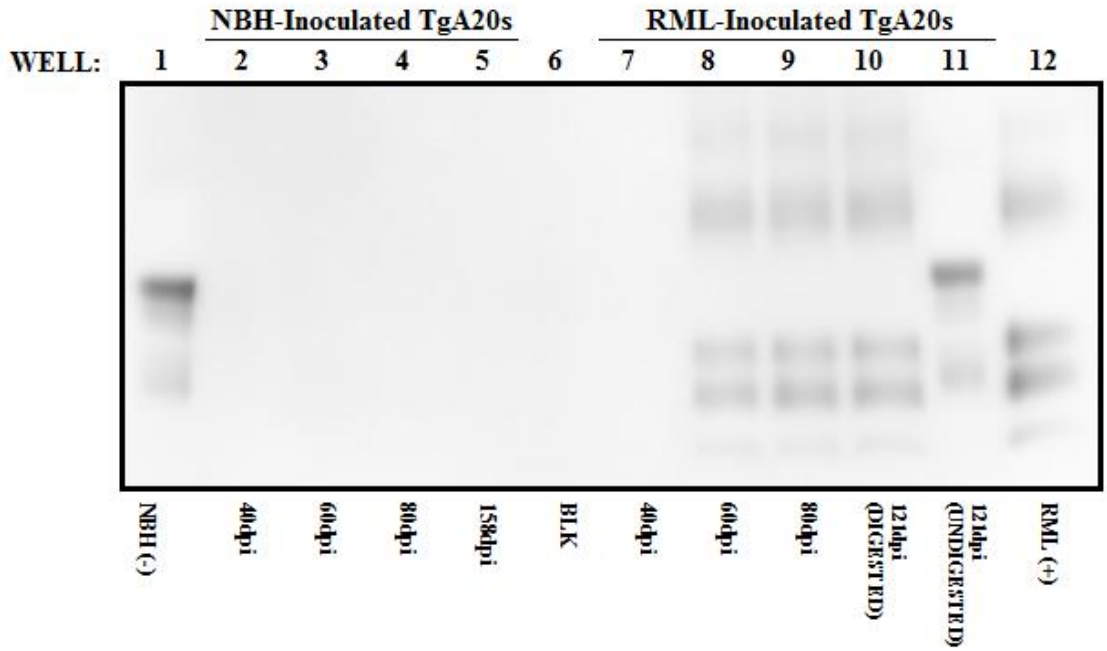

Figure 5 (A & B): Western Blots of TgA20 Brain Homogenate from Longitudinal Cytokine Study

TgA20 NBH - negative for prions - was included in well 1 on both blots as a representative of undigested negative brain material and TgA20 RML was loaded into well 12 on both blots as a positive control. **(A)** 10% brain homogenate from NBH-inoculated animals is shown in wells 2-6 and RML-inoculated animals in wells 8-11 in the order of 40dpi, 60dpi, 80dpi and terminal. Well 7 was left blank to prevent sample spill-over. **(B)** NBH-inoculated brain material from each time point is shown in wells 2-5 and RML-inoculated animals from each time point are shown in wells 7-10. Well 11 shows undigested brain material from RML-infected mouse 136539-1, whose PK-digested sample is shown in well 10. Well 6 was left blank to prevent sample spill-over.

BioPlex:

Cytokine levels for GM-CSF, IFN-γ, IL-1β, IL-4, IL-6, IL-12p70, IL-13, IL-18, TNF-α, and IL-10 were overall below detection limit (out-of-range low, OOR<), set by the lowest value from the standard curve. IL-2 and IL-5 showed the most robust and consistent signals throughout the longitudinal study, with a few mice showing pro- and/or anti-inflammatory cytokine responses at varying time points (see Appendix, Table 1A—Supplementary, Cytokine Mega Table). A repeated-measure statistical analysis using SAS revealed that although no significant differences were observed between the RML and NBH treatment groups, there was a significant difference over time for IL-2 and IL-5 (Table 2). Due to unequal numbers between treatment groups and numerous OOR< values, a repeated measures analysis could not be performed using SAS for the other cytokines. In an attempt to overcome this issue, and not miss other significant differences between genders, treatment groups and time for other analytes, cytokine data was bootstrapped to fill in missing values and a repeated measures two-way ANOVA was performed using Prism software (version 5.0d). This secondary statistical analysis revealed a number of additional significant differences for the other cytokines, as well as confirmed the statistical significance seen for IL-2 and IL-5 in the SAS analysis (Table 3).

Table 2 (A - D):
Results of SAS analysis (repeated measures performed by Ann Hess). Tables 2A and 2B pertain to IL-2, and tables 2C and 2D pertain to IL-5. Tables 2A and 2C show maximum and minimum (usually <OOR) observed cytokine concentration (pg/ml) along with mean and standard deviation for longitudinal data. Tables 2B and 2D show p-values associated with factors that were analyzed, such as gender, time, treatment groups, etc.

Table 2A: IL-2 SAS Statistical Analysis
At 20dpi, the observed serum concentration of IL-2 peaks for both NBH and RML treatment groups, but is overall expressed at higher levels in the RML-infected mice at this time point.

Treatment Group	DPI	N Obs	Mean	Std Dev	Minimum	Maximum
NBH	**0**	10	2.827	5.836	0.140	16.550
	1	10	8.044	8.378	0.080	23.880
	20	10	24.369	18.920	0.080	**51.160**
	40	10	11.375	10.503	0.080	26.180
	60	8	11.109	11.365	0.090	31.490
	80	6	14.940	6.623	7.520	23.500
	Term	4	0.085	0	0.080	0.085
RML	**0**	21	4.973	9.779	0.080	41.030
	1	20	12.689	11.176	0.080	31.120
	20	21	21.014	18.154	0.090	**63.950**
	40	21	14.132	11.278	0.090	37.920
	60	17	11.278	9.132	0.085	27.020
	80	13	12.237	11.195	0.085	30.420
	Term	8	2.696	6.092	0.080	17.460

Table 2B: IL-2 SAS Type 3 Tests of Fixed Effects
IL-2 was only shown to have a significant differences over time (p-value <0.0001), but not for any other interactions.

Effect	**F Value**	**Pr > F**
Gender	0.06	0.8010
TX_Group	0.12	0.7277
Gender*TX_Group	0.33	0.5703
DPI	9.48	**<0.0001**
Gender*DPI	0.61	0.7220
TX_Group*DPI	0.73	0.6285
Gender*TX_Group*DPI	0.52	0.7882

Table 2C: IL-5 SAS Statistical Analysis
Similar to IL-2, IL-5 peaked at 20dpi for the NBH animals, whereas the peak was observed at 40dpi for the RML-inoculated cohort.

Treatment Group	DPI	N Obs	Mean	Std Dev	Minimum	Maximum
NBH	**0**	10	1.893	2.351	0.300	7.190
	1	10	8.009	10.341	0.305	27.970
	20	10	5.143	8.680	0.305	**29.180**
	40	10	7.457	7.389	0.220	27.200
	60	8	4.151	5.944	0.220	17.330
	80	6	1.227	1.587	0.210	3.570
	Term	4	2.780	1.858	0.210	4.590
RML	**0**	21	1.532	2.044	0.210	7.190
	1	20	2.828	3.553	0.210	12.800
	20	21	4.153	5.527	0.210	20.730
	40	21	4.903	5.355	0.210	**22.770**
	60	17	4.405	3.960	0.210	16.650
	80	13	3.115	3.333	0.210	10.170
	Term	8	3.279	4.834	0.210	13.230

Table 2D: IL-5 SAS Type 3 Tests of Fixed Effects
IL-5 showed significant differences between males and females (p-value 0.0021), as well as a statistically significant variation over the course of disease (p-value 0.0016).

Effect	**F Value**	**Pr > F**
Gender	11.19	**0.0021**
TX_Group	1.29	0.2647
Gender*TX_Group	0.14	0.7061
DPI	4.30	**0.0016**
Gender*DPI	1.07	0.3961
TX_Group*DPI	1.07	0.3941
Gender*TX_Group*DPI	0.87	0.5274

Table 3: Repeated Measures Two-Way ANOVA of Cytokine Data
Two-way ANOVA repeated measures analysis performed using PRISM software (version 5.0d) on bootstrapped cytokine data. IL-2 and IL-5 significance over time was reconfirmed using this method of statistical analysis with IL-2 having a p-value of <0.0001 (same as SAS analysis), and IL-5 also at <0.0001 (compared with 0.0016 on SAS). Additionally, IL-6, TNF-α, and IL-18 were shown to have significance over time, IFN-γ and IL-5 were significantly different between treatment groups, and IL-5, IL-6, and TNF-α had statistically significant interactions between treatments and time.

Cytokine	Significant Trends (p-value)	Significant DPI
IFN-γ	Treatment* (0.0286)	n/a
IL-2	Time**** (<0.0001)	Baseline to 20dpi: NBH Males**** (<0.0001), NBH Females* (<0.05), RML Males*** (<0.001) 20dpi to Terminal: NBH Males**** (<0.0001), NBH Females**** (<0.0001), RML Males **** (<0.0001)
IL-5	Interaction** (0.0029) Treatment*** (0.0005) Time**** (<0.0001)	NBH Females 1dpi** (<0.01), 80dpi** (<0.01)
IL-6	Interaction* (0.0344) Time** (0.0021)	NBH Females 40dpi*** (<0.001)
IL-18	Time *** (0.0003)	n/a
TNF-α	Interaction** (0.0019) Time* (0.0130)	NBH Females 1dpi**; NBH Males 40dpi*
IL-10	n/a	RML Females 20dpi* (<0.05)

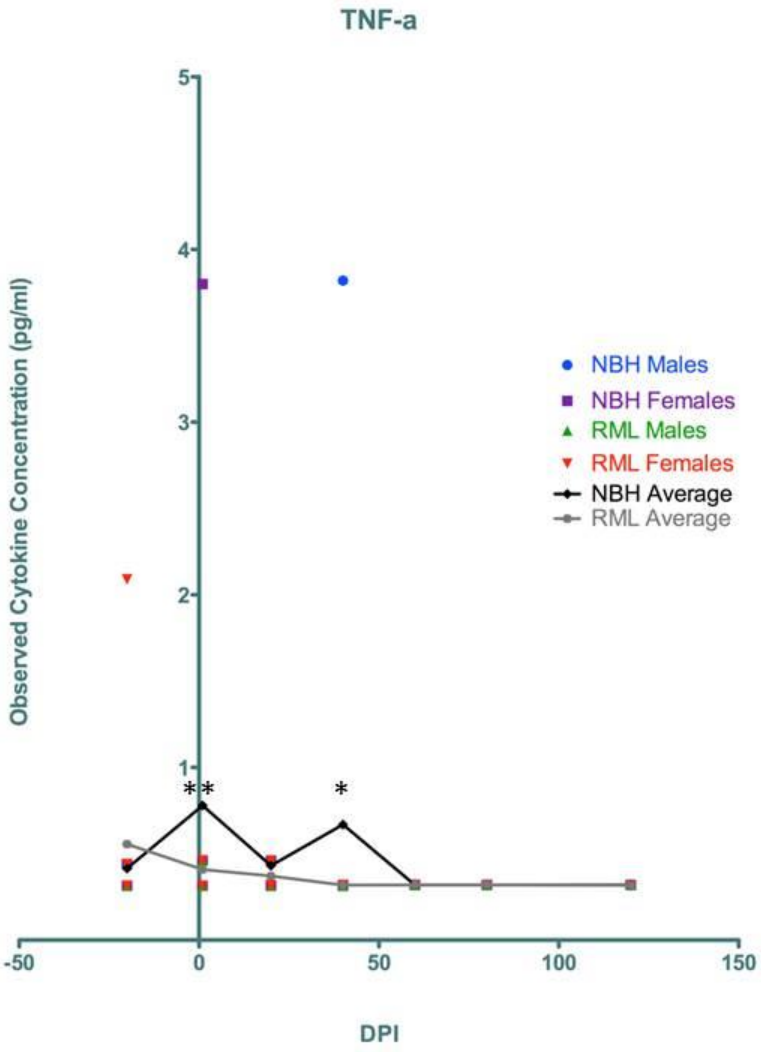

Figure 6: TNF-α Longitudinal Expression Levels in NBH- and RML-infected mice

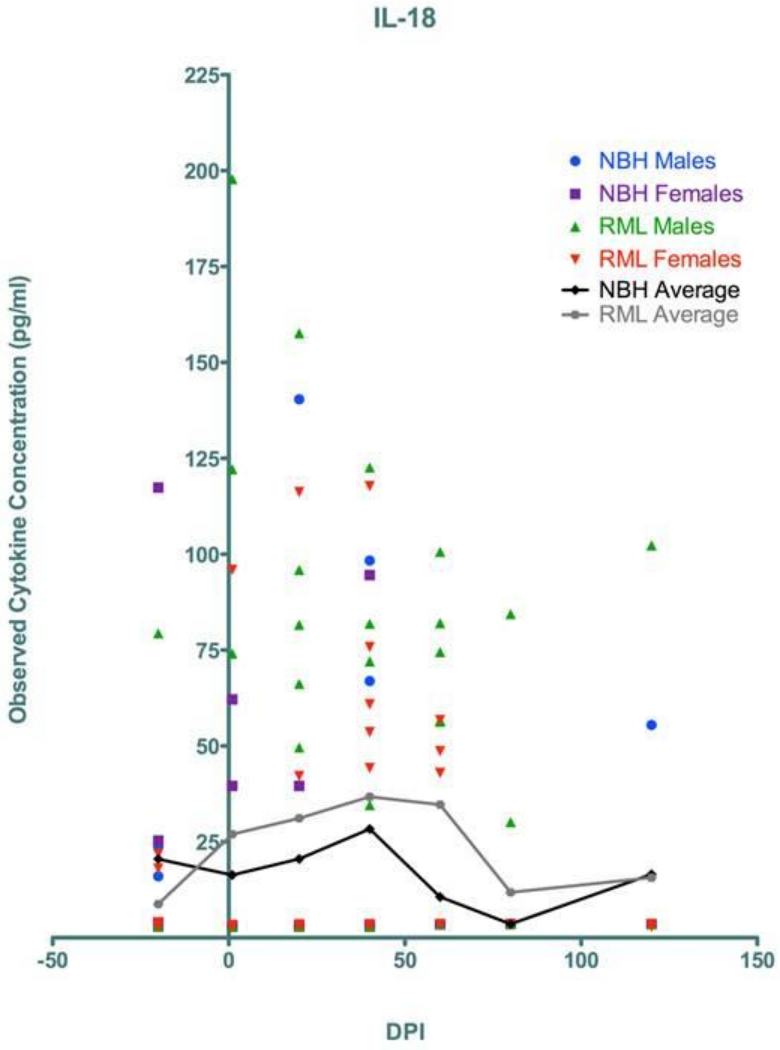

Figure 7: IL-18 Longitudinal Expression Levels in NBH- and RML-infected mice

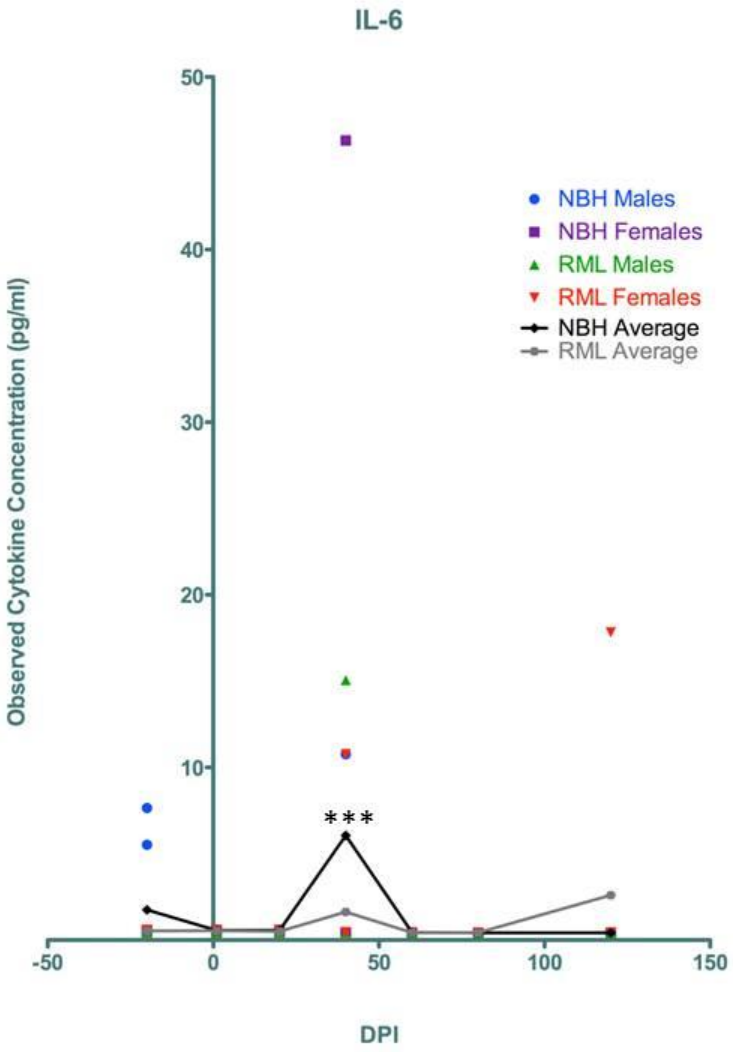

Figure 8: IL-6 Longitudinal Expression Levels in NBH- and RML-infected mice

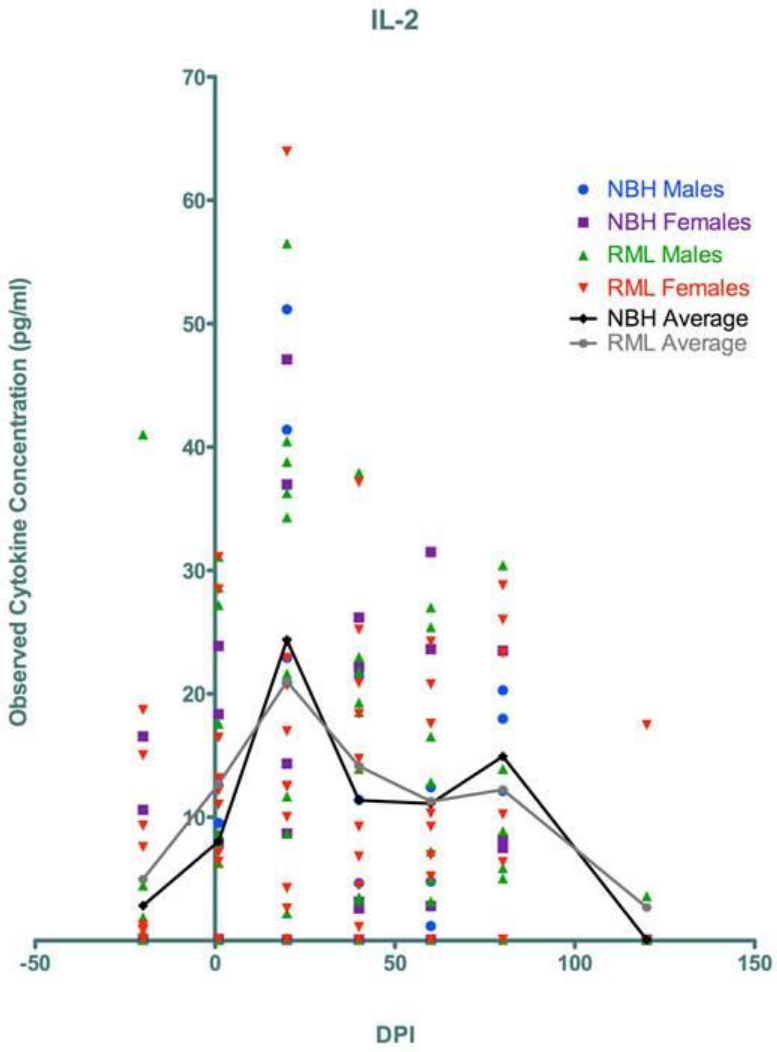

Figure 9: IL-2 Longitudinal Expression Levels in NBH- and RML-infected mice

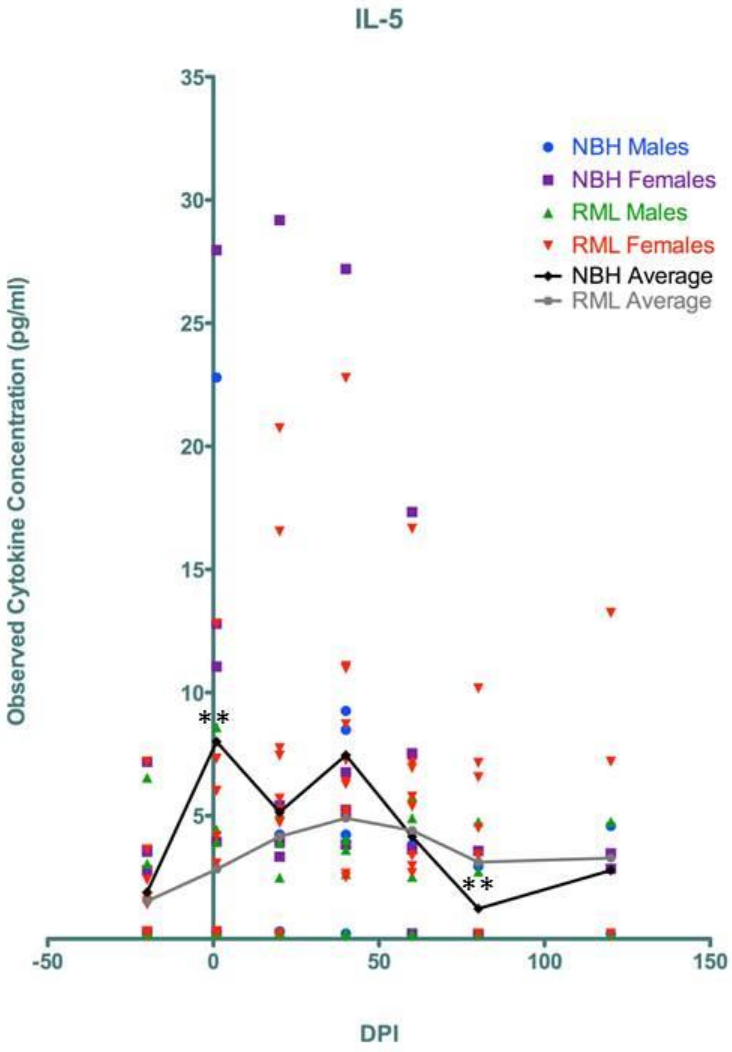

Figure 10: IL-5 Longitudinal Expression Levels in NBH- and RML-infected mice

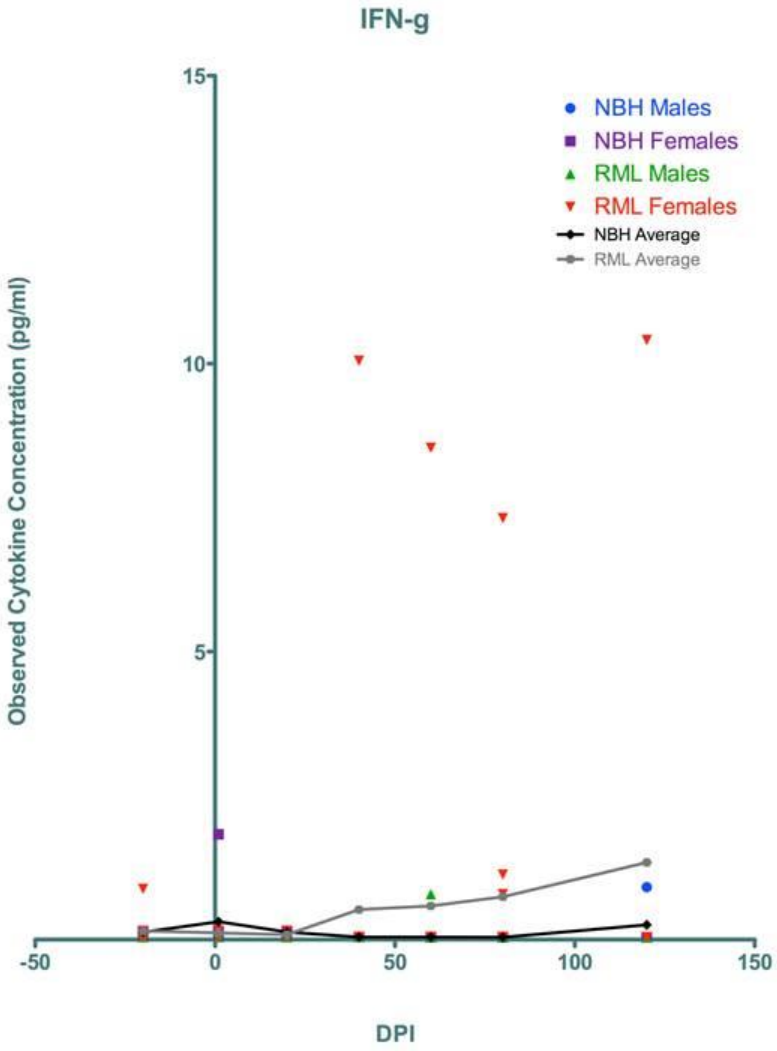

Figure 11: IFN-γ Longitudinal Expression Levels in NBH- and RML-infected mice

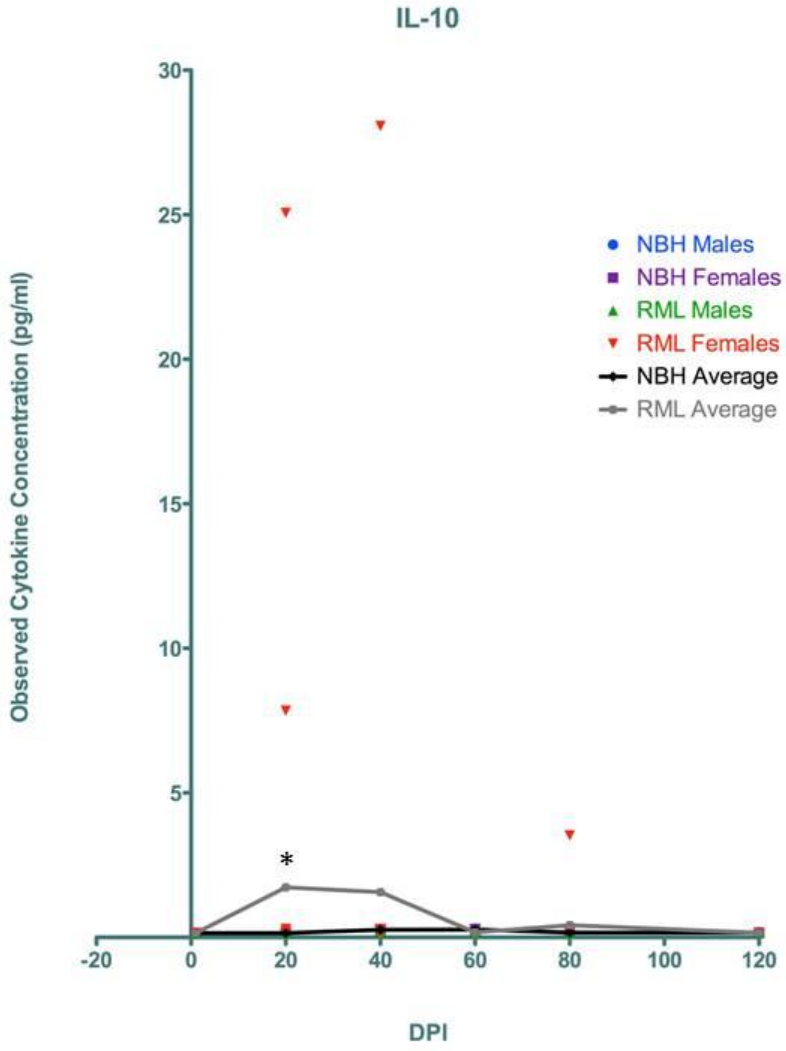

Figure 12: IL-10 Longitudinal Expression Levels in NBH- and RML-infected mice

Flow Cytometry:

TgA20 mice overexpress PrP^C in the CNS at reported levels of 4- to 10-fold higher than wild type mice. We performed an experiment utilizing flow cytometry to determine whether peripheral PrP^C expression level correlated to the higher expression level seen in the CNS. If PrP^C expression is much lower in the spleen—an organ known to play an important role in peripheral prion replication and propagation as well as immunity—then the overall cytokine expression could be altered and may influence downstream effects in disease progression and resulting pathology. Since PrP^C is required for prion-associated neuronal death, expression level in the periphery versus the brain could directly affect cellular signals of neurotoxicitiy/neuroprotection and ultimately cellular survival. In order to investigate this, we euthanized four TgA20 mice—two males and two females—and analyzed filtered brain and spleen homogenates tagged with PE-Texas Red and antibody-probed for PrP^C. Cells were analyzed via flow cytometry and the percent of PrP-expressing cells from brain and spleen homogenates was determined using mean fluorescence intensity (MFI).

We found that males showed slightly higher PrP^C-expression in both the brain and the spleen over females, although this difference was subtle (Figure 13). Interestingly, we observed PrP^C expression levels 20-fold higher in the brain than the spleen in TgA20s (Figure 13, C & D).

A.

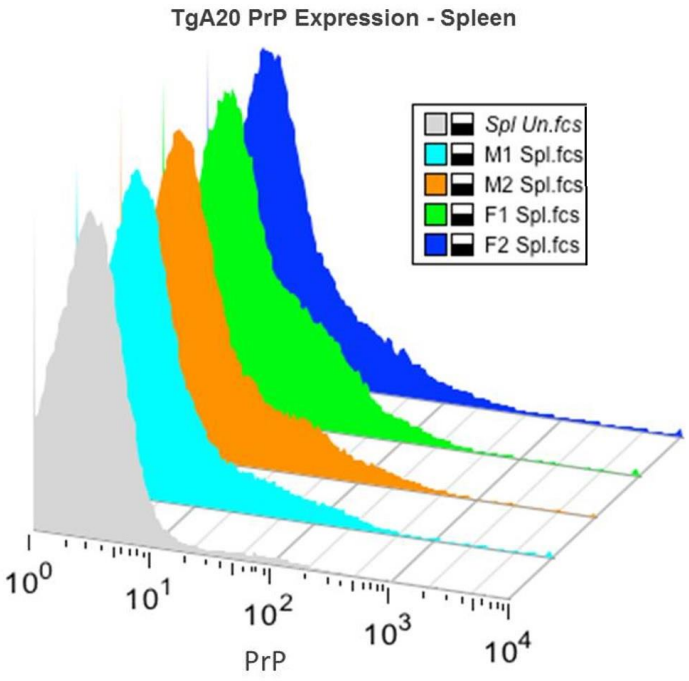
TgA20 PrP Expression - Spleen
Spl Un.fcs
M1 Spl.fcs
M2 Spl.fcs
F1 Spl.fcs
F2 Spl.fcs
10^0
10^1
10^2
10^3
10^4
PrP

B.

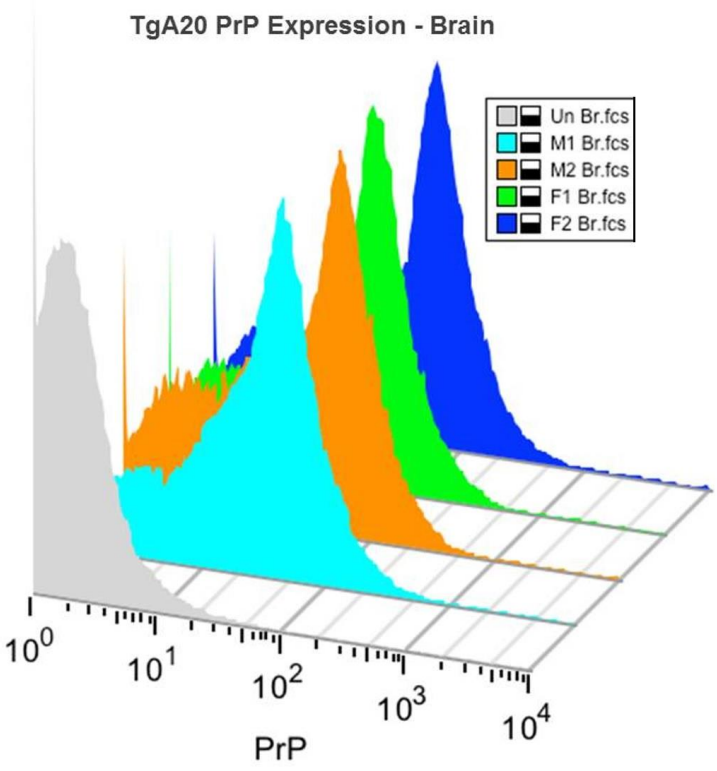
TgA20 PrP Expression - Brain
Un Br.fcs
M1 Br.fcs
M2 Br.fcs
F1 Br.fcs
F2 Br.fcs
10^0
10^1
10^2
10^3
10^4
PrP

C.

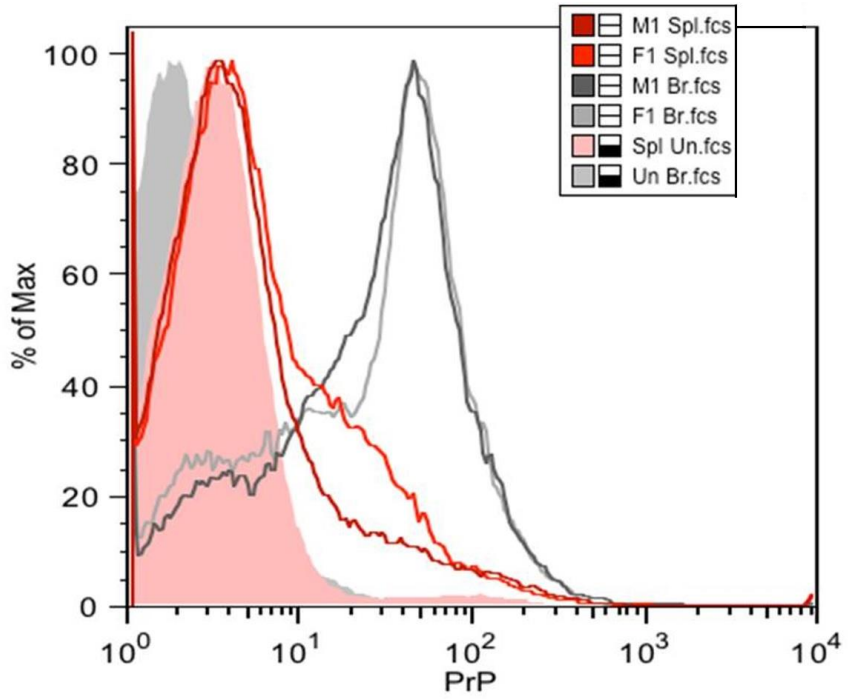

D.

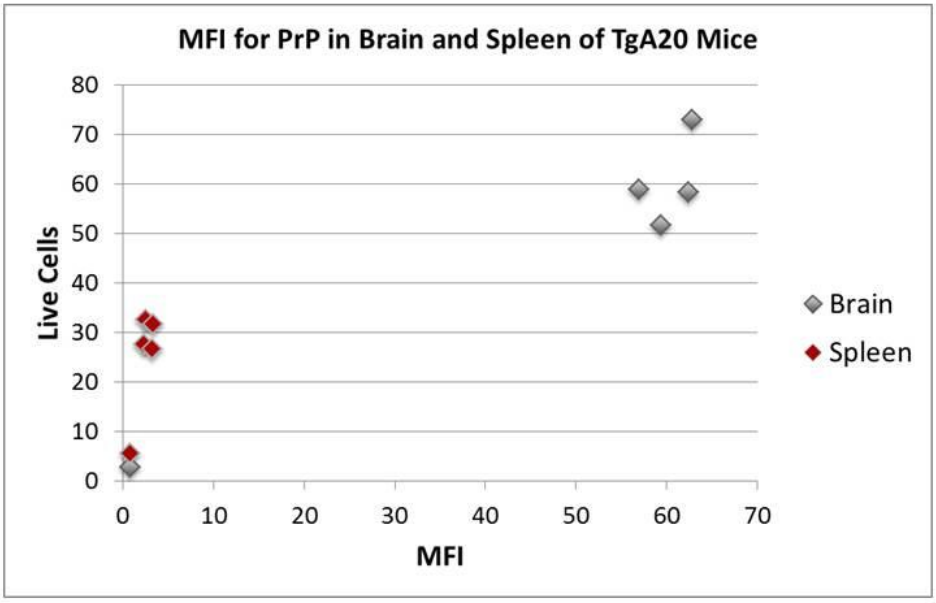

BRAIN		
Sample	**Live Cells**	**MFI (PrP+)**
Female 1	51.6	59.4
Female 2	72.9	62.8
Male 1	58.4	62.4
Male 2	58.8	56.9
Unstained	2.67	0.77
Mean	48.9	48.5
StdDev	27	26.8

SPLEEN		
Sample	**Live Cells**	**MFI (PrP+)**
Female 1	32.5	2.54
Female 2	27.6	2.33
Male 1	31.6	3.32
Male 2	26.7	3.21
Unstained	5.4	0.8
Mean	24.8	2.44
StdDev	11.1	1.01

Figure 13 (A-D): Flow Cytometry Characterization of PrP^C Expression Levels
Four age-related TgA20s, two male (M1 & M2) and two female (F1 & F2) were euthanized and brains and spleen homogenates were stained for PrP^C and quantitated by flow cytometry. (A) Levels of PrP^C(+) splenic cells compared to unstained (Spl Un) in grey. (B) Levels of PrP^C(+) brain cells compared to unstained (Un Br) in grey. (C) Overlap of Figure 13, A & B with spleen represented in red and brain in grey, solid background correlates to unstained. (D) Graphical interpretation of MFI for PrP^C(+)

ELISA:

Overall, MCP-1 levels in the serum of study animals are lower in prion-infected animals, with animals from both treatment groups displaying low levels compared to LPS-induced positive control mice. Whereas in the brain, MCP-1 levels from RML male mice increase above the levels seen in LPS-controls. Likely due to a single mouse which showed chronic, significantly increase inflammatory responses.

A.

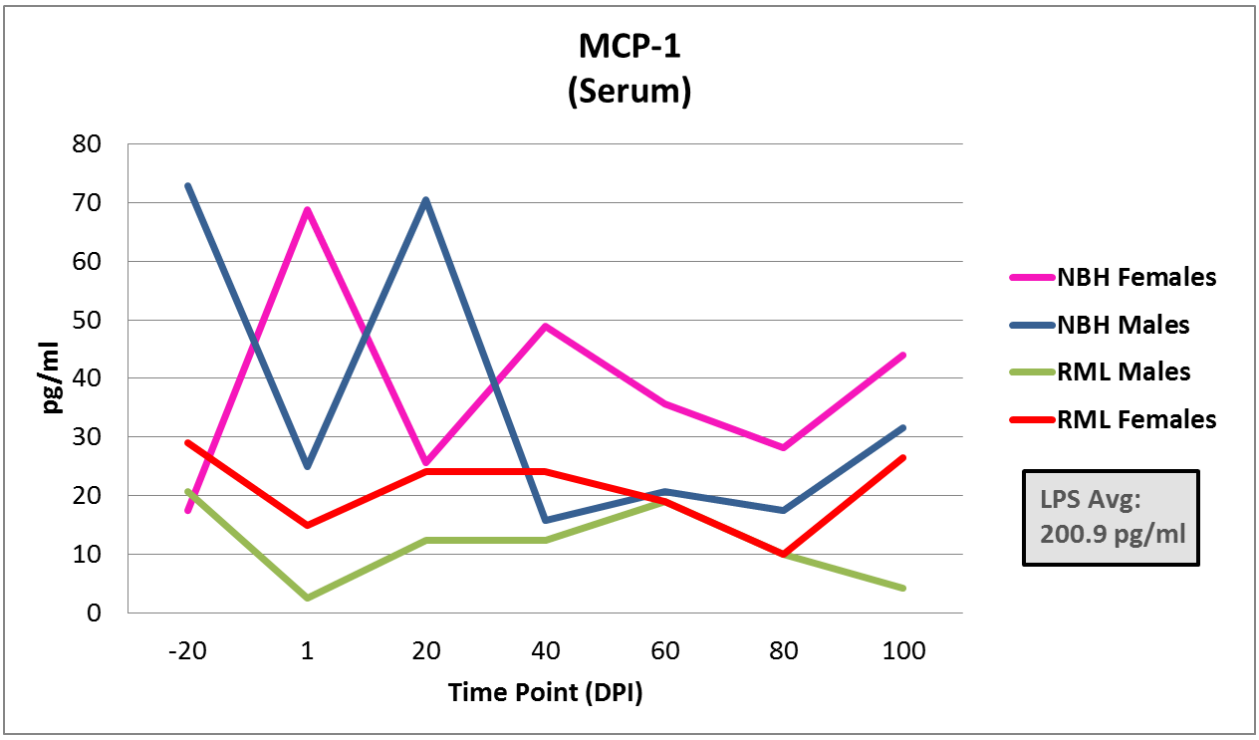

B.

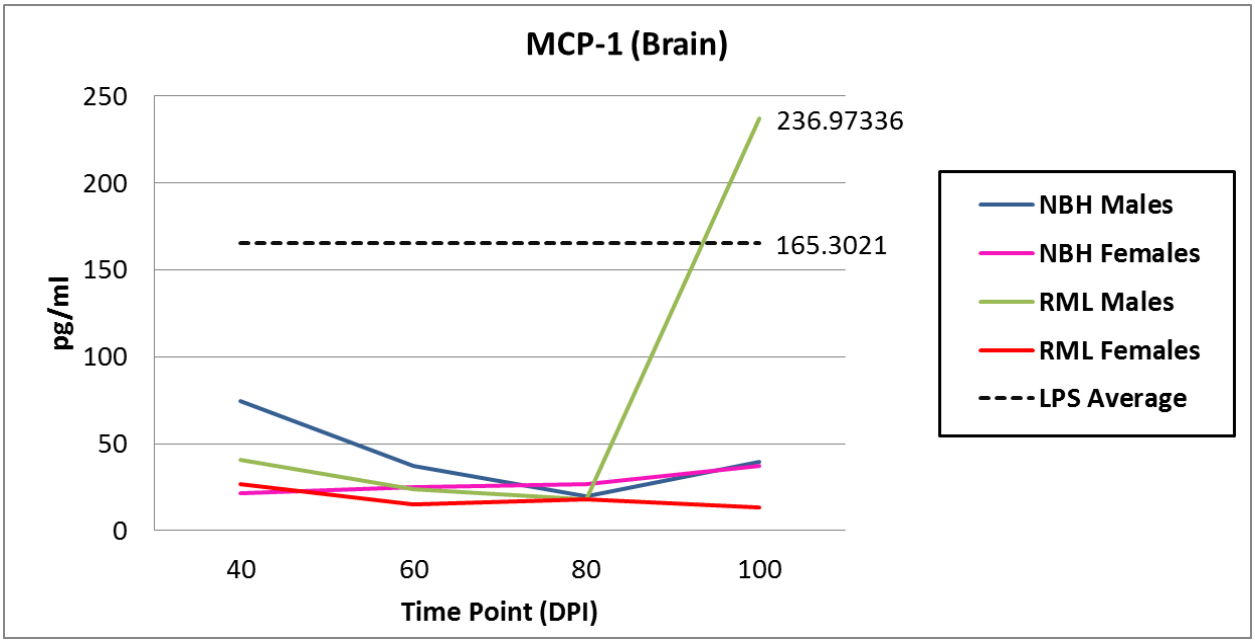

Figure 14 (A & B): MCP-1 ELISA in serum (A) and brain (B)
Pooled samples due to limited volume show lower MCP-1 expression in the serum of RML-infected mice compared to NBH, but both were significantly below LPS average (A). MCP-1 in the brain homogenate from RML males is exceptionally high (B), likely due to the chronic inflammation from expression of other pro-inflammatory cytokine signals apparent in a single mouse in the cytokine multiplex assay (see supplementary cytokine Mega Table).

IHC/H&E/GFAP:

Histological staining techniques are often used for assessing prion-induced neuropathology and include immunohistochemistry for PrP^{res} and H&E stain for neuronal vacuolation and spongiosis. Glial Fibrillary Acidic Protein (GFAP) is an intermediate filament protein encoded by the GFAP gene. Within the CNS, GFAP is expressed during reactive gliosis and is mostly associated with astrocytes, and thus is a classic stain used to illustrate the astrogliosis associated with prion infection.

Figure 15 (A-C) shows IHC staining of PrP^{res} material in mice sacrificed at 80dpi and at terminal disease. Staining for GFAP and H&E for spongiosis yielded unexpected results, showing mild vacuolation in both RML- and NBH- inoculated mice (pictures not shown), with atypical GFAP staining in the hypothalamus and caudal medulla region, ventral to the cerebellum at the level of the cerebellar peduncles and lateral cerebellar nuclei (Figure 16).

A. 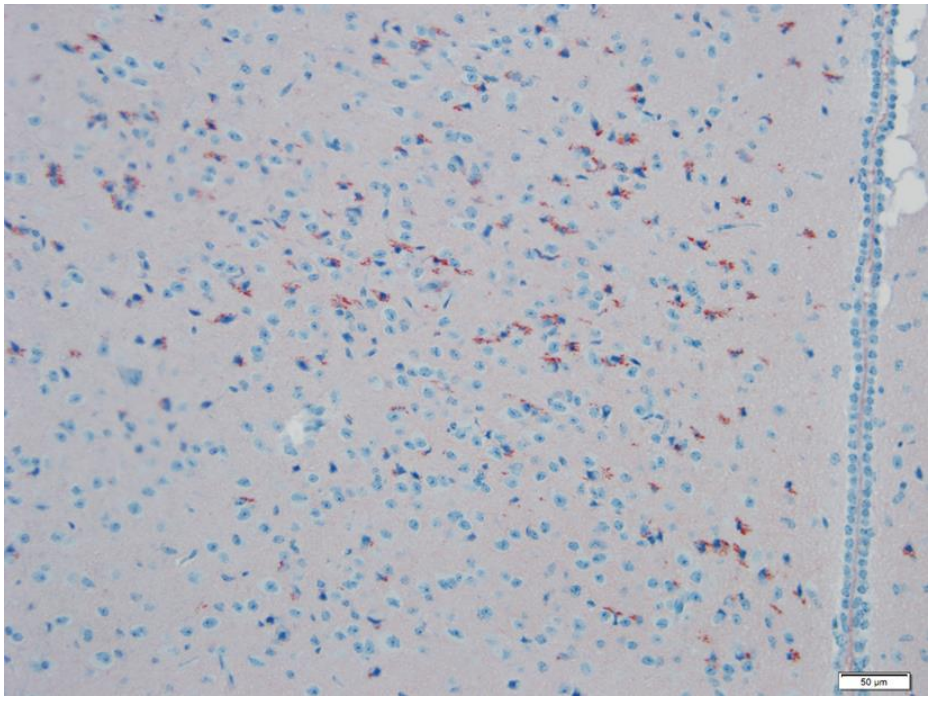

B.

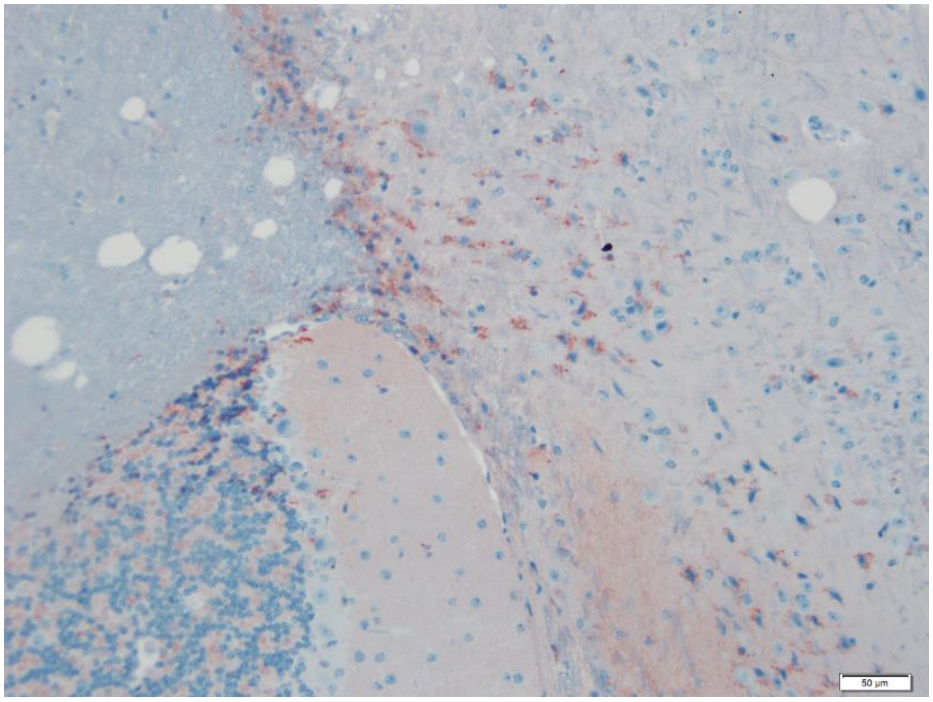

C.

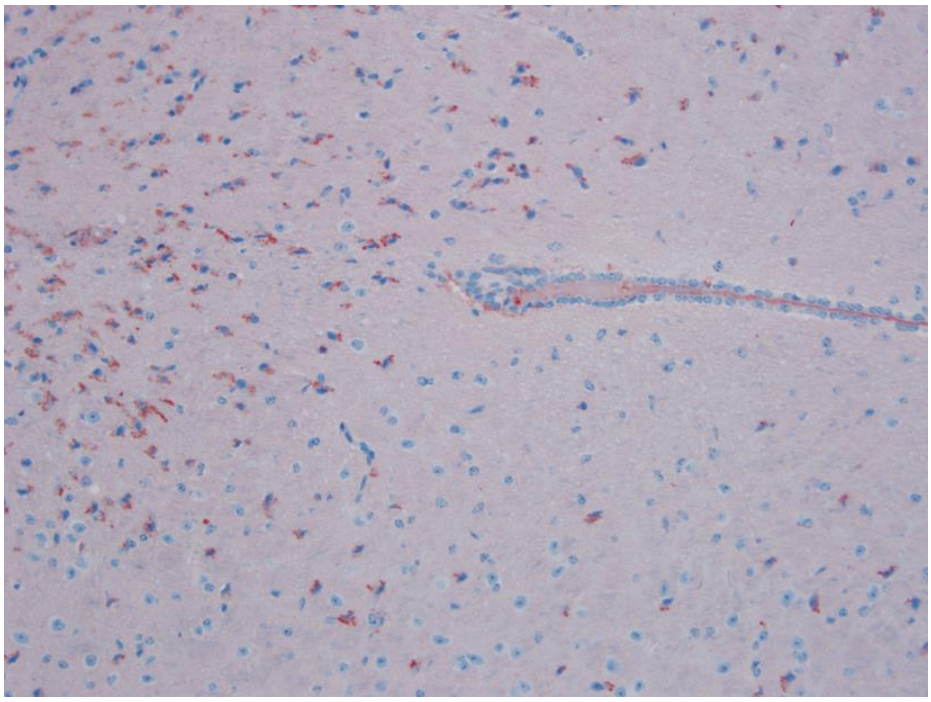

Figure 15: IHC for PrP^{Sc} in the brains of mice infected with RML mouse-adapted scrapie
IHC + staining in RML-infected female mouse sacrificed at 83dpi in the hypothalamus near the 3rd ventricle (A) and in the region of the cerebellar peduncle (B), coinciding with the region where higher intensity GFAP staining was observed. PrP^{res} was also detected in and surrounding the 3rd ventricle of a male mouse with terminal prion disease, sacrificed at 121dpi (C).

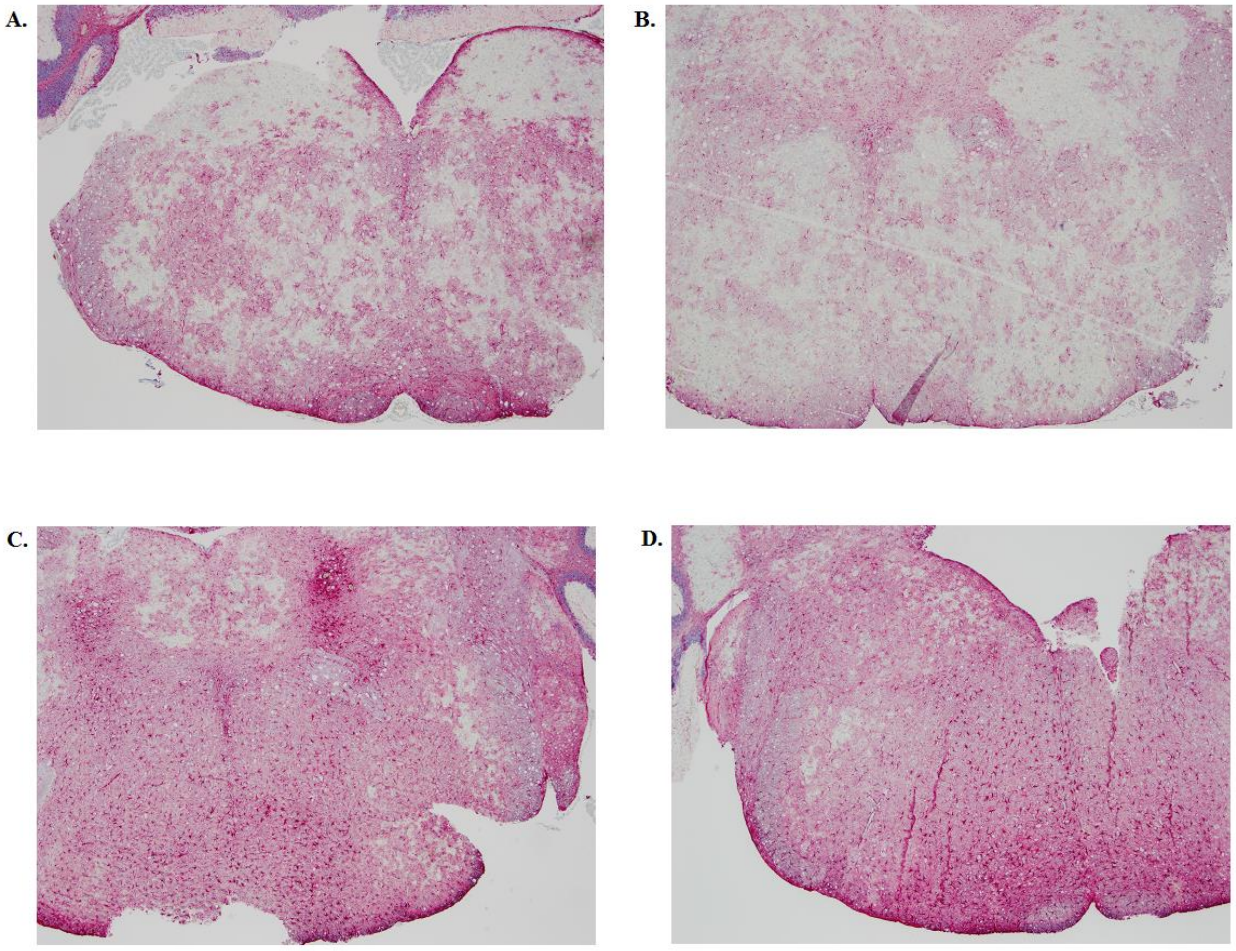

Figure 16, A-D: GFAP Staining in NBH- and RML-Inoculated TgA20 Mouse Brains
A & B show GFAP stain uptake in caudal medulla of NBH-inoculated male and female mice, respectively. This diffuse, light staining is indicative of normal, low-level astrogliosis present in overexpressing mouse models. Compared to figures C and D, which display darker, heavier GFAP staining with occasional "hotspots" in RML-inoculated mice. This stain pattern is suggestive of more extensive astrogliosis in prion-infected animals, in spite of overall low-level PrP^{Sc} accumulation, and atypical location of early astrogliosis (usually near hippocampus).

CLARITY:

Due to IHC/GFAP/H&E histologic findings that were atypical for naturally-occurring and other experimental models of prion disease, we investigated the activation of the NFκB transcription

factor in GFP-NFκB expressing mice infected with RML and euthanized at 60dpi. We used a newly-developed CLARITY protocol to clarify intact whole sections of mouse brains, ridding them of lipid content following crosslinking of proteins and cytoskeletal elements, allowing for 3-dimensional visualization of GFP expression where NFκB activation was present. Using confocal microscopy, we found the only significant GFP expression within the region of the caudal medulla underlying and extending into the cerebellum (Figure 17).

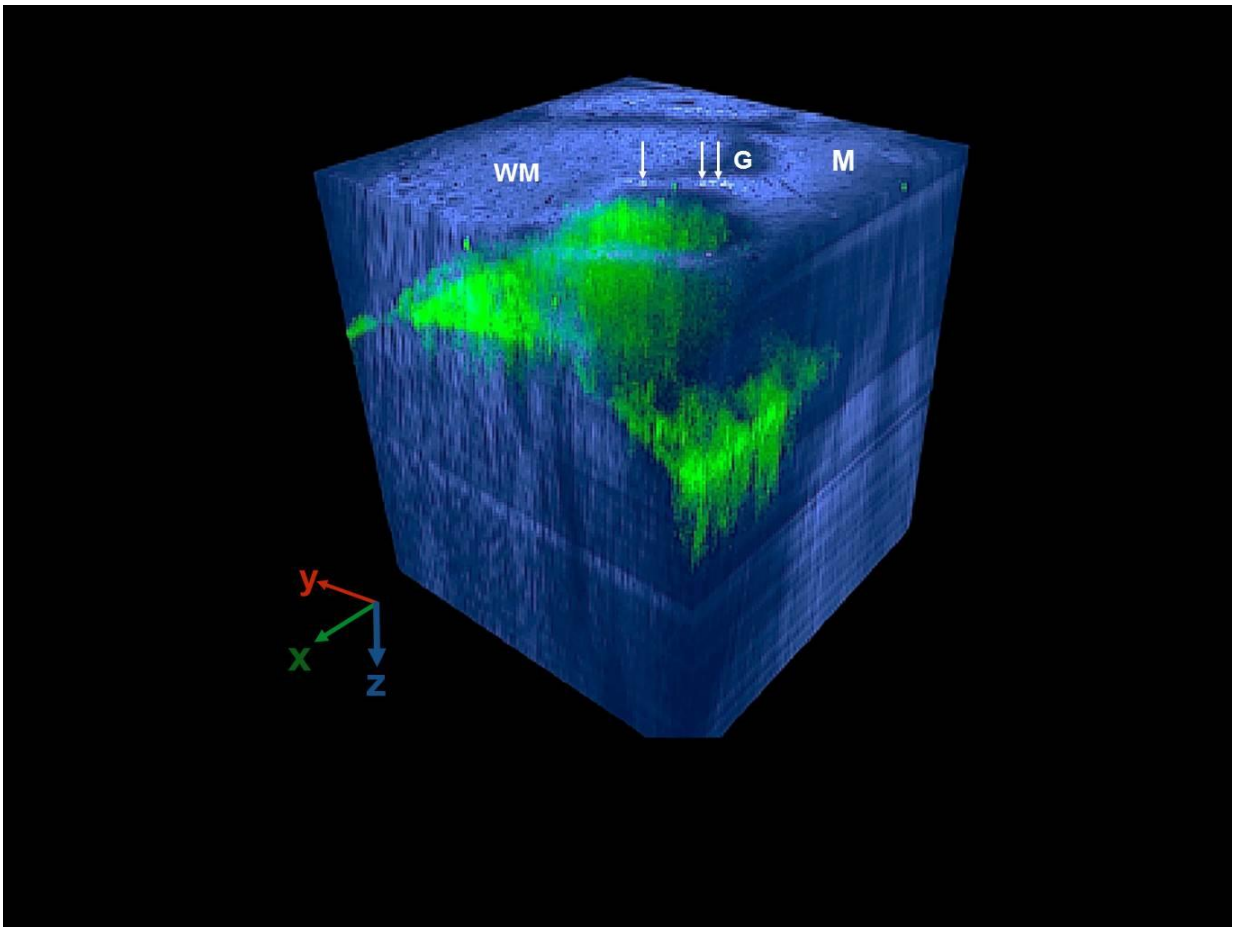

Figure 17: CLARITY brain section from NFκB-GFP mouse
Confocal microscopy of a 60dpi scrapie-infected GFP-NFκB mouse showed GFP expression in the region of the caudal medulla, underlying and extending into the cerebellum (WM).

Discussion

Prion diseases are characterized by a state of progressive and invariably fatal neurodegeneration manifesting as cognitive decline and chronic wasting. Prions are misfolded, infectious, proteinaceous particles that break the biological dogma of what we understood of transmissible disease prior to their discovery (Prusiner, S., 1982). In the normal cellular form, the prion protein appears to be ubiquitous among mammals with highly conserved primary biochemical structure (Krakauer et al., 1998; Schätzl et al., 1995). High PrP^{C} homology, auto-conversion to pathogenicity, and striking environmental persistence of prions in the face of common decontamination methods would suggest widespread distribution and a high prevalence of disease among host species—however, naturally-occurring prion diseases seem to maintain host-specificity (Gajdusek, D., 1977), with certain mammalian species showing complete resistance to prion-induced neurodegeneration (Bartz et al., 1994; Diaz-San Segundo et al., 2006; Lysek et al., 2005). The low prevalence of "naturally-occurring" human prion diseases is evidenced by a one-in-a-million chance of developing sCJD. Naturally-occurring animal prion diseases, however, are a larger problem with historical reports of scrapie extending back to the 1700s and a new emergence of CWD in North American cervid populations. The distribution of CWD continues to expand, along with environmental contamination, and current studies are underway revisiting the zoonotic potential of both scrapie and CWD prions (Saunders, Bartelt-Hunt, & Bartz, 2012). It is difficult to ascertain the risk factors involved with the consumption of CWD positive brain or peripheral tissues from hunter-killed deer, elk, and moose when so much remains unknown about the prion protein's behavior.

The outbreak of BSE in the UK heightened our awareness of the unknowns of prion disease and stands as an important reminder that species barriers in prion disease transmission are not well understood (Billeter et al., 1997). Additionally, recent comparisons between prion disease and other "proteinopathies" such as AD, Parkinson's, ALS, traumatic brain injury (TBI), and dementia provide helpful insight into cellular and molecular pathways that potentially cause disease. In the absence of informative genetic material, little is known about the structure and function of PrP^{Sc}, making the studies of prion epidemiology and pathogenesis challenging—other factors potentially involved in prion propagation between different host species become an appealing focus. This study recognizes lymphoid involvement as a key feature unique to specific prion diseases and quantitated cellular immune signaling molecules in the same animals throughout their disease to expose information pertinent to prion disease mechanisms.

A number of past studies have described neuroinflammation involved in neurodegenerative processes. In AD it is thought that expression of pro-inflammatory cytokines such as IL-1β, IL-6, IFN-γ, and TNF-α contribute to astrocytosis and exacerbate neuronal oxidative stress through the production of NO through the iNOS pathway (Chiarini et al., 2005; Eikelenboom et al., 1994, McGeer & McGeer, 1995; Sudduth et al., 2013). Chiarini et al. further characterized this signaling and found that cytokines themselves were mildly neurotoxic, but when combined with the presence of Aβ the neurotoxic effect significantly increased. Their group also looked at the involvement of p75, a neuronal cell surface receptor in the same family as other death receptors, which has been shown to bind both Aβ and NGF (Lu et al., 2005; Nagata et al., 1997; Smith et al., 1994). It was determined that Aβ-p75 binding can in fact induce cell death through generation of ROS (Chiarini et al., 2005). Within a murine scrapie model, it was demonstrated that IL-1 is a significant inducer

of astrogliosis, and IL-$1^{-/-}$ mice had prolonged incubation periods (Schultz et al., 2004). However, they also noted increased microgliosis in the murine IL-$1^{-/-}$ model and progression to terminal disease in the absence of IL-1.

Histopathological findings associated with scrapie infection include spongiosis, neuronal and neuropil vacuolation, PrP^{res}, gliosis (Fraser, 1988; Jendroska et al., 1991), as well as synaptic loss (Budka, 2003). A lack of inflammatory infiltrate of peripheral immune cells during TSE infection makes studying central immune responses represented by cytokines important. Astrocytes and microglia make up the two most important cell types contributing to neuroinflammation, as they are stimulated to undergo proliferation early on during prion disease (Betmouni, Perry, & Gordon, 1996; Campbell et al., 1994; DeArmond, Kristensson, & Bowler, 1992; Giese et al., 1998; Williams et al., 1994; Williams et al, 1997), and both cell types have been shown to produce cytokines and have an impact on neuronal survivability (Campbell et al., 1994; Kim et al., 1999; Williams et al., 1994). Microgliosis co-localizing with areas of pathology (i.e. PrP^{res} deposition and/or vacuolization) is commonly observed in CJD brains and murine scrapie models (Sasaki, Hirato, & Nakazato, 1993; Williams et al., 1994).

Other groups have reported that the typical pro-inflammatory cytokine profile was not observed in certain prion disease models, as was the case for the ME-7 form of murine scrapie (Cunningham, Boche, & Perry, 2002; Walsh, Betmouni, & Perry, 2001). Studies in this animal model show a preponderance of TGF-β1 expression, which can directly down-regulate iNOS (Minghetti & Levi, 1998). While we were interested in the possibility of anti-inflammatory cytokine expression, the unstable nature of TGF-β prompted us to, instead, analyze IL-10 in the multiplex assay. Multiple

investigators have demonstrated involvement of TGF-β and IL-10 in prion disease models (Baker et al., 1999), as both TGF-β and IL-10 negatively impact cytokine expression from microglia in vitro (Lodge & Sriram, 1996). Additionally, it has been shown that IL-10 can down-regulate IL-1β and TNF-α (Bogdan et al., 1992; Chao et al., 1995; Lodge & Sriram, 1996).

It should be noted that specific cytokine expression and cellular pathways vary depending on disease, genetic factors, PrP expression level, and chosen experimental animal model. For example, oxidative stress and apoptotic pathways are a known component of AD pathogenesis and other protein-misfolding disorders. The cytokine profiles and mechanisms of neuronal death are less clear for prion-induced TSEs, but may also involve apoptotic pathways (Giese et al., 1995; Williams et al., 1997). The findings from this study cytokine variations possibly relevant to the physiologic role of PrP^{C} and unveil a distinctive neuropathological profile that may provide clues about early stage neuroinvasion and disease progression.

BioPlex

A repeated measures statistical analysis revealed significant differences for both IL-2 (p-value <0.0001) and Il-5 (p-value 0.0016) over time for the longitudinal cytokine data (Table 2, A-D). However, no significant difference was observed between treatment groups throughout the disease for these two cytokines, suggesting that either the TgA20 transgenic mouse model or over-expression of the prion protein resulted in continual expression of IL-2 and/or IL-5 in the study animals.

Interleukin-2 acts as a T cell growth factor in an autocrine manner to induce proliferation and activation of T lymphocytes. The consistent expression of IL-2 throughout the longitudinal study in both infected and uninfected mice is somewhat surprising, as the involvement of T cells in prion pathogenesis appears to be non-essential (Klein et al., 1997). Disease progression and incubation periods in prion-infected SCID mice, a strain devoid of functional B and T cells (Bosma et al., 1983) as well as FDCs (Szakal et al., 1990), show resistance to murine CJD through peripheral route of inoculation (Kitamoto et al., 1991).

Another hypothesis relating IL-2 expression to the TgA20 transgenic model involves the location of the insertional transgene for *Prnp*. Zabel et al. (2009) characterized the immune composition of lymphocytes in PrP^{C}-expressing transgenic models at 0- (PrP-/-), 1- (wild-type), 3-5 (Tg19), and 4-7- (TgA20) fold higher than wild-type and found an altered T lymphocyte phenotype in TgA20 over-expressing mice. Their TgA20s showed a lower number of αβ(+) T cells compared to γδ(+) T cells, reflected in overall lower numbers of CD4 and CD8 T cells. Despite an atypical T lymphocyte phenotype, the normal 2:1 ratio of CD4+:CD8+ T cells remained and T cell function was not compromised. It was suggested that this is due to the *Prnp* transgene insertion centrally within murine chromosome 17, a location correlated to a number of genes involved in T cell development (Fehling et al., 1995; Havelkova et al., 1999). TgA20 mice have reduced TCRα mRNA transcript and protein, which has been shown to induce expression of the high affinity IL-2α receptor (Kim & Leonard, 2002). Failure to up-regulate IL-2αR could cause increased compensatory expression of IL-2 that we observed for this mouse line.

Interleukin-2 is multifunctional and displays roles extending beyond T lymphocyte activation and proliferation. In fact, within the rat brain IL-2 is expressed, with the highest concentration of its binding sites localized to the hippocampal formation (Arujo et al., 1989; Lapchak & Hefti, 1991; Nieto-Sampedro & Chandy, 1987). Within the brain it is proposed that IL-2 contributes to elongation and branching of neurites and positively effects neuronal survival in a dose-dependent fashion (Awatsuji et al., 1993; Sarder, Saito, & Abe, 1993; Sarder et al., 1996; Shimojo et al., 1993). This effect was blocked when anti-IL-2 antibodies were added (Awatsuji et al., 1993). Although IL-2R may be most concentrated in the hippocampal formation, Awatsuji et al. (1993) proved IL-2 to have similar effects on cortical, septal, and striatal neurons. Importantly, IL-2 appears to be involved in spatial learning and memory, as well as hippocampal neurodevelopment (Petitto et al., 1999).

It is clear that IL-2 plays a crucial role in neuronal survivability and neurite elongation and branching, promoting spatial learning and memory. However, the current findings from this study demonstrate consistent IL-2 expression in both NBH- and RML- inoculated TgA20s, perhaps suggesting a correlation between IL-2 and the over-expressed PrP^{C} protein. It has been documented that PrP-/- mice show impaired T cell activation and proliferation in response to mitogens, compared with PrP +/+ mice (Bainbridge & Walker, 2005). PrP^{C} has also been implicated in human lymphocyte activation (Cashman et al., 1990). T lymphocytes may not be essential for prion disease progression, but *Prnp* -/- mice inoculated with rα-PrP or rβ-PrP exhibited proliferation of T cells and appear to recognize the same epitope (Khalili-Shirazi et al., 2005). It was mentioned that the observed proliferation was weak, however, because PrP expression plays a role in T cell activation it could be that proliferation was dampened in the

knockout model. PrP^C is significantly upregulated on the surface of T cells stimulated with concanavalin-A, while PrP-/- mice display a reduction in PrP^C upregulation, further supporting the idea that PrP^C participates in T cell activation (Mabbott et al., 1997). This group also observed the importance of the GPI anchor of the prion protein in this process. Ingram et al. (2009) found that activated T cells in PrP-/- mice displayed a significant reduction in Th1, Th2, and Th17 cytokine expression levels, although others such as TNF-a and IL-9 were unchanged. It could be that the opposite is true in this study, and the over-expression of PrP^C in TgA20s altered T lymphocyte phenotype, as well as increased cytokine expression for IL-5 and/or IL-2.

Interleukin-5 expression showed a significant variation over time (p-value 0.0016), as well as between genders (p-value 0.0021) (Table 2, C & D), perhaps suggesting a role for IL-5 in sex-related differences in prion pathogenesis. Figure 4 from the current study shows terminal clinical illness and morbidity scores warranting euthanasia in RML-infected female mice prior to onset of apparent clinical symptoms in any of the male RML-infected mice. Within the literature, reports of IL-5 acting independently are extremely limited, as it is usually co-expressed with IL-4 in a Th2 immune response to allergens and parasites. Within a prion disease model, a Th2 immune response in PrP-/- mice inoculated with rα-PrP showed IL-5 and IL-10 expression, whereas inoculation of rβ-PrP induced a Th1 response shown by IFN-γ (Kahlili-Shirazi et al., 2005). More importantly, IL-5 is involved in B-cell growth and proliferation (Takatsu, K., 1998) and may have a relevant function in the induction of nerve growth factor (NGF) synthesis/secretion in astrocytes (Awatsuji et al., 1993)—the former possibly involved in B cell stimulation of FDCs, an immune cell under significant investigation for its proposed role in prion protein propagation within the LRS prior to neuroinvasion (Fraser et al., 1989; Fraser et al., 1996; Fraser & Farquhar, 1987).

FDCs play a key role in stimulation and viability of memory B cells through antigen presentation on the cell surface via CR21/CR35, in contrast to internalized antigens that are processed for T cell activation (van Nierop & de Groot, 2002). Within the scope of prion disease, FDCs express the prion protein at high levels compared to other immune cells and are an essential component of peripheral prion propagation (Brown et al., 1999, McBride et al., 1992). PrP^C has been shown to co-localize with FDCs in lymph node germinal centers (Kitamoto et al., 1991; McBride et al, 1992; Muramoto et al, 1992) and accumulation of the abnormal prion protein is diminished in the spleens of mice lacking functional FDCs (Montrasio et al., 2000). Normal maturation of FDCs is dependent upon normal functioning B lymphocytes, but interestingly PrP^C expression is only required on FDCs to sustain peripheral prion replication and initiate neuroinvasion (Klein et al, 1998; Montrasio et al, 2001). B lymphocytes provide TNF-α and lymphotoxins (LTα and LTβ) as required signals for FDC development and maintenance within lymph node germinal centers and splenic white pulp (Alimzhanov et al., 1997; Koni et al., 1997; Matsumoto et al., 1997; Montrasio, 2000). This is supported by the fact that down regulation of the LTβ-R reduces prion pathogenesis (Mabbott et al., 2000; Mabbott et al., 2003; Montrasio et al., 2000) and FDCs in an autoimmune, chronic-inflammatory disease state resulted in prion detection and replication in atypical organs where PrP-expressing FDCs were found, such as the kidney, pancreas, and liver (Heikenwalder et al., 2005). Prinz et al. (2002) demonstrated the necessity of B cell follicles for successful FDC-associated prion replication, and later, that KO of the CCR5 chemokine placed FDCs in closer proximity to arterioles and nerves, resulting in accelerated prion neuroinvasion in WT and CCR5-/- mice (Prinz et al., 2003). B cells were also found to comprise the majority of prion-bearing cells within lymph nodes early after IP infection with prions, suggesting an important role in intranodal prion trafficking to FDCs (Michel et al., 2013). Therefore, B lymphocytes are crucial players in

peripheral prion replication (Klein et al., 1997) through interdependence with FDCs, and altered B cell or FDC development/function can affect prion pathogenesis (Brown et al., 1999; Fraser et al., 1996; O'Rourke et al., 1994; Prinz et al., 2002; Prinz et al., 2003).

While it has been shown that IL-4 and IL-5 induce the synthesis and secretion of NGF, this did not have any positive effect on neuronal survivability (Awatsuji et al., 1993). NGF has many functions pertaining to neurons within the CNS, but one function that may be pertinent to prion-induced disease is the induction of B cell growth and differentiation (Otten, Ehrhard, & Peck, 1989). This same group also identified the presence of functional NGF receptors on B and T lymphocytes. Adding to this idea is the finding that T cell-derived B cell growth factors (i.e. cytokines produced by T cells that stimulate B cell growth) induce astrocytic proliferation and GFAP expression (Benveniste et al., 1989) in response to cytokines IL-1 (Otten et al., 1989) and IL-6 (Frei et al., 1989) and possibly others. This is likely through NF-κB activation from cytokine signal transduction. Interestingly, NGF may be expressed following activation of certain T-helper subtypes (Ehrhard et al., 1993), and it has been shown that NGF stimulates expression of IL-2R, and vice versa (Brodie & Gelfand, 1992). If PrP^{C} overexpression in TgA20s is responsible for constant IL-2 and IL-5 expression, positive signals sent to B and T cells directly from the above cytokine signaling pathways and indirectly through NGF expression may result in up-regulation of PrP^{C} in the immune cell compartment (Mabbott et al., 1997; Wion et al., 1988) and over stimulation of FDCs, promoting prion propagation. PrP^{C}-mediated cytokine-induction could potentially be activating NF- κB as well as up-regulating NGF, but whether the overall effect of this activation is anti-apoptotic (Mattson & Camandola, 2001) or cytotoxic through p75 signaling and generation of NO (Chiarini et al., 2005) is unknown. The fact that this transgenic model shows

expedited disease in the presence of scrapie prions suggests that possibly these cell signaling pathways are contributing to neurodegeneration.

Flow Cytometry

There are mixed reports about the level of PrP^C-overexpression in the TgA20 mouse model (Fischer et al., 1996; Zabel et al., 2009) and as to whether this level of overexpression is observed equally in brain and lymphoid compartments. Flow cytometry of spleens and brains from TgA20 male and female mice revealed a 20-fold increase of PrP^C expression in the brain over what was observed in the spleens of these mice (Figure 13). While this finding contradicts PrP^C expression patterns reported by others (Glatzel & Aguzzi, 2000), we hypothesize that peripheral cytokine levels may have been influenced by PrP^C-expression in the periphery of TgA20s more similar to that of wild-type mice. If this is true, then a decreased inflammatory state in early stages of disease in the LRS may have affected overall prion pathogenesis, including neuroinvasion and neurodegeneration, contributing to the atypical cytokine profile observed.

Histopathology

Prion diseases have a complex diagnosis, involving clinical signs, sensitive and time-consuming lab assays (western blot and protein-misfolding cyclic amplification, PMCA) of contaminated tissues or fomites, immunohistochemical detection of insoluble, partially PK resistant prion protein deposits—both ante mortem and post mortem via lymphoid biopsy, or brain IHC/H&E, respectively—or combinations of these. Unfortunately no in-house or field rapid detection assay

exists with a high efficacy for ante mortem diagnosis. Neurohistopathology is useful for detection of the prion protein within brain tissue and to visualize neuronal vacuolation and spongiosis. Attempts to classify clinical and histological characteristics of IHC and other special stain-uptake patterns in human CJD have been published (Budka et al., 1995; Parchi et al., 1999) but are complicated by many different disease manifestations (Gambetti et al., 2003; Kong et al., 2004; Monari et al., 1994). Similarly, in experimental prion models, disease characteristics are skewed by the genetics of the animal model, transgenes, type and strain of prion inoculum, number of serial passages within endogenous/exogenous host, dose, and inoculation site/route. For example, murine scrapie strain ME7 inoculated intracerebrally into C57BL and VM/Dk mice showed PrP accumulation within the hippocampus as the first indicator of neurodegenerative disease (Jeffrey et al., 2001), whereas infection with 87V murine scrapie caused vacuolation primarily concentrated to the brainstem (Jeffrey et al., 1997).

The findings in this study showed minimal vacuolation and PrP^{Sc}-deposition in the region of the caudal medulla of terminally ill, RML-infected TgA20s. IHC staining for PrP^{Sc} in RML-infected animals was in the region of hypothalamus near the 3rd ventricle and in the cerebellar peduncle (Figure 15). The most prominent finding supporting "hallmark" characteristics of prion-induced neuropathology was (+)GFAP staining in brain regions coinciding with PrP^{Sc} deposition and at a considerably higher intensity than in NBH TgA20s, but the extent of overall astrogliosis throughout other regions of the brain was low (Figure 16, A-D).

The presence of PK-resistant scrapie prions in the brain homogenates of RML-infected mice were confirmed by Western blot (Figure 5, A & B), and the presence or absence of clinical disease warranting terminal morbidity scores in RML- or NBH- infected animals, respectively, was documented on video and uploaded to the laboratory's private YouTube library (see appendix for URL).

Other prion researchers have documented cases of atypical histopathology in various disease models, with similar findings of low PrP^{res} concentration, vacuolation and/or astrocytosis (Hegde et al., 1998; Hsiao et al., 1994; Jeffrey et al., 2001, Lasmezas et al., 1996; Lasmezas et al., 1997; Sisó et al., 2002). Furthermore, a number of papers exist supporting our observed lesion profile, involving the cerebellum, brainstem, and/or spinal cord in both natural (Parchi et al., 1999; Wood & Done, 1992) and experimental (Baringer et al., 1983; Glatzel & Aguzzi, 2000; Sisó et al., 2002; Tamgüney et al., 2009) prion disease models. However, there are different theories as to why this observation occurs.

It is difficult to characterize the differences in disease caused by an agent that is a misfolded host-encoded protein, lacking nucleic acids. While many researchers have recognized prion "strains" by variations in clinical signs, incubation period, neuropathology, and deposition patterns of PrP^{Sc} within host tissues, it is generally accepted that these variations are caused by differences in host genetics of *Prnp* and the biochemical conformation of PrP^{Sc} (Bessen & Marsh, 1994; Prusiner, 1998; Telling et al., 1996). Neuropathological profile can also be modified by route of infection, as inoculation-induced trauma from IC injection generated hippocampal plaques in a murine

scrapie model but are reduced or absent following IP inoculation (Bruce & Fraser, 1981). Modification of the prion protein itself can also alter neuropathological phenotype, as shown by cerebellar and brainstem deposits of amyloid-like plaques in mice not expressing the GPI anchor of PrP (Chesebro et al., 2005).

Moreover, it is anticipated that these observations are providing clues about the timeline and mechanisms underlying prion pathogenesis. Focalized areas of neuropathology perhaps caught earlier in the progression of disease could provide insightful information about early neuropathological events preceding neuronal death but capable of causing terminal illness. Yun et al. observed the progression of lesion profiles in RML-infected C57BL/6J mice throughout multiple time points during disease. Specifically, his group witnessed lesions within the cervical spinal cord at 105dpi, in the brainstem at 123dpi, and then a more disseminated disease profile in 142dpi terminally-ill mice. They also measured mRNA of heme oxygenase-1 (HO-1), as a maker of oxidative stress, and stained for GFAP and synaptophysin, a pre-synaptic vesicle membrane protein marker of synaptic loss (Honer, 2003). They found a progressive increase in HO-1 mRNA corresponding with later time points and advanced disease, an increase in GFAP over the course of time points sampled, and a significant decrease in synaptophysin expression. This study, and others, indicated an increased state of oxidative stress and evidence of synaptic loss as disease progressed (Johnston et al., 1997; Schipper, 2004; Yun et al., 2006). When considering the anatomy of the nervous system and the path of other neurotropic diseases (not disseminated to the brain through circulation), it makes sense that prions would result in a neuropathological lesion profile starting with peripheral nerves, ascend the spinal cord, affect brainstem and cerebellum then progress in a caudal to rostral fashion. This theory, however, would not take into account

prions that takes other routes for neuroinvasion, such as through circulation or olfactory epithelium.

What is most interesting is how minimally-extensive apparent neuropathology was within clinical, terminally-ill mice infected with prions. Cases of prion-induced neuropathologies exist with both clinical symptoms in the absence of apparent disease—down to the histological level—as well as with evidence of significant PrP^{res} deposition without fatal and/or transmissible disease (Piccardo et al., 2007). We believe that minimal neuropathology as evidenced by histological IHC/H&E staining and moderate but focal astrogliosis may have contributed to the overt lack of cytokine and chemokine expression within brain homogenates of infected mice. These findings, in addition to the considerations mentioned above, suggest that we do not have a good understanding of the cellular and signaling pathways that are resulting in apparent clinical disease. Clearly, it is warranted to further investigate synaptic loss and other potential mechanisms that might disrupt normal neuronal function prior to manifestation of histological and gross findings that are suggestive of disease

CHAPTER 2:

PRO-INFLAMMATORY CYTOKINES AND MECHANISMS OF NEURONAL DEATH

As extracellular signaling proteins involved in cell proliferation and differentiation, cytokines are useful for identifying the immune cellular players involved in prion pathogenesis. Certain cytokines have been proposed to play a direct role in neurodegeneration through activation of the transcription factor NADPH oxidase (NOX) (Griffin & Barger, 2010; Mrak & Griffin, 2005). Activation of NOX results in the production of reactive oxygen species (ROS) and may contribute to neuronal death and cognitive decline (Ansari & Scheff, 2011; Barth et al., 2009; Bruce-Keller et al., 2011). Interestingly, it has been shown that Aβ present in AD patients may activate the same NOX pathway as pro-inflammatory cytokines IL-1B, TNF-a, and IL-6 (Chiarini et al., 2005; Walsh et al., 2014). As mentioned previously, both PrP^C-dependent signaling pathways and PrP106-126 can upregulate pro-inflammatory cytokine gene expression and iNOS (Lu et al., 2012; Sonati et al., 2013). By blocking the interaction between Aβ and its co-receptor, PrP^C, long-term potentiation and Aβ-induced cognitive deficits were prevented in an AD mouse model (Barry et al., 2011; Chung et al., 2010).

Cofilin-actin rods are modified, space-occupying actin filaments within neuronal axons that interfere with vesicle transport and contribute to Aβ-induced synaptic loss (Bamburg et al., 2010; Cichon et al., 2012; Davis et al., 2009; Maloney et al., 2005; Minamide et al., 2000). A protein called RanBP9 is involved in cofilin activation, generation of ROS, and is also required in the Aβ-induced apoptotic pathway (Roh et al., 2013). The biochemical environment necessary for rod

formation requires both dephosphorylation of cofilin and the presence of ROS to create disulfide-linked cofilin dimers (Bernstein, 2012). Therefore, the neuroinflammation resulting from gliosis, which is present early on in TSEs and other neurodegenerative diseases, supports the formation of potentially neurotoxic rods. Conversely, rods may positively impact neuronal viability by blocking cofilin's involvement in apoptotic pathways when it becomes completely oxidized (Bernstein et al., 2006).

Longitudinal cytokine analysis of TgA20s over-expressing murine PrP^{C} showed consistent expression of IL-2 and IL-5 in both scrapie-infected and NBH control mice. We attributed this to downstream effects associated with *Prnp* transgene insertion and/or over-expression of the prion protein itself. This transgenic model shortens incubation periods by expediting prion disease progression. One would hypothesize that prion-induced pathology would be increased in a disease model where the prion protein is over-expressed. However, we observed minimal vacuolation or spongiosis, and diagnosis of prion infection was made based off outward signs of terminal illness, PrP^{Sc} detection via Western blot, IHC staining in the caudal medulla and surrounding the third ventricle, and an increase in distribution and intensity of GFAP stain uptake in in RML-infected mice.

These findings support the idea that cognitive decline and clinical disease during prion infection are a result of neuronal dysfunction (i.e. synaptic loss) prior to histologic evidence of neuronal loss. Both of these cytokines have indirect implications in immune-mediated peripheral prion replication (Alimzhanov et al., 1997; Koni et al., 1997; Matsumoto et al., 1997; Montrasio, 2000) as well as NGF synthesis/secretion (Awatsuji et al., 1993; Brodie & Gelfand, 1992; Ehrhard et al.,

1993; Otten, Ehrhard, & Peck, 1989). Additionally, NGF appears to promote B cell growth and differentiation (Otten, Ehrhard, & Peck, 1989), is produced by specific T-helper subtypes (Ehrhard et al., 1993) and cooperatively stimulates expression of IL-2R on T lymphocytes (Brodie & Gelfand, 1992). This suggests some sort of feedback loop mechanism resulting in NF-κB activation and production of ROS through NOX expression and, ultimately, the production of cofilin-actin rods and synaptic loss.

The presence of cytokines in neuronal cell culture was analyzed to confirm that Aβ was activating NOX-induced generation of ROS independent of cytokine signal transduction (Walsh et al., 2014). Aβ can stimulate the production of pro-inflammatory cytokines (Griffin & Barger, 2010), and it is known that cytokine profiles can vary widely between individuals affected by AD (Sudduth et al., 2013). It appears that both Aβ and pro-inflammatory cytokines may be inducing the production of ROS in cells of the central nervous system, through a similar pathway but independent of each other. Both Aβ and TNF-a can induce rod formation through a PrP^{C}-dependent pathway, and importantly, overexpression of PrP^{C} itself is sufficient to induce rod formation (Walsh et al., 2014). It may be that increased density of GPI-linked PrP^{C} expression concentrated at lipid rafts within the cell membrane is influencing redox-signaling resulting in synaptic damage (Bate and Williams, 2012; Brown & London, 1998), as lipid rafts are crucial players in synaptic development and maintenance (Mauch et al., 2001; Willmann et al., 2006). Mice lacking the GPI anchor of PrP^{C} fail to develop clinical disease regardless of significant deposition of infectious PrP^{Sc} (Chesebro et al., 2005).

We now know that oxidative stress plays a role early on in many neurodegenerative disorders (Keller et al., 2005). In getting at the molecular signaling pathways that could be influencing protein-misfolding diseases, it is relevant to investigate endogenous as well as exogenous molecules/compounds. Dietary and environmental constituents such as ursolic acid (UA) and the micronutrients copper (Cu), manganese (Mn), magnesium (Mg), and iron (Fe) are the recent and current focus of many investigators studying neurodegeneration. UA is derived from the skin of many fruits and plants—blueberries, cranberries, basil, and rosemary, to name a few—and has many proposed health benefits (Ikeda et al., 2008; Kim et al., 2011; Kunkel et al., 2012; Prasad et al., 2012; Zhou et al., 2013). Briefly, UA has been shown to inhibit rod formation in neurons stimulated by both Aβ and pro-cytokines, specifically, TNF-α (Barth et al., 2012; Walsh et al., 2014), and attenuate cognitive deficits (Mortiboys et al., 2013; Wang et al., 2011; Wu et al., 2013).

The role of micronutrients is more complex. Copper binds to PrP^{C} with high affinity on octapeptide repeats within the N-terminal region, inducing conformational changes (Brown et al., 1997a; Hornshaw et al., 1995; Stöckel et al., 1998; Whittal et al., 2000; You et al., 2012), and may possibly increase infectivity of PrP^{Sc} (Sigurdsson et al., 2003). The uptake of Cu into cells appears to involve cellular PrP (Brown, 1999; Pauly & Harris, 1998) as wild-type mice have higher membrane-bound Cu than *Prnp*$^{-/-}$ mice within the CNS where Cu is abundant (Brown et al., 1997a). The brains of CJD patients are reported to be deficient in Cu (Wong et al., 2003) as well as mice infected with scrapie, with the lowest levels corresponding with onset of clinical disease (Thackray et al., 2002; Wong et al., 2001). Mn has been shown to competitively bind with Cu on PrP^{C} octapeptide domains (Brown et al., 2000). Copper may not be essential for PrP → PrP^{Sc} conversion, but its levels within the CNS throughout disease may play a role in signaling, synaptic

loss, and/or oxidative damage (Collinge et al., 1994; Vassallo & Herms, 2003). Decreased copper binding and/or knockout of PrP^{C} has been correlated with diminished neuronal integrity and increased susceptibility to oxidative stress when infected with PrP^{Sc} (Brown et al., 1997b; Brown & Besinger, 1998; Miranda et al., 2000; Rachidi et al., 2003; Wong et al., 2000). Conversely, Cu^{+} and Fe^{2+} are known to generate ROS via Fenton-like or Haber-Weiss physiologic reactions (Butterfield & Stadtman, 1997; Halliwell & Gutteridge, 1990) and experimentally when stimulated by Aβ (Huang et al., 1999). It may be that distinct levels of micronutrients, as well as expression of amyloid/fibril-forming peptides and their precursors, may dictate the outcome of the particular disease state (Huang et al. 2004; Kralovicova et al., 2009; Multhaup et al., 1998; Opazo et al., 2000; Opazo et al., 2003; Ruiz et al., 1999, Sigurdsson et al., 2003).

In order to investigate the potential effects of metal cations on CWD prevalence and pathogenesis, water and soil were analyzed from CWD-endemic and non-endemic areas to quantitate individual concentrations of Cu, Mg, Mn, and Fe, as well as their associated ratios. Initial sampling by Nichols et al. (in process of submission) revealed high Mg ratios [Mg/Cu, Mg/Mn, and Mg/Fe] present in the water of CWD-negative areas, with Mg/Cu having the highest significance and thus receiving the most emphasis within the study. Transgenic Tg12 mice expressing elk PrP^{C} were IC-inoculated with CWD-positive or -negative brain homogenate and were offered a customized diet lacking Mg and Cu (Harlan/Teklad), with different treatment groups receiving various Mg/Cu ratios supplemented in drinking water offered *ad lib*. It was discovered that mice fed the custom diet which received the highest Mg/Cu drinking water, and also contained the lowest concentration of Cu, lived significantly longer than mice in other treatment groups. Although, interestingly, the levels of Cu within the brains of CWD-positive and –negative mice within the same group did not

differ significantly, while Mg concentration was significantly increased in CWD-positive animals from this same group.

Differences in survival times between animals fed various ratios of Cu, Mg, Mn, and Fe, could be explained by metal cation effects on neuroinflammatory processes (Eikelenboom et al., 2002; Sigurdsson et al., 2003). In a murine scrapie model, experimental copper-chelation prolonged disease incubation period but simultaneously induced caspase-3—a pro-apoptotic factor—overexpression in the cerebellum, midbrain, hippocampus and frontal cortex of infected mice (Bolea et al., 2010). In this same study yet another pro-apoptotic factor, Bax, was expressed in the medulla where it co-localized with PrP^{Sc} deposition, however caspase-3 nor Bax significantly contributed to neuronal loss. Although, caspase-3 has also been reported within the cerebellum of patients with CJD (Puig & Ferrer, 2001).

To deduce whether or not pro-inflammatory mediators were present within the Tg12 cervidized elk mice, brain material was screened for a panel of chemokine and cytokine mRNAs using an RT-PCR, and protein quantitation was carried out using a Th1/Th2 cytokine multiplex assay. Some mice fed a high Cu diet showed alterations in mRNA transcripts for TNF-α and IFN-γ at terminal disease. To corroborate these results, it was determined that pro-inflammatory cytokines IL-1β, IFN-γ, and IL-18 were expressed in mice fed high [Cu], in addition to IL-2, IL-12p70, and IL-13. These results suggest that neuroinflammation may be occurring in CWD-infected mice exposed to high concentrations of Cu orally prior to and throughout disease.

REFERENCES

Aguzzi, A., & Weissmann, C. (1996). A suspicious signature. *Nature, 383*(6602), 666-667. doi: 10.1038/383666a0

Alimzhanov, M. B., Kuprash, D. V., Kosco-Vilbois, M. H., Luz, A., Turetskaya, R. L., Tarakhovsky, A., . . . Pfeffer, K. (1997). Abnormal development of secondary lymphoid tissues in lymphotoxin β-deficient mice. *Proceedings of the National Academy of Sciences, 94*(17), 9302-9307.

Ansari, M. A., & Scheff, S. W. (2011). NADPH-oxidase activation and cognition in Alzheimer disease progression. *Free Radical Biology and Medicine, 51*(1), 171-178.

Araujo, D. M., Lapchak, P. A., & Collier, B. (1989). Localization of interleukin-2 immunoreactivity and interleukin-2 receptors in the rat brain: interaction with the cholinergic system. *Brain research, 498*(2), 257-266.

Aucouturier, P., Carp, R. I., Carnaud, C., & Wisniewski, T. (2000). Prion diseases and the immune system. *Clinical Immunology, 96*(2), 79-85.

Aucouturier, P., Geissmann, F., Damotte, D., Saborio, G. P., Meeker, H. C., Kascsak, R., . . . Wisniewski, T. (2001). Infected splenic dendritic cells are sufficient for prion transmission to the CNS in mouse scrapie. *Journal of Clinical Investigation, 108*(5), 703.

Awatsuji, H., Furukawa, Y., Nakajima, M., Furukawa, S., & Hayashi, K. (1993). Interleukin-2 as a neurotrophic factor for supporting the survival of neurons cultured from various regions of fetal rat brain. *Journal of neuroscience research, 35*(3), 305-311.

Bacot, S. M., Lenz, P., Frazier-Jessen, M. R., & Feldman, G. M. (2003). Activation by prion peptide PrP106–126 induces a NF-κB-driven proinflammatory response in human monocyte-derived dendritic cells. *Journal of leukocyte biology, 74*(1), 118-125.

Bainbridge, J., & Walker, K. B. (2005). The normal cellular form of prion protein modulates T cell responses. *Immunology letters, 96*(1), 147-150.

Baker, C. A., Lu, Z. Y., Zaitsev, I., & Manuelidis, L. (1999). Microglial activation varies in different models of Creutzfeldt-Jakob disease. *Journal of Virology, 73*(6), 5089-5097.

Baldwin, M., Stahl, N., Hecker, R., Pan, K., Burlingame, A., & Prusiner, S. (1992). Glycosylinositol phospholipid anchors of prion proteins. *Prion Diseases of Humans and Animals*, 380-397.

Ballerini, C., Gourdain, P., Bachy, V., Blanchard, N., Levavasseur, E., Grégoire, S., . . . Carnaud, C. (2006). Functional implication of cellular prion protein in antigen-driven interactions between T cells and dendritic cells. *The Journal of Immunology, 176*(12), 7254-7262.

Bamburg, J., Bernstein, B., Davis, R., Flynn, K., Goldsbury, C., Jensen, J., . . . Pak, C. (2010). ADF/Cofilin-actin rods in neurodegenerative diseases. *Current Alzheimer Research, 7*(3), 241-250.

Baringer, J. R., Bowman, K. A., & Prusiner, S. B. (1983). Replication of the scrapie agent in hamster brain precedes neuronal vacuolation. *Journal of Neuropathology & Experimental Neurology, 42*(5), 539-547.

Barry, A. E., Klyubin, I., Mc Donald, J. M., Mably, A. J., Farrell, M. A., Scott, M., . . . Rowan, M. J. (2011). Alzheimer's disease brain-derived amyloid-β-mediated inhibition of LTP in vivo is prevented by immunotargeting cellular prion protein. *The Journal of Neuroscience, 31*(20), 7259-7263.

Barth, B. M., Gustafson, S. J., Hankins, J. L., Kaiser, J. M., Haakenson, J. K., Kester, M., & Kuhn, T. B. (2012). Ceramide kinase regulates TNFα-stimulated NADPH oxidase activity and eicosanoid biosynthesis in neuroblastoma cells. *Cellular signalling, 24*(6), 1126-1133.

Barth, K. R., Isabella, V. M., Wright, L. F., & Clark, V. L. (2009). Resistance to peroxynitrite in Neisseria gonorrhoeae. *Microbiology, 155*(8), 2532-2545.

Bartz, J. C., McKenzie, D. I., Bessen, R. A., Marsh, R. F., & Aiken, J. M. (1994). Transmissible mink encephalopathy species barrier effect between ferret and mink: PrP gene and protein analysis. *Journal of General Virology, 75*(11), 2947-2954.

Bate, C., & Williams, A. (2012). Neurodegeneration induced by clustering of sialylated glycosylphosphatidylinositols of prion proteins. *Journal of Biological Chemistry, 287*(11), 7935-7944.

Bauer, H., Willert, J., Koschorz, B., & Herrmann, B. G. (2005). The t complex–encoded GTPase-activating protein Tagap1 acts as a transmission ratio distorter in mice. *Nature genetics, 37*(9), 969-973.

Benveniste, E. N., Whitaker, J. N., Gibbs, D. A., Sparacio, S. M., & Butler, J. L. (1989). Human B cell growth factor enhances proliferation and glial fibrillary acidic protein gene expression in rat astrocytes. *International immunology, 1*(3), 219-228.

Berg, L. J. (1994). Insights into the role of the immune system in prion diseases. *Proceedings of the National Academy of Sciences of the United States of America, 91*(2), 429.

Beringue, V., Couvreur, P., & Dormont, D. (2002). Involvement of macrophages in the pathogenesis of transmissible spongiform encephalopathies. *Journal of Immunology Research, 9*(1), 19-27.

Beringue, V., Demoy, M., Lasmézas, C. I., Gouritin, B., Weingarten, C., Deslys, J. P., . . . Dormont, D. (2000). Role of spleen macrophages in the clearance of scrapie agent early in pathogenesis. *The Journal of pathology, 190*(4), 495-502.

Bernstein, B. W., Chen, H., Boyle, J. A., & Bamburg, J. R. (2006). Formation of actin-ADF/cofilin rods transiently retards decline of mitochondrial potential and ATP in stressed neurons. *American Journal of Physiology-Cell Physiology, 291*(5), C828-C839.

Bernstein, B. W., Shaw, A. E., Minamide, L. S., Pak, C. W., & Bamburg, J. R. (2012). Incorporation of cofilin into rods depends on disulfide intermolecular bonds: implications for actin regulation and neurodegenerative disease. *The Journal of Neuroscience, 32*(19), 6670-6681.

Bessen, R. A., & Marsh, R. F. (1994). Distinct PrP properties suggest the molecular basis of strain variation in transmissible mink encephalopathy. *Journal of Virology, 68*(12), 7859-7868.

Betmouni, S., Perry, V., & Gordon, J. (1996). Evidence for an early inflammatory response in the central nervous system of mice with scrapie. *Neuroscience, 74*(1), 1-5.

Billeter, M., Riek, R., Wider, G., Hornemann, S., Glockshuber, R., & Wüthrich, K. (1997). Prion protein NMR structure and species barrier for prion diseases. *Proceedings of the National Academy of Sciences, 94*(14), 7281-7285.

Blanquet-Grossard, F., Thielens, N. M., Vendrely, C., Jamin, M., & Arlaud, G. J. (2005). Complement protein C1q recognizes a conformationally modified form of the prion protein. *Biochemistry, 44*(11), 4349-4356.

Block, M. L., Zecca, L., & Hong, J.-S. (2007). Microglia-mediated neurotoxicity: uncovering the molecular mechanisms. *Nature Reviews Neuroscience, 8*(1), 57-69.

Blum-Degena, D., Müller, T., Kuhn, W., Gerlach, M., Przuntek, H., & Riederer, P. (1995). Interleukin-1β and interleukin-6 are elevated in the cerebrospinal fluid of Alzheimer's and de novo Parkinson's disease patients. *Neuroscience letters, 202*(1), 17-20.

Bogdan, C., Paik, J., Vodovotz, Y., & Nathan, C. (1992). Contrasting mechanisms for suppression of macrophage cytokine release by transforming growth factor-beta and interleukin-10. *Journal of Biological Chemistry, 267*(32), 23301-23308.

Bolea, R., Hortells, P., Martín-Burriel, I., Vargas, A., Ryffel, B., Monzon, M., & Badiola, J. (2010). Consequences of dietary manganese and copper imbalance on neuronal apoptosis in a murine model of scrapie. *Neuropathology and applied neurobiology, 36*(4), 300-311.

Bosma, G. C., Custer, R. P., & Bosma, M. J. (1983). A severe combined immunodeficiency mutation in the mouse. *Nature, 301*(5900), 527-530. doi: 10.1038/301527a0

Brodie, C., & Gelfand, E. (1992). Functional nerve growth factor receptors on human B lymphocytes. Interaction with IL-2. *The Journal of Immunology, 148*(11), 3492-3497.

Brown, D., & Besinger, A. (1998). Prion protein expression and superoxide dismutase activity. *Biochem. J, 334*, 423-429.

Brown, D., & London, E. (1998). Functions of lipid rafts in biological membranes. *Annual review of cell and developmental biology, 14*(1), 111-136.

Brown, D. R., Hafiz, F., Glasssmith, L. L., Wong, B. S., Jones, I. M., Clive, C., & Haswell, S. J. (2000). Consequences of manganese replacement of copper for prion protein function and proteinase resistance. *The EMBO journal, 19*(6), 1180-1186.

Brown, D. R., Qin, K., Herms, J. W., Madlung, A., Manson, J., Strome, R., . . . Schulz-Schaeffer, W. (1997a). The cellular prion protein binds copper in vivo. *Nature, 390*(6661), 684-687.

Brown, D. R., Schulz-Schaeffer, W. J., Schmidt, B., & Kretzschmar, H. A. (1997b). Prion protein-deficient cells show altered response to oxidative stress due to decreased SOD-1 activity. *Experimental neurology, 146*(1), 104-112.

Brown, K., Stewart, K., Ritchie, D., Mabbott, N., Williams, A., Fraser, H., . . . Bruce, M. (1999). Scrapie replication in lymphoid tissues depends on prion protein-expressing follicular dendritic cells. *Nature medicine, 5*(11), 1308-1312.

Bruce, M. E., & Fraser, H. (1981). Effect of route of infection on the frequency and distribution of cerebral amyloid plaques in scrapie mice. *Neuropathology and applied neurobiology, 7*(4), 289-298.

Bruce, M. E., Will, R., Ironside, J., McConnell, I., Drummond, D., Suttie, A., . . . Birkett, C. (1997). Transmissions to mice indicate that ‘new variant’CJD is caused by the BSE agent. *Nature, 389*(6650), 498-501.

Bruce-Keller, A. J., Gupta, S., Knight, A. G., Beckett, T. L., McMullen, J. M., Davis, P. R., . . . Keller, J. N. (2011). Cognitive impairment in humanized APP× PS1 mice is linked to Aβ 1–42 and NOX activation. *Neurobiology of disease, 44*(3), 317-326.

Budka, H. (2003). Neuropathology of prion diseases. *British medical bulletin, 66*(1), 121-130.

Budka, H., Aguzzi, A., Brown, P., Brucher, J. M., Bugiani, O., Gullotta, F., . . . Jellinger, K. (1995). Neuropathological diagnostic criteria for Creutzfeldt-Jakob disease (CJD) and other human spongiform encephalopathies (Prion diseases). *Brain Pathology, 5*(4), 459-466.

Büeler, H., Aguzzi, A., Sailer, A., Greiner, R.-A., Autenried, P., Aguet, M., & Weissmann, C. (1993). Mice devoid of PrP are resistant to scrapie. *Cell, 73*(7), 1339-1347.

Büeler, H., Fischer, M., Lang, Y., Bluethmann, H., Lipp, H.-P., DeArmond, S. J., . . . Weissmann, C. (1992). Normal development and behaviour of mice lacking the neuronal cell-surface PrP protein. *Nature, 356*(6370), 577-582. doi: 10.1038/356577a0

Butterfield, D. A., & Stadtman, E. R. (1997). Protein oxidation processes in aging brain. *Advances in Cell Aging and Gerontology, 2*, 161-191.

Campbell, I., Eddleston, M., Kemper, P., Oldstone, M., & Hobbs, M. (1994). Activation of cerebral cytokine gene expression and its correlation with onset of reactive astrocyte and acute-phase response gene expression in scrapie. *Journal of Virology, 68*(4), 2383-2387.

Cashman, N. R., Loertscher, R., Nalbantoglu, J., Shaw, I., Kascsak, R. J., Bolton, D. C., & Bendheim, P. E. (1990). Cellular isoform of the scrapie agent protein participates in lymphocyte activation. *Cell, 61*(1), 185-192.

Chandler, R. L. (1961). Encephalopathy in mice produced by inoculation with scrapie brain material. *The Lancet, 277*(7191), 1378-1379.

Chao, C. C., Hu, S., Ehrlich, L., & Peterson, P. K. (1995). Interleukin-1 and tumor necrosis factor-α synergistically mediate neurotoxicity: involvement of nitric oxide and of N-methyl-D-aspartate receptors. *Brain Behavior and Immunity, 9*(4), 355-365.

Chazot, G., Broussolle, E., Lapras, C., Blättler, T., Aguzzi, A., & Kopp, N. (1996). New variant of Creutzfeldt-Jakob disease in a 26-year-old French man. *The Lancet, 347*(9009), 1181.

Chesebro, B., Trifilo, M., Race, R., Meade-White, K., Teng, C., LaCasse, R., . . . Priola, S. (2005). Anchorless prion protein results in infectious amyloid disease without clinical scrapie. *Science, 308*(5727), 1435-1439.

Chiarini, A., Dal Pra, I., Whitfield, J., & Armato, U. (2005). The killing of neurons by beta-amyloid peptides, prions, and pro-inflammatory cytokines. *Italian journal of anatomy and embryology= Archivio italiano di anatomia ed embriologia, 111*(4), 221-246.

Chung, E., Ji, Y., Sun, Y., Kascsak, R. J., Kascsak, R. B., Mehta, P. D., . . . Wisniewski, T. (2010). Anti-PrPC monoclonal antibody infusion as a novel treatment for cognitive deficits in an Alzheimer's disease model mouse. *BMC neuroscience, 11*(1), 130.

Cichon, J., Sun, C., Chen, B., Jiang, M., Chen, X. A., Sun, Y., . . . Chen, G. (2012). Cofilin aggregation blocks intracellular trafficking and induces synaptic loss in hippocampal neurons. *Journal of Biological Chemistry, 287*(6), 3919-3929.

Clarke, M., & Kimberlin, R. (1984). Pathogenesis of mouse scrapie: distribution of agent in the pulp and stroma of infected spleens. *Veterinary microbiology, 9*(3), 215-225.

Collinge, J. (1997). Human prion diseases and bovine spongiform encephalopathy (BSE). *Human molecular genetics, 6*(10), 1699-1705.

Collinge, J., Sidle, K. C., Meads, J., Ironside, J., & Hill, A. F. (1996). Molecular analysis of prion strain variation and the aetiology of'new variant'CJD. *Nature, 383*, 685-690. doi: 10.1038/383685a0

Collinge, J., Whittington, M. A., Sidle, K. C., Smith, C. J., Palmer, M. S., Clarke, A. R., & Jefferys, J. G. (1994). Prion protein is necessary for normal synaptic function. *Nature, 370*(6487), 295-297. doi: 10.1038/370295a0

Cunningham, C., Boche, D., & Perry, V. (2002). Transforming growth factor β1, the dominant cytokine in murine prion disease: influence on inflammatory cytokine synthesis and alteration of vascular extracellular matrix. *Neuropathology and applied neurobiology, 28*(2), 107-119.

Davis, R. C., Maloney, M. T., Minamide, L. S., Flynn, K. C., Stonebraker, M. A., & Bamburg, J. R. (2009). Mapping cofilin-actin rods in stressed hippocampal slices and the role of cdc42 in amyloid-β-induced rods. *Journal of Alzheimer's Disease, 18*(1), 35-50.

DeArmond, S., Kretzschmar, H., McKinley, M., Barry, R., Meyer, R., Westaway, D., & Prusiner, S. (1986). Chemical and biological properties of the prion protein and its cellular isoform. *Journal of Neuropathology & Experimental Neurology, 45*(3), 329.

DeArmond, S. J., Kristensson, K., & Bowler, R. P. (1992). PrP Sc causes nerve cell death and stimulates astrocyte proliferation: a paradox. *Progress in brain research, 94*, 437-446.

DeJoia, C., Moreaux, B., O'Connell, K., & Bessen, R. A. (2006). Prion infection of oral and nasal mucosa. *Journal of Virology, 80*(9), 4546-4556.

Díaz-San Segundo, F., Salguero, F. J., de Ávila, A., Espinosa, J. C., Torres, J. M., & Brun, A. (2006). Distribution of the cellular prion protein (PrPC) in brains of livestock and domesticated species. *Acta neuropathologica, 112*(5), 587-595.

Dodelet, V. C., & Cashman, N. R. (1998). Prion protein expression in human leukocyte differentiation. *Blood, 91*(5), 1556-1561.

Doh-ura, K., Tateishi, J., Sasaki, H., Kitamoto, T., & Sakaki, Y. (1989). Pro→ Leu change at position 102 of prinon protein is the most common but not the sole mutation related to Gerstmann-Sträussler syndrome. *Biochemical and biophysical research communications, 163*(2), 974-979.

Donaldson, D., Kobayashi, A., Ohno, H., Yagita, H., Williams, I., & Mabbott, N. (2012). M cell-depletion blocks oral prion disease pathogenesis. *Mucosal immunology, 5*(2), 216-225.

Doran, M., & Larner, A. (2004). EEG findings in dementia with Lewy bodies causing diagnostic confusion with sporadic Creutzfeldt–Jakob disease. *European Journal of Neurology, 11*(12), 838-841.

Dürig, J., Giese, A., Schulz-Schaeffer, W., Rosenthal, C., Schmücker, U., Bieschke, J., . . . Kretzschmar, H. A. (2000). Differential constitutive and activation-dependent expression of prion protein in human peripheral blood leucocytes. *British journal of haematology, 108*(3), 488-495.

Ehrhard, P. B., Erb, P., Graumann, U., & Otten, U. (1993). Expression of nerve growth factor and nerve growth factor receptor tyrosine kinase Trk in activated CD4-positive T-cell clones. *Proceedings of the National Academy of Sciences, 90*(23), 10984-10988.

Eikelenboom, P., Bate, C., Van Gool, W., Hoozemans, J., Rozemuller, J., Veerhuis, R., & Williams, A. (2002). Neuroinflammation in Alzheimer's disease and prion disease. *Glia, 40*(2), 232-239.

Eikelenboom, P., Zhan, S.-S., van Gool, W. A., & Allsop, D. (1994). Inflammatory mechanisms in Alzheimer's disease. *Trends in pharmacological sciences, 15*(12), 447-450.

Fabrizi, C., Silei, V., Menegazzi, M., Salmona, M., Bugiani, O., Tagliavini, F., . . . Lauro, G. M. (2001). The stimulation of inducible nitric-oxide synthase by the prion protein fragment 106–126 in human microglia is tumor necrosis factor-α-dependent and involves p38 mitogen-activated protein kinase. *Journal of Biological Chemistry, 276*(28), 25692-25696.

Fehling, H. J., Krotkova, A., Saint-RufT, C., & von Boehmer, H. (1995). Crucial role of the pre-T-cell receptor a gene in development of. *Nature, 375*, 29.

Fischer, M., Rülicke, T., Raeber, A., Sailer, A., Moser, M., Oesch, B., . . . Weissmann, C. (1996). Prion protein (PrP) with amino-proximal deletions restoring susceptibility of PrP knockout mice to scrapie. *The EMBO journal, 15*(6), 1255.

Flechsig, E., & Weissmann, C. (2004). The role of PrP in health and disease. *Current molecular medicine, 4*(4), 337-353.

Fraser, H., Brown, K., Stewart, K., McConnell, I., McBride, P., & Williams, A. (1996). Replication of scrapie in spleens of SCID mice follows reconstitution with wild-type mouse bone marrow. *Journal of General Virology, 77*(8), 1935-1940.

Fraser, H., Bruce, M., Chree, A., Mcconnell, I., & Wells, G. (1988). Transmission of bovine spongiform encephalopathy to mice. *Veterinary Record*.

Fraser, H., Bruce, M., Chree, A., McConnell, I., & Wells, G. (1992). Transmission of bovine spongiform encephalopathy and scrapie to mice. *J Gen Virol, 73*(8), 1891-1897.

Fraser, H., & Farquhar, C. (1987). Ionising radiation has no influence on scrapie incubation period in mice. *Veterinary microbiology, 13*(3), 211-223.

Fraser, J. R., Halliday, W. G., Brown, D., Belichenko, P. V., & Jeffrey, M. (1996). Mechanisms of scrapie-induced neuronal cell death. *Transmissible subacute spongiform encephalopathies: prion diseases (Eds. L. Court and B. Dodet). Elsevier, Paris*, 107-112.

Frei, K., Malipiero, U. V., Leist, T. P., Zinkernagel, R. M., Schwab, M. E., & Fontana, A. (1989). On the cellular source and function of interleukin 6 produced in the central nervous system in viral diseases. *European journal of immunology, 19*(4), 689-694.

Gajdusek, D. C., & Science, A. A. f. t. A. o. (1977). Unconventional viruses and the origin and disappearance of kuru. 161-215.

Gambetti, P., Kong, Q., Zou, W., Parchi, P., & Chen, S. G. (2003). Sporadic and familial CJD: classification and characterisation. *British medical bulletin, 66*(1), 213-239.

Gellman, R., & Gibson, J. (1996). Role of microglia and host prion protein in neurotoxicity of a prion protein fragment. *Nature, 380*, 28.

Giese, A., Brown, D. R., Groschup, M. H., Feldmann, C., Haist, I., & Kretzschmar, H. A. (1998). Role of microglia in neuronal cell death in prion disease. *Brain Pathology, 8*(3), 449-457.

Giese, A., Groschup, M. H., Hess, B., & Kretzschmar, H. A. (1995). Neuronal cell death in scrapie-infected mice is due to apoptosis. *Brain Pathology, 5*(3), 213-221.

Glatzel, M., & Aguzzi, A. (2000). PrPC expression in the peripheral nervous system is a determinant of prion neuroinvasion. *Journal of General Virology, 81*(11), 2813-2821.

Goldfarb, L. G., Brown, P., Goldgaber, D., Asher, D. M., Rubenstein, R., Brown, W. T., . . . Gajdusek, D. C. (1990). Creutzfeldt-Jakob disease and kuru patients lack a mutation consistently found in the Gerstmann-Sträussler-Scheinker syndrome. *Experimental neurology, 108*(3), 247-250.

Goldfarb, L. G., Brown, P., McCombie, W. R., Goldgaber, D., Swergold, G. D., Wills, P. R., . . . Gajdusek, D. C. (1991). Transmissible familial Creutzfeldt-Jakob disease associated with five, seven, and eight extra octapeptide coding repeats in the PRNP gene. *Proceedings of the National Academy of Sciences, 88*(23), 10926-10930.

Griffin, W. S. T., & Barger, S. W. (2010). Neuroinflammatory Cytokines—The Common Thread in Alzheimer's Pathogenesis. *US neurology, 6*(2), 19.

Halliwell, B., & Gutteridge, J. M. (1990). The antioxidants of human extracellular fluids. *Archives of biochemistry and biophysics, 280*(1), 1-8.

Havelková, H., Kosařová, M., Krulová, M., Demant, P., & Lipoldová, M. (1999). T-cell proliferative response is controlled by loci Tria4 and Tria5 on mouse chromosomes 7 and 9. *Mammalian genome, 10*(7), 670-674.

Hegde, R. S., Mastrianni, J. A., Scott, M. R., DeFea, K. A., Tremblay, P., Torchia, M., . . . Lingappa, V. R. (1998). A transmembrane form of the prion protein in neurodegenerative disease. *Science, 279*(5352), 827-834.

Heikenwalder, M., Zeller, N., Seeger, H., Prinz, M., Klöhn, P.-C., Schwarz, P., . . . Aguzzi, A. (2005). Chronic lymphocytic inflammation specifies the organ tropism of prions. *Science, 307*(5712), 1107-1110.

Hill, A. F., Zeidler, M., Ironside, J., & Collinge, J. (1997). Diagnosis of new variant Creutzfeldt-Jakob disease by tonsil biopsy. *The Lancet, 349*(9045), 99-100.

Honer, W. G. (2003). Pathology of presynaptic proteins in Alzheimer's disease: more than simple loss of terminals. *Neurobiology of aging, 24*(8), 1047-1062.

Hornshaw, M., McDermott, J., & Candy, J. (1995). Copper binding to the N-terminal tandem repeat regions of mammalian and avian prion protein. *Biochemical and biophysical research communications, 207*(2), 621-629.

Hou, F., Sun, L., Zheng, H., Skaug, B., Jiang, Q.-X., & Chen, Z. J. (2011). MAVS forms functional prion-like aggregates to activate and propagate antiviral innate immune response. *Cell, 146*(3), 448-461.

Houston, F., Foster, J., Chong, A., Hunter, N., & Bostock, C. (2000). Transmission of BSE by blood transfusion in sheep. *The Lancet, 356*(9234), 999-1000.

Hsiao, K., Baker, H. F., Crow, T. J., Poulter, M., Owen, F., Terwilliger, J. D., . . . Prusiner, S. B. (1989). Linkage of a prion protein missense variant to Gerstmann-Sträussler syndrome. *Nature, 338*(6213), 342-345.

Hsiao, K., & Prusiner, S. B. (1990). Inherited human prion diseases. *Neurology, 40*(12), 1820-1820.

Hsiao, K. K., Groth, D., Scott, M., Yang, S.-L., Serban, H., Rapp, D., . . . Prusiner, S. B. (1994). Serial transmission in rodents of neurodegeneration from transgenic mice expressing mutant prion protein. *Proceedings of the National Academy of Sciences, 91*(19), 9126-9130.

Hsiao, K. K., Scott, M., Foster, D., Groth, D. F., Dearmond, S. J., & Prusiner, S. B. (1990). Spontaneous neurodegeneration in transgenic mice with mutant prion protein. *Science, 250*(4987), 1587-1590.

Huang, X., Atwood, C. S., Hartshorn, M. A., Multhaup, G., Goldstein, L. E., Scarpa, R. C., . . . Moir, R. D. (1999). The Aβ peptide of Alzheimer's disease directly produces hydrogen peroxide through metal ion reduction. *Biochemistry, 38*(24), 7609-7616.

Huang, X., Atwood, C. S., Moir, R. D., Hartshorn, M. A., Tanzi, R. E., & Bush, A. I. (2004). Trace metal contamination initiates the apparent auto-aggregation, amyloidosis, and oligomerization of Alzheimer's Aβ peptides. *JBIC Journal of Biological Inorganic Chemistry, 9*(8), 954-960.

Ikeda, Y., Murakami, A., & Ohigashi, H. (2008). Ursolic acid: An anti-and pro-inflammatory triterpenoid. *Molecular nutrition & food research, 52*(1), 26-42.

Ingram, R. J., Isaacs, J. D., Kaur, G., Lowther, D. E., Reynolds, C. J., Boyton, R. J., . .Altmann, D. M. (2009). A role of cellular prion protein in programming T-cell cytokine responses in disease. *The FASEB Journal, 23*(6), 1672-1684.

Ironside, J., Sutherland, K., Bell, J., McCardle, L., Barrie, C., Estebeiro, K., . . . Will, R. (1996). *A new variant of Creutzfeldt-Jakob disease: neuropathological and clinical features.* Paper presented at the Cold Spring Harbor symposia on quantitative biology.

Jeffrey, M., Goodsir, C., Bruce, M., McBride, P., & Fraser, J. (1997). In vivo toxicity of prion protein in murine scrapie: ultrastructural and immunogold studies. *Neuropathology and applied neurobiology, 23*(2), 93-101.

Jeffrey, M., Martin, S., Barr, J., Chong, A., & Fraser, J. (2001). Onset of accumulation of PrP res in murine ME7 scrapie in relation to pathological and PrP immunohistochemical changes. *Journal of comparative pathology, 124*(1), 20-28.

Jendroska, K., Heinzel, F., Torchia, M., Stowring, L., Kretzschmar, H., Kon, A., . . . DeArmond, S. (1991). Proteinase-resistant prion protein accumulation in Syrian hamster brain correlates with regional pathology and scrapie infectivity. *Neurology, 41*(9), 1482-1482.

Jiang, H., Burdick, D., Glabe, C. G., Cotman, C. W., & Tenner, A. J. (1994). beta-Amyloid activates complement by binding to a specific region of the collagen-like domain of the C1q A chain. *The Journal of Immunology, 152*(10), 5050-5059.

Johnston, A. R., Black, C., Fraser, J., & MacLeod, N. (1997). Scrapie infection alters the membrane and synaptic properties of mouse hippocampal CA1 pyramidal neurones. *The Journal of physiology, 500*(1), 1-15.

Keller, J., Schmitt, F., Scheff, S., Ding, Q., Chen, Q., Butterfield, D., & Markesbery, W. (2005). Evidence of increased oxidative damage in subjects with mild cognitive impairment. *Neurology, 64*(7), 1152-1156.

Khalili-Shirazi, A., Summers, L., Linehan, J., Mallinson, G., Anstee, D., Hawke, S., . . . Collinge, J. (2005). PrP glycoforms are associated in a strain-specific ratio in native PrPSc. *Journal of General Virology, 86*(9), 2635-2644.

Kiachopoulos, S., Heske, J., Tatzelt, J., & Winklhofer, K. F. (2004). Misfolding of the prion protein at the plasma membrane induces endocytosis, intracellular retention and degradation. *Traffic, 5*(6), 426-436.

Kim, H. P., & Leonard, W. J. (2002). The basis for TCR-mediated regulation of the IL-2 receptor α chain gene: role of widely separated regulatory elements. *The EMBO journal, 21*(12), 3051-3059.

Kim, H.-Y., Edsall, L., Garcia, M., & Zhang, H. (1999). The release of polyunsaturated fatty acids and their lipoxygenation in the brain *Lipoxygenases and their Metabolites* (pp. 75-85): Springer.

Kim, K. H., Seo, H. S., Choi, H. S., Choi, I., Shin, Y. C., & Ko, S.-G. (2011). Induction of apoptotic cell death by ursolic acid through mitochondrial death pathway and extrinsic death receptor pathway in MDA-MB-231 cells. *Archives of pharmacal research, 34*(8), 1363-1372.

Kincaid, A. E., & Bartz, J. C. (2007). The nasal cavity is a route for prion infection in hamsters. *Journal of Virology, 81*(9), 4482-4491.

Kitamoto, T., Muramoto, T., Mohri, S., Doh-Ura, K., & Tateishi, J. (1991). Abnormal isoform of prion protein accumulates in follicular dendritic cells in mice with Creutzfeldt-Jakob disease. *Journal of Virology, 65*(11), 6292-6295.

Klein, M. A., Frigg, R., Flechsig, E., Raeber, A. J., Kalinke, U., Bluethmann, H., . . . Aguzzi, A. (1997). A crucial role for B cells in neuroinvasive scrapie. *Nature, 390*(6661), 687-690.

Klein, M. A., Frigg, R., Raeber, A. J., Flechsig, E., Hegyi, I., Zinkernagel, R. M., . . . Aguzzi, A. (1998). PrP expression in B lymphocytes is not required for prion neuroinvasion. *Nature medicine, 4*(12), 1429-1433.

Klein, M. A., Kaeser, P. S., Schwarz, P., Weyd, H., Xenarios, I., Zinkernagel, R. M., . . . Walport, M. J. (2001). Complement facilitates early prion pathogenesis. *Nature medicine, 7*(4), 488-492.

Kobayashi, A., Parchi, P., Yamada, M., Brown, P., Saverioni, D., Matsuura, Y., . . . Kitamoto, T. (2015). Transmission properties of atypical Creutzfeldt-Jakob disease: a clue to disease etiology? *Journal of Virology*, JVI. 03183-03114.

Kong, Q., Surewicz, W. K., Petersen, R. B., Zou, W., Chen, S. G., Gambetti, P., . . . Montagna, P. (2004). 14 Inherited Prion Diseases. *Cold Spring Harbor Monograph Archive, 41*, 673-775.

Koni, P. A., Sacca, R., Lawton, P., Browning, J. L., Ruddle, N. H., & Flavell, R. A. (1997). Distinct roles in lymphoid organogenesis for lymphotoxins α and β revealed in lymphotoxin β–deficient mice. *Immunity, 6*(4), 491-500.

Krakauer, D. C., Paolo, M. d. A., & Pagel, M. (1998). Prion's progress: patterns and rates of molecular evolution in relation to spongiform disease. *Journal of molecular evolution, 47*(2), 133-145.

Kralovicova, S., Fontaine, S. N., Alderton, A., Alderman, J., Ragnarsdottir, K. V., Collins, S. J., & Brown, D. R. (2009). The effects of prion protein expression on metal metabolism. *Molecular and Cellular Neuroscience, 41*(2), 135-147.

Kunkel, S. D., Elmore, C. J., Bongers, K. S., Ebert, S. M., Fox, D. K., Dyle, M. C., . . . Adams, C. M. (2012). Ursolic acid increases skeletal muscle and brown fat and decreases diet-induced obesity, glucose intolerance and fatty liver disease. *PloS one, 7*(6), e39332.

Lapchak, P., & Hefti, F. (1991). Effect of recombinant human nerve growth factor on presynaptic cholinergic function in rat hippocampal slices following partial septohippocampal lesions: measures of [3 H] acetylcholine synthesis,[3 H] acetylcholine release and choline acetyltransferase activity. *Neuroscience, 42*(3), 639-649.

Lasmézas, C. I., Deslys, J.-P., Demaimay, R., Adjou, K. T., Hauw, J.-J., & Dormont, D. (1996). Strain specific and common pathogenic events in murine models of scrapie and bovine spongiform encephalopathy. *Journal of General Virology, 77*(7), 1601-1609.

Lasmézas, C. I., Deslys, J.-P., Robain, O., Jaegly, A., Beringue, V., Peyrin, J.-M., . . . Dormont, D. (1997). Transmission of the BSE agent to mice in the absence of detectable abnormal prion protein. *Science, 275*(5298), 402-404.

Lindholm, H., Meyer, Thoenen. (1987). Interleukin-1 regulates synthesis of nerve growth factor in non-neuronal cell of rat sciatic nerve. *Nature, 230*, 658-659. doi: 10.1038/330658a0

Llewelyn, C., Hewitt, P., Knight, R., Amar, K., Cousens, S., Mackenzie, J., & Will, R. (2004). Possible transmission of variant Creutzfeldt-Jakob disease by blood transfusion. *The Lancet, 363*(9407), 417-421.

Lodge, P. A., & Sriram, S. (1996). Regulation of microglial activation by TGF-beta, IL-10, and CSF-1. *Journal of leukocyte biology, 60*(4), 502-508.

Lu, B., Pang, P. T., & Woo, N. H. (2005). The yin and yang of neurotrophin action. *Nature Reviews Neuroscience, 6*(8), 603-614.

Lu, Y., Liu, A., Zhou, X., Kouadir, M., Zhao, W., Zhang, S., . . . Zhao, D. (2012). Prion peptide PrP106-126 induces inducible nitric oxide synthase and proinflammatory cytokine gene expression through the activation of NF-κB in macrophage cells. *DNA and cell biology, 31*(5), 833-838.

Lysek, D. A., Schorn, C., Nivon, L. G., Esteve-Moya, V., Christen, B., Calzolai, L., . . . Güntert, P. (2005). Prion protein NMR structures of cats, dogs, pigs, and sheep. *Proceedings of the National Academy of Sciences of the United States of America, 102*(3), 640-645.

Mabbott, N., Brown, K., Manson, J., & Bruce, M. (1997). T-lymphocyte activation and the cellular form of the prion protein. *Immunology, 92*(2), 161-165.

Mabbott, N. A., Mackay, F., Minns, F., & Bruce, M. E. (2000). Temporary inactivation of follicular dendritic cells delays neuroinvasion of scrapie. *Nature medicine, 6*(7), 719-720.

Mabbott, N. A., Young, J., McConnell, I., & Bruce, M. E. (2003). Follicular dendritic cell dedifferentiation by treatment with an inhibitor of the lymphotoxin pathway dramatically reduces scrapie susceptibility. *Journal of Virology, 77*(12), 6845-6854.

Mallucci, G., Dickinson, A., Linehan, J., Klöhn, P.-C., Brandner, S., & Collinge, J. (2003). Depleting neuronal PrP in prion infection prevents disease and reverses spongiosis. *Science, 302*(5646), 871-874.

Maloney, M. T., Minamide, L. S., Kinley, A. W., Boyle, J. A., & Bamburg, J. R. (2005). β-secretase-cleaved amyloid precursor protein accumulates at actin inclusions induced in neurons by stress or amyloid β: a feedforward mechanism for Alzheimer's disease. *The Journal of Neuroscience, 25*(49), 11313-11321.

Matsumoto, M., Fu, Y.-X., Molina, H., Huang, G., Kim, J., Thomas, D. A., . . . Chaplin, D. D. (1997). Distinct roles of lymphotoxin α and the type I tumor necrosis factor (TNF) receptor in the establishment of follicular dendritic cells from non–bone marrow–derived cells. *The Journal of experimental medicine, 186*(12).

Mattson, M. P., & Camandola, S. (2001). NF-κB in neuronal plasticity and neurodegenerative disorders. *Journal of Clinical Investigation, 107*(3), 247.

Mauch, D. H., Nägler, K., Schumacher, S., Göritz, C., Müller, E.-C., Otto, A., & Pfrieger, F. W. (2001). CNS synaptogenesis promoted by glia-derived cholesterol. *Science, 294*(5545), 1354-1357.

McBride, P. A., Eikelenboom, P., Kraal, G., Fraser, H., & Bruce, M. E. (1992). PrP protein is associated with follicular dendritic cells of spleens and lymph nodes in uninfected and scrapie-infected mice. *The Journal of pathology, 168*(4), 413-418.

McGeer, P. L., & McGeer, E. G. (1995). The inflammatory response system of brain: implications for therapy of Alzheimer and other neurodegenerative diseases. *Brain Research Reviews, 21*(2), 195-218.

Michel, B., Ferguson, A., Johnson, T., Bender, H., Meyerett-Reid, C., Pulford, B., . . . Telling, G. C. (2012). Genetic depletion of complement receptors CD21/35 prevents terminal prion disease in a mouse model of chronic wasting disease. *The Journal of Immunology, 189*(9), 4520-4527.

Michel, B., Ferguson, A., Johnson, T., Bender, H., Meyerett-Reid, C., Wyckoff, A. C., . . . Zabel, M. D. (2013). Complement protein C3 exacerbates prion disease in a mouse model of chronic wasting disease. *International immunology, 25*(12), 697-702.

Minamide, L. S., Striegl, A. M., Boyle, J. A., Meberg, P. J., & Bamburg, J. R. (2000). Neurodegenerative stimuli induce persistent ADF/cofilin–actin rods that disrupt distal neurite function. *Nature cell biology, 2*(9), 628-636.

Minghetti, L., & Levi, G. (1998). Microglia as effector cells in brain damage and repair: focus on prostanoids and nitric oxide. *Progress in neurobiology, 54*(1), 99-125.
Miranda, S., Opazo, C., Larrondo, L. F., Muñoz, F. J., Ruiz, F., Leighton, F., & Inestrosa, N. C. (2000). The role of oxidative stress in the toxicity induced by amyloid β-peptide in Alzheimer's disease. *Progress in neurobiology, 62*(6), 633-648.
Mitchell, D. A., Kirby, L., Paulin, S. M., Villiers, C. L., & Sim, R. B. (2007). Prion protein activates and fixes complement directly via the classical pathway: implications for the mechanism of scrapie agent propagation in lymphoid tissue. *Molecular immunology, 44*(11), 2997-3004.
Mogi, M., Harada, M., Kondo, T., Riederer, P., Inagaki, H., Minami, M., & Nagatsu, T. (1994). Interleukin-1β, interleukin-6, epidermal growth factor and transforming growth factor-α are elevated in the brain from parkinsonian patients. *Neuroscience letters, 180*(2), 147-150.
Mogi, M., Harada, M., Narabayashi, H., Inagaki, H., Minami, M., & Nagatsu, T. (1996). Interleukin (IL)-1β, IL-2, IL-4, IL-6 and transforming growth factor-α levels are elevated in ventricular cerebrospinal fluid in juvenile parkinsonism and Parkinson's disease. *Neuroscience letters, 211*(1), 13-16.
Monari, L., Chen, S. G., Brown, P., Parchi, P., Petersen, R. B., Mikol, J., . . . Ghetti, B. (1994). Fatal familial insomnia and familial Creutzfeldt-Jakob disease: different prion proteins determined by a DNA polymorphism. *Proceedings of the National Academy of Sciences, 91*(7), 2839-2842.
Montrasio, F., Cozzio, A., Flechsig, E., Rossi, D., Klein, M. A., Rülicke, T., . . . Aguzzi, A. (2001). B lymphocyte-restricted expression of prion protein does not enable prion replication in prion protein knockout mice. *Proceedings of the National Academy of Sciences, 98*(7), 4034-4037.
Montrasio, F., Frigg, R., Glatzel, M., Klein, M. A., Mackay, F., Aguzzi, A., & Weissmann, C. (2000). Impaired prion replication in spleens of mice lacking functional follicular dendritic cells. *Science, 288*(5469), 1257-1259.
Mortiboys, H., Aasly, J., & Bandmann, O. (2013). Ursocholanic acid rescues mitochondrial function in common forms of familial Parkinson's disease. *Brain, 136*(10), 3038-3050.
Mrak, R. E., & Griffin, W. S. T. (2005). Glia and their cytokines in progression of neurodegeneration. *Neurobiology of aging, 26*(3), 349-354.
Multhaup, G., Ruppert, T., Schlicksupp, A., Hesse, L., Bill, E., Pipkorn, R., . . . Beyreuther, K. (1998). Copper-binding amyloid precursor protein undergoes a site-specific fragmentation in the reduction of hydrogen peroxide. *Biochemistry, 37*(20), 7224-7230.
Muramoto, T., Kitamoto, T., Tateishi, J., & Goto, I. (1992). The sequential development of abnormal prion protein accumulation in mice with Creutzfeldt-Jakob disease. *The American journal of pathology, 140*(6), 1411.
Nagata, S. (1997). Apoptosis by death factor. *Cell, 88*(3), 355-365.
Naslavsky, N., Weigert, R., & Donaldson, J. G. (2004). Characterization of a nonclathrin endocytic pathway: membrane cargo and lipid requirements. *Molecular biology of the cell, 15*(8), 3542-3552.
Nieto-Sampedro, M., & Chandy, K. G. (1987). Interleukin-2-like activity in injured rat brain. *Neurochemical research, 12*(8), 723-727.

O'Rourke, K. I., Baszler, T. V., Miller, J. M., Spraker, T. R., Sadler-Riggleman, I., & Knowles, D. P. (1998). Monoclonal antibody F89/160.1. 5 defines a conserved epitope on the ruminant prion protein. *Journal of Clinical Microbiology, 36*(6), 1750-1755.

Opazo, C., Barría, M. I., Ruiz, F. H., & Inestrosa, N. C. (2003). Copper reduction by copper binding proteins and its relation to neurodegenerative diseases. *Biometals, 16*(1), 91-98.

Opazo, C., Ruiz, F. H., & Inestrosa, N. C. (2000). Amyloid-ß-peptide reduces copper (II) to copper (I) independent of its aggregation state. *Biological research, 33*(2), 125-131.

O'Rourke, K. I., Huff, T., Leathers, C., Robinson, M., & Gorham, J. (1994). SCID mouse spleen does not support scrapie agent replication.

Otten, U., Ehrhard, P., & Peck, R. (1989). Nerve growth factor induces growth and differentiation of human B lymphocytes. *Proceedings of the National Academy of Sciences, 86*(24), 10059-10063.

Owen, F., Lofthouse, R., Crow, T., Baker, H., Poulter, M., Collinge, J., . . . Prusiner, S. (1989). Insertion in prion protein gene in familial Creutzfeldt-Iakob disease. *The Lancet, 333*(8628), 51-52.

Palmer, M. S., Dryden, A. J., Hughes, J. T., & Collinge, J. (1991). Homozygous prion protein genotype predisposes to sporadic Creutzfeldt–Jakob disease. *Nature, 352*(6333), 340-342. doi: 10.1038/352340a0

Parchi, P., Giese, A., Capellari, S., Brown, P., Schulz-Schaeffer, W., Windl, O., . . . Piccardo, P. (1999). Classification of sporadic Creutzfeldt-Jakob disease based on molecular and phenotypic analysis of 300 subjects. *Annals of neurology, 46*(2), 224-233.

Pauly, P. C., & Harris, D. A. (1998). Copper stimulates endocytosis of the prion protein. *Journal of Biological Chemistry, 273*(50), 33107-33110.

Perera, W. S. S., & Hooper, N. M. (2001). Ablation of the metal ion-induced endocytosis of the prion protein by disease-associated mutation of the octarepeat region. *Current Biology, 11*(7), 519-523.

Petitto, J. M., McNamara, R. K., Gendreau, P. L., Huang, Z., & Jackson, A. J. (1999). Impaired learning and memory and altered hippocampal neurodevelopment resulting from interleukin-2 gene deletion. *Journal of neuroscience research, 56*(4), 441-446.

Piccardo, P., Manson, J. C., King, D., Ghetti, B., & Barron, R. M. (2007). Accumulation of prion protein in the brain that is not associated with transmissible disease. *Proceedings of the National Academy of Sciences, 104*(11), 4712-4717.

Porter, D. D., Porter, H. G., & Cox, N. A. (1973). Failure to demonstrate a humoral immune response to scrapie infection in mice. *The Journal of Immunology, 111*(5), 1407-1410.

Prasad, S., Yadav, V. R., Sung, B., Reuter, S., Kannappan, R., Deorukhkar, A., . . . Krishnan, S. (2012). Ursolic acid inhibits growth and metastasis of human colorectal cancer in an orthotopic nude mouse model by targeting multiple cell signaling pathways: chemosensitization with capecitabine. *Clinical Cancer Research, 18*(18), 4942-4953.

Prinz, M., Heikenwalder, M., Junt, T., Schwarz, P., Glatzel, M., Heppner, F. L., . . . Aguzzi, A. (2003). Positioning of follicular dendritic cells within the spleen controls prion neuroinvasion. *Nature, 425*(6961), 957-962.

Prinz, M., Montrasio, F., Klein, M. A., Schwarz, P., Priller, J., Odermatt, B., . . . Aguzzi, A. (2002). Lymph nodal prion replication and neuroinvasion in mice devoid of follicular dendritic cells. *Proceedings of the National Academy of Sciences, 99*(2), 919-924.

Prusiner, S. B. (1982). Novel proteinaceous infectious particles cause scrapie. *Science, 216*(4542), 136-144.

Prusiner, S. B. (1998). The priori diseases. *Brain Pathology, 8*(3), 499-513.
Prusiner, S. B., Groth, D., Serban, A., Koehler, R., Foster, D., Torchia, M., . . . DeArmond, S. J. (1993). Ablation of the prion protein (PrP) gene in mice prevents scrapie and facilitates production of anti-PrP antibodies. *Proceedings of the National Academy of Sciences, 90*(22), 10608-10612.
Puig, B., & Ferrer, I. (2001). Cell death signaling in the cerebellum in Creutzfeldt-Jakob disease. *Acta neuropathologica, 102*(3), 207-215.
Rachidi, W., Mangé, A., Senator, A., Guiraud, P., Riondel, J., Benboubetra, M., . . . Lehmann, S. (2003). Prion infection impairs copper binding of cultured cells. *Journal of Biological Chemistry, 278*(17), 14595-14598.
Roberson, E., Hesse, J., Rose, K., Slama, H., Johnson, J., Yaffe, K., . . . Kramer, J. (2005). Frontotemporal dementia progresses to death faster than Alzheimer disease. *Neurology, 65*(5), 719-725.
Rogers, M., Yehiely, F., Scott, M., & Prusiner, S. B. (1993). Conversion of truncated and elongated prion proteins into the scrapie isoform in cultured cells. *Proceedings of the National Academy of Sciences, 90*(8), 3182-3186.
Roh, S.-E., Woo, J. A., Lakshmana, M. K., Uhlar, C., Ankala, V., Boggess, T., . . . Kim, S. J. (2013). Mitochondrial dysfunction and calcium deregulation by the RanBP9-cofilin pathway. *The FASEB Journal, 27*(12), 4776-4789.
Roucou, X., & LeBlanc, A. C. (2005). Cellular prion protein neuroprotective function: implications in prion diseases. *Journal of molecular medicine, 83*(1), 3-11.
Ruiz, F. H., González, M., Bodini, M., Opazo, C., & Inestrosa, N. C. (1999). Cysteine 144 Is a Key Residue in the Copper Reduction by the β-Amyloid Precursor Protein. *Journal of neurochemistry, 73*(3), 1288-1292.
Sarder, M., Abe, K., Saito, H., & Nishiyama, N. (1996). Comparative effect of IL-2 and IL-6 on morphology of cultured hippocampal neurons from fetal rat brain. *Brain research, 715*(1), 9-16.
Sarder, M., Saito, H., & Abe, K. (1993). Interleukin-2 promotes survival and neurite extension of cultured neurons from fetal rat brain. *Brain research, 625*(2), 347-350.
Sasaki, A., Hirato, J., & Nakazato, Y. (1993). Immunohistochemical study of microglia in the Creutzfeldt-Jakob diseased brain. *Acta neuropathologica, 86*(4), 337-344.
Saunders, S. E., Bartelt-Hunt, S. L., & Bartz, J. C. (2012). Occurrence, transmission, and zoonotic potential of chronic wasting disease. *Emerg Infect Dis, 18*(3), 369-376.
Schätzl, H. M., Da Costa, M., Taylor, L., Cohen, F. E., & Prusiner, S. B. (1995). Prion protein gene variation among primates. *Journal of molecular biology, 245*(4), 362-374.
Schipper, H. M. (2004). Heme Oxygenase-1: Transducer of Pathological Brain Iron Sequestration under Oxidative Stress. *Annals of the New York Academy of Sciences, 1012*(1), 84-93.
Schultz, J., Schwarz, A., Neidhold, S., Burwinkel, M., Riemer, C., Simon, D., . . . Baier, M. (2004). Role of interleukin-1 in prion disease-associated astrocyte activation. *The American journal of pathology, 165*(2), 671-678.
Shimojo, M., Imai, Y., Nakajima, K., Mizushima, S., Uemura, A., & Kohsaka, S. (1993). Interleukin-2 enhances the viability of primary cultured rat neocortical neurons. *Neuroscience letters, 151*(2), 170-173.

Sigurdson, C. J., Heikenwalder, M., Manco, G., Barthel, M., Schwarz, P., Stecher, B., . . . MacPherson, A. J. (2009). Bacterial colitis increases susceptibility to oral prion disease. *Journal of Infectious Diseases, 199*(2), 243-252.

Sigurdsson, E. M., Brown, D. R., Alim, M. A., Scholtzova, H., Carp, R., Meeker, H. C., . . . Wisniewski, T. (2003). Copper chelation delays the onset of prion disease. *Journal of Biological Chemistry, 278*(47), 46199-46202.

Silveira, J. R. (2005). - The most infectious prion protein particles. *Nature, 437*(7056), 257-261. doi: 10.1038/nature03989

Sim, R. B., Kishore, U., Villiers, C. L., Marche, P. N., & Mitchell, D. A. (2007). C1q binding and complement activation by prions and amyloids. *Immunobiology, 212*(4), 355-362.

Siso, S., Puig, B., Varea, R., Vidal, E., Acin, C., Prinz, M., . . . Pumarola, M. (2002). Abnormal synaptic protein expression and cell death in murine scrapie. *Acta neuropathologica, 103*(6), 615-626.

Smith, C. A., Farrah, T., & Goodwin, R. G. (1994). The TNF receptor superfamily of cellular and viral proteins: activation, costimulation, and death. *Cell, 76*(6), 959-962.

Sonati, T., Reimann, R. R., Falsig, J., Baral, P. K., O'Connor, T., Hornemann, S., . . . Wieland, B. (2013). The toxicity of antiprion antibodies is mediated by the flexible tail of the prion protein. *Nature, 501*(7465), 102-106.

Stahl, N., Baldwin, M., Hecker, R., Pan, K.-M., Burlingame, A., & Prusiner, S. (1992). Glycosylinositol phospholipid anchors of the scrapie and cellular prion proteins contain sialic acid. *Biochemistry, 31*(21), 5043-5053.

Stöckel, J., Safar, J., Wallace, A. C., Cohen, F. E., & Prusiner, S. B. (1998). Prion protein selectively binds copper (II) ions. *Biochemistry, 37*(20), 7185-7193.

Sudduth, T. L., Schmitt, F. A., Nelson, P. T., & Wilcock, D. M. (2013). Neuroinflammatory phenotype in early Alzheimer's disease. *Neurobiology of aging, 34*(4), 1051-1059.

Szakal, A. K., Taylor, J. K., Smith, J. P., Kosco, M. H., Burton, G. F., & Tew, J. J. (1990). Kinetics of germinal center development in lymph nodes of young and aging immune mice. *The Anatomical Record, 227*(4), 475-485.

Takatsu, K. (1998). Interleukin 5 and B cell differentiation. *Cytokine & growth factor reviews, 9*(1), 25-35.

Tamgüney, G., Miller, M. W., Giles, K., Lemus, A., Glidden, D. V., DeArmond, S. J., & Prusiner, S. B. (2009). Transmission of scrapie and sheep-passaged bovine spongiform encephalopathy prions to transgenic mice expressing elk prion protein. *Journal of General Virology, 90*(4), 1035-1047.

Telling, G. C., Parchi, P., DeArmond, S. J., Cortelli, P., Montagna, P., Gabizon, R., . . . Prusiner, S. B. (1996). Evidence for the conformation of the pathologic isoform of the prion protein enciphering and propagating prion diversity. *Science, 274*(5295), 2079-2082.

Thackray, A., Knight, R., Haswell, S., Bujdoso, R., & Brown, D. (2002). Metal imbalance and compromised antioxidant function are early changes in prion disease. *Biochem. J, 362*, 253-258.

Tobler, I., Gaus, S., Deboer, T., Achermann, P., Fischer, M., Rülicke, T., . . . Manson, J. (1996). Altered circadian activity rhythms and sleep in mice devoid of prion protein. *Nature, 380*(6575), 639-642. doi: 10.1038/380639a0

Tribouillard-Tanvier, D., Striebel, J. F., Peterson, K. E., & Chesebro, B. (2009). Analysis of protein levels of 24 cytokines in scrapie agent-infected brain and glial cell cultures from mice differing in prion protein expression levels. *Journal of Virology, 83*(21), 11244-11253.

Tsivgoulis, G., Bonakis, A., Papathanasiou, M. A., Chondrogianni, M., Papageorgiou, S. G., Voumvourakis, K., & Stefanis, L. (2014). Magnetic resonance imaging reveals Creutzfeldt–Jakob disease in a patient with apparent dementia with Lewy bodies. *Journal of the neurological sciences, 340*(1), 130-132.

van Nierop, K., & de Groot, C. (2002). *Human follicular dendritic cells: function, origin and development.* Paper presented at the Seminars in immunology.

Vassallo, N., & Herms, J. (2003). Cellular prion protein function in copper homeostasis and redox signalling at the synapse. *Journal of neurochemistry, 86*(3), 538-544.

Walsh, D. T., Betmouni, S., & Perry, V. H. (2001). Absence of Detectable IL-1β Production in Murine Prion Disease: A Model of Chronic Neurodegeneration. *Journal of Neuropathology & Experimental Neurology, 60*(2), 173-182.

Walsh, K. P., Kuhn, T. B., & Bamburg, J. R. (2014). Cellular prion protein: a co-receptor mediating neuronal cofilin-actin rod formation induced by β-amyloid and proinflammatory cytokines. *Prion* (just-accepted), 00-00.

Walsh, K. P., Minamide, L. S., Kane, S. J., Shaw, A. E., Brown, D. R., Pulford, B., . . . Bamburg, J. R. (2014). Amyloid-β and proinflammatory cytokines utilize a prion protein-dependent pathway to activate NADPH oxidase and induce cofilin-actin rods in hippocampal neurons. *PloS one, 9*(4), e95995.

Wang, Y.-J., Lu, J., Wu, D.-m., Zheng, Z.-h., Zheng, Y.-L., Wang, X.-h., . . . Zhang, Z.-f. (2011). Ursolic acid attenuates lipopolysaccharide-induced cognitive deficits in mouse brain through suppressing p38/NF-κB mediated inflammatory pathways. *Neurobiology of learning and memory, 96*(2), 156-165.

Wathne, G. J., & Mabbott, N. A. (2012). The diverse roles of mononuclear phagocytes in prion disease pathogenesis. *Prion, 6*(2), 124-133.

Weissmann, C., Fischer, M., Raeber, A., Büeler, H., Sailer, A., Shmerling, D., . . . Aguzzi, A. (1996). *The role of PrP in pathogenesis of experimental scrapie.* Paper presented at the Cold Spring Harbor Symposia on Quantitative Biology.

Westergard, L., Christensen, H. M., & Harris, D. A. (2007). The cellular prion protein (PrP C): its physiological function and role in disease. *Biochimica et Biophysica Acta (BBA)-Molecular Basis of Disease, 1772*(6), 629-644.

Whittal, R. M., Ball, H. L., Cohen, F. E., Burlingame, A. L., Prusiner, S. B., & Baldwin, M. A. (2000). Copper binding to octarepeat peptides of the prion protein monitored by mass spectrometry. *Protein Science, 9*(2), 332-343.

Williams, A., Lawson, L., Perry, V., & Fraser, H. (1994). Characterization of the microglial response in murine scrapie. *Neuropathology and applied neurobiology, 20*(1), 47-55.

Williams, A., Lucassen, P., Ritchie, D., & Bruce, M. (1997). PrP deposition, microglial activation, and neuronal apoptosis in murine scrapie. *Experimental neurology, 144*(2), 433-438.

Willmann, R., Pun, S., Stallmach, L., Sadasivam, G., Santos, A. F., Caroni, P., & Fuhrer, C. (2006). Cholesterol and lipid microdomains stabilize the postsynapse at the neuromuscular junction. *The EMBO journal, 25*(17), 4050-4060.

Wion, D., Le Bert, M., & Brachet, P. (1988). Messenger RNAs of β-amyloid precursor protein and prion protein are regulated by nerve growth factor in PC12 cells. *International journal of developmental neuroscience, 6*(4), 387-393.

Wong, B. S., Brown, D. R., Pan, T., Whiteman, M., Liu, T., Bu, X., . . . Rubenstein, R. (2001). Oxidative impairment in scrapie-infected mice is associated with brain metals perturbations and altered antioxidant activities. *Journal of neurochemistry, 79*(3), 689-698.

Wong, B.-S., Li, R., Sassoon, J., Kang, S.-C., Liu, T., Pan, T., . . . Sy, M.-S. (2003). Mapping the antigenicity of copper-treated cellular prion protein with the scrapie isoform. *Cellular and Molecular Life Sciences CMLS, 60*(6), 1224-1234.

Wong, B.-S., Pan, T., Liu, T., Li, R., Petersen, R. B., Jones, I. M., . . . Sy, M.-S. (2000). Prion disease: A loss of antioxidant function? *Biochemical and biophysical research communications, 275*(2), 249-252.

Wood, J., & Done, S. (1992). Natural scrapie in goats: neuropathology. *The Veterinary record, 131*(5), 93-96.

Wu, D.-m., Lu, J., Zhang, Y.-q., Zheng, Y.-l., Hu, B., Cheng, W., . . . Li, M.-q. (2013). Ursolic acid improves domoic acid-induced cognitive deficits in mice. *Toxicology and applied pharmacology, 271*(2), 127-136.

You, H., Tsutsui, S., Hameed, S., Kannanayakal, T. J., Chen, L., Xia, P., . . . Zamponi, G. W. (2012). Aβ neurotoxicity depends on interactions between copper ions, prion protein, and N-methyl-D-aspartate receptors. *Proceedings of the National Academy of Sciences, 109*(5), 1737-1742.

Yun, S.-W., Gerlach, M., Riederer, P., & Klein, M. A. (2006). Oxidative stress in the brain at early preclinical stages of mouse scrapie. *Experimental neurology, 201*(1), 90-98.

Zabel, M., Greenwood, C., Thackray, A. M., Pulford, B., Rens, W., & Bujdoso, R. (2009). Perturbation of T-cell development by insertional mutation of a PrP transgene. *Immunology, 127*(2), 226-236.

Zabel, M. D., Heikenwalder, M., Prinz, M., Arrighi, I., Schwarz, P., Kranich, J., . . . Tedder, T. F. (2007). Stromal complement receptor CD21/35 facilitates lymphoid prion colonization and pathogenesis. *The Journal of Immunology, 179*(9), 6144-6152.

Zeidler, M., Stewart, G., Barraclough, C., Bateman, D., Bates, D., Burn, D., . . . Hawkins, S. (1997). New variant Creutzfeldt-Jakob disease: neurological features and diagnostic tests. *The Lancet, 350*(9082), 903-907.

Zhang, T., He, Y.-M., Wang, J.-S., Shen, J., Xing, Y.-Y., & Xi, T. (2011). Ursolic acid induces HL60 monocytic differentiation and upregulates C/EBPβ expression by ERK pathway activation. *Anti-cancer drugs, 22*(2), 158-165.

Zhou, L., Ding, Y., Chen, W., Zhang, P., Chen, Y., & Lv, X. (2013). The in vitro study of ursolic acid and oleanolic acid inhibiting cariogenic microorganisms as well as biofilm. *Oral diseases, 19*(5), 494-500.

Zhou, X., Xu, G., & Zhao, D. (2008). In vitro effect of prion peptide PrP 106–126 on mouse macrophages: Possible role of macrophages in transport and proliferation for prion protein. *Microbial pathogenesis, 44*(2), 129-134.

APPENDIX

Supplementary Material

TgA20 Bioassay—YouTube Videos of Study Animals Sacrificed

https://www.youtube.com/playlist?list=PLX3zsHGI0Yf0q5tko_MXLNsywtDbbIj_A

Bioplex Cytokine Array

Table 1—Supplementary (sA & sB): TgA20 Cytokine Mega Table
Mega table showing cytokine expression in TgA20 mice from the longitudinal cytokine study. Cytokine levels are shown in tables that are separated by treatment group, and by serum cytokine analysis (table 2A) or brain-homogenate cytokine analysis (table 2B). LPS-induced positive control mice are shown at the top of each table as a positive control. Expression of any analyte (within detectable limit of the standard curve) is shown by a colored cell background corresponding with the color of the analyte listed at the top of each table. Samples that were below detection limit (OOR<) are shown with a white background and defined as half of the lowest detectable limit (LDL) as determined by the lowest point on the standard curve for each analyte. **(sA)** Serum cytokine levels broken down by individual animals for each treatment group, then by dpi. **(sB)** Cytokine expression in brain homogenate of TgA20s, with RML groups pooled by gender for 40, 60, and 80dpi.

Table 1(sA): Cytokine Mega Table - Serum

					Cytokine Data (Serum)										
Animal ID	TX Grp	M/F	DPI	GM-CSF	IFN-γ	IL-1β	IL-2	IL-4	IL-5	IL-6	IL-12p70	IL-13	IL-18	TNF-α	IL-10
141158	LPS	M	n/a	0.2	0.05	0.115	0.09	0.12	10.15	8.46	0.17	0.22	3.315	7.09	0.145
140726	LPS	F	n/a	0.2	0.88	2.36	0.09	0.12	29.69	160.17	5.93	0.22	64.51	29.41	19.04
133157-1	NBH	M	0	0.28	0.15	0.14	0.14	0.15	0.3	5.52	0.3	0.29	4.015	0.44	ND
			1	0.29	0.155	0.145	0.13	0.15	0.305	0.59	0.305	0.285	3.3	0.46	0.145
			20	0.29	0.155	0.145	22.91	0.15	0.305	0.59	0.305	0.285	3.3	0.46	0.145
			40	0.205	0.045	0.115	11.41	0.12	0.22	0.44	0.17	0.23	3.51	0.32	0.29
			60	0.205	0.045	0.115	12.44	0.12	0.22	0.44	0.17	0.23	3.51	0.32	0.29
			80	0.205	0.04	0.115	12.14	0.12	0.21	0.425	0.17	0.22	3.58	0.32	0.165
			Term	0.205	0.04	0.115	0.085	0.12	0.21	0.425	0.17	0.22	3.58	0.32	0.165
133157-2	NBH	M	0	0.28	0.15	0.14	0.14	0.15	0.3	0.58	0.3	0.29	4.015	0.44	ND
			1	0.29	0.155	0.145	7.64	0.15	0.305	0.59	0.305	0.285	3.3	0.46	0.145
			20	0.29	0.155	0.145	20.9	0.15	0.305	0.59	0.305	0.285	3.3	0.46	0.145
			40	0.205	0.045	0.115	4.67	0.12	4.23	0.44	0.17	0.23	3.51	3.82	0.29
			60	0.205	0.045	0.115	4.8	0.12	0.22	0.44	0.17	0.23	3.51	0.32	0.29
			80	0.205	0.04	0.115	17.98	0.12	2.95	0.425	0.17	0.22	3.58	0.32	0.165
			Term	0.205	0.91	0.115	0.085	0.12	4.59	0.425	0.17	0.22	55.5	0.32	0.165
133157-3	NBH	M	0	0.28	0.15	0.14	0.14	0.15	0.3	0.58	0.3	0.29	16.05	0.44	ND
			1	0.29	0.155	0.145	9.54	0.15	0.305	0.59	0.305	0.285	39.6	0.46	0.145
			20	0.29	0.155	0.145	51.16	0.15	0.305	0.59	0.305	0.285	140.37	0.46	0.145
			40	0.205	0.045	0.115	21.45	0.12	4.23	0.44	0.17	0.23	98.37	0.32	0.29
			60	0.205	0.045	0.115	12.44	0.12	0.22	0.44	0.17	0.23	3.51	0.32	0.29
			80	0.205	0.04	0.115	20.29	0.12	0.21	0.425	0.17	0.22	3.58	0.32	0.165
133157-4	NBH	M	0	0.28	0.15	0.14	0.14	0.15	0.3	0.58	0.3	0.29	4.015	0.44	ND
			1	0.29	0.155	0.145	12.61	0.15	22.79	0.59	0.305	0.285	3.3	0.46	0.145
			20	0.29	0.155	0.145	41.41	0.15	4.24	0.59	0.305	0.285	3.3	0.46	0.145
			40	0.205	0.045	0.115	21.93	0.12	9.26	0.44	0.17	0.23	66.94	0.32	0.29
			60	0.205	0.045	0.115	1.19	0.12	3.83	0.44	0.17	0.23	3.51	0.32	0.29
133157-5	NBH	M	0	0.28	0.15	0.14	0.14	0.15	0.3	7.65	0.3	0.29	23.63	0.44	ND
			1	0.29	0.155	0.145	0.13	0.15	0.305	0.59	0.305	0.285	3.3	0.46	0.145
			20	0.29	0.155	0.145	0.13	0.15	0.305	0.59	0.305	0.285	3.3	0.46	0.145
			40	0.205	0.045	0.115	0.09	0.12	8.49	10.77	0.17	0.23	3.51	0.32	0.29

						Cytokine Data (Serum)								
Animal ID	TX Grp	M/F	DPI	GM-CSF	IFN-ϒ	IL-1β	IL-2	IL-4	IL-5	IL-6	IL-12p70	IL-13	IL-18	TNF-α	IL-10
141158	LPS	M	n/a	0.2	0.05	0.115	0.09	0.12	10.15	8.46	0.17	0.22	3.315	7.09	0.145
140726	LPS	F	n/a	0.2	0.88	2.36	0.09	0.12	29.69	160.17	5.93	0.22	64.51	29.41	19.04
133158-1	NBH	F	0	0.28	0.15	0.14	0.14	0.15	0.3	0.58	0.3	0.29	4.015	0.44	ND
			1	0.29	0.155	0.145	0.13	0.15	0.305	0.59	0.305	0.285	3.3	0.46	0.145
			20	0.29	0.155	0.145	14.35	0.15	4.09	0.59	0.305	0.285	3.3	0.46	0.145
			40	0.205	0.045	0.115	2.61	0.12	5.11	0.44	0.17	0.23	3.51	0.32	0.29
			60	0.205	0.045	0.115	0.09	0.12	7.53	0.44	0.17	0.23	3.51	0.32	0.29
			80	0.205	0.04	0.115	8.21	0.12	0.21	0.425	0.17	0.22	3.58	0.32	0.165
			Term	0.205	0.04	0.115	0.085	0.12	2.85	0.425	0.17	0.22	3.58	0.32	0.165
133158-3	NBH	F	0	0.28	0.15	0.14	0.14	0.15	3.62	0.58	0.3	0.29	4.015	0.44	ND
			1	0.29	0.155	0.145	7.94	0.15	12.8	0.59	0.305	0.285	39.6	0.46	0.145
			20	0.29	0.155	0.145	8.68	0.15	3.94	0.59	0.305	0.285	39.6	0.46	0.145
			40	0.205	0.045	0.115	3.16	0.12	6.76	0.44	0.17	0.23	3.51	0.32	0.29
			60	0.205	0.045	0.115	2.8	0.12	3.64	0.44	0.17	0.23	3.51	0.32	0.29
			80	0.205	0.04	0.115	7.52	0.12	3.57	0.425	0.17	0.22	3.58	0.32	0.165
			Term	0.205	0.04	0.115	0.085	0.12	3.47	0.425	0.17	0.22	3.58	0.32	0.165
133158-5	NBH	F	0	0.28	0.15	0.14	0.14	0.15	3.54	0.58	0.3	0.29	25.36	0.44	ND
			1	0.29	0.155	0.145	18.36	0.15	3.94	0.59	0.305	0.285	62.15	0.46	0.145
			20	0.29	0.155	0.145	47.1	0.15	5.42	0.59	0.305	0.285	3.3	0.46	0.145
			40	0.205	0.045	0.115	22.17	0.12	3.83	0.44	0.17	0.23	3.51	0.32	0.29
			60	0.205	0.045	0.115	23.62	0.12	0.22	0.44	0.17	0.23	3.51	0.32	0.29
			80	0.205	0.04	0.115	23.5	0.12	0.21	0.425	0.17	0.22	3.58	0.32	0.165
136540-1	NBH	F	0	0.18	0.045	0.11	10.6	0.12	2.78	0.445	0.175	0.215	117.39	0.315	0.155
			1	0.18	0.045	0.11	0.08	0.12	27.97	0.445	0.175	0.215	2.885	0.315	0.155
			20	0.18	0.045	0.11	0.08	0.12	3.34	0.445	0.175	0.215	2.885	0.315	0.155
			40	0.18	0.045	0.11	0.08	0.12	5.24	46.32	0.175	0.215	94.54	0.315	0.155
136540-2	NBH	F	0	0.18	0.045	0.11	16.55	0.12	7.19	0.445	0.175	0.215	2.885	0.315	0.155
			1	0.18	1.83	0.11	23.88	0.12	11.06	0.445	0.175	0.215	2.885	3.8	0.155
			20	0.18	0.045	0.11	36.97	0.12	29.18	0.445	0.175	0.215	2.885	0.315	0.155
			40	0.18	0.045	0.11	26.18	0.12	27.2	0.445	0.175	0.215	2.885	0.315	0.155
			60	0.2	0.05	0.115	31.49	0.12	17.33	0.44	0.17	0.22	60.68	0.32	0.145

						Cytokine Data (Serum)									
Animal ID	TX Grp	M/F	DPI	GM-CSF	IFN-ϒ	IL-1β	IL-2	IL-4	IL-5	IL-6	IL-12p70	IL-13	IL-18	TNF-α	IL-10
141158	LPS	M	n/a	0.2	0.05	0.115	0.09	0.12	10.15	8.46	0.17	0.22	3.315	7.09	0.145
140726	LPS	F	n/a	0.2	0.88	2.36	0.09	0.12	29.69	160.17	5.93	0.22	64.51	29.41	19.04
133707-1	RML	M	0	0.28	0.15	0.14	0.14	0.15	0.3	0.58	0.3	0.29	4.015	0.44	ND
			1	0.29	0.155	0.145	27.21	0.15	0.305	0.59	0.305	0.285	122.17	0.46	0.145
			20	0.29	0.155	0.145	34.32	0.15	0.305	0.59	0.305	0.285	81.66	0.46	0.145
			40	0.205	0.045	0.115	21.78	0.12	0.22	0.44	0.17	0.23	72.04	0.32	0.29
			60	0.205	0.045	0.115	27.02	0.12	5.79	0.44	0.17	0.23	56.35	0.32	0.29
			80	0.205	0.04	0.115	30.42	0.12	0.21	0.425	0.17	0.22	3.58	0.32	0.165
133707-2	RML	M	0	0.28	0.15	0.14	4.48	0.15	0.3	0.58	0.3	0.29	4.015	0.44	ND
			1	0.29	0.155	0.145	31.12	0.15	8.6	0.59	0.305	0.285	74.12	0.46	0.145
			20	0.29	0.155	0.145	38.81	0.15	0.305	0.59	0.305	0.285	66.24	0.46	0.145
			40	0.205	0.045	0.115	13.94	0.12	2.64	0.44	0.17	0.23	72.04	0.32	0.29
			60	0.205	0.045	0.115	12.84	0.12	4.91	0.44	0.17	0.23	74.54	0.32	0.29
			80	0.205	0.04	0.115	5.88	0.12	2.74	0.425	0.17	0.22	84.43	0.32	0.165
133707-4	RML	M	0	0.28	0.15	0.14	0.14	0.15	0.3	0.58	0.3	0.29	4.015	0.44	ND
			1	0.29	0.155	0.145	0.13	0.15	3.94	0.59	0.305	0.285	3.3	0.46	0.145
			20	0.29	0.155	0.145	40.47	0.15	5.13	0.59	0.305	0.285	157.65	0.46	0.145
			40	0.205	0.045	0.115	18.54	0.12	4.03	0.44	0.17	0.23	81.91	0.32	0.29
			60	0.205	0.04	0.115	4.98	0.12	2.53	0.425	0.17	0.22	100.63	0.32	0.165
134097-1	RML	M	0	0.28	0.15	0.14	1.56	0.15	0.3	0.58	0.3	0.29	4.015	0.44	ND
			1	0.29	0.155	0.145	28.62	0.15	0.305	0.59	0.305	0.285	197.8	0.46	0.145
			20	0.29	0.155	0.145	56.51	0.15	0.305	0.59	0.305	0.285	95.94	0.46	0.145
			40	0.205	0.045	0.115	37.92	0.12	0.22	15.07	0.17	0.23	122.65	0.32	0.29
			60	0.205	0.04	0.115	25.42	0.12	0.21	0.425	0.17	0.22	82.05	0.32	0.165
134097-2	RML	M	0	0.28	0.15	0.14	0.14	0.15	0.3	0.58	0.3	0.29	4.015	0.44	ND
			1	0.29	0.155	0.145	8.68	0.15	0.305	0.59	0.305	0.285	3.3	0.46	0.145
			20	0.29	0.155	0.145	2.22	0.15	0.305	0.59	0.305	0.285	3.3	0.46	0.145
			40	0.205	0.045	0.115	3.52	0.12	0.22	0.44	0.17	0.23	3.51	0.32	0.29
			60	0.205	0.04	0.115	3.19	0.12	0.21	0.425	0.17	0.22	3.58	0.32	0.165
			80	0.205	0.04	0.115	5.05	0.12	0.21	0.425	0.17	0.22	3.58	0.32	0.165
			Term	0.205	0.04	0.115	0.085	0.12	0.21	0.425	0.17	0.22	3.58	0.32	0.165

						Cytokine Data (Serum)								
Animal ID	TX Grp	M/F	DPI	GM-CSF	IFN-ϒ	IL-1β	IL-2	IL-4	IL-5	IL-6	IL-12p70	IL-13	IL-18	TNF-α	IL-10
141158	LPS	M	n/a	0.2	0.05	0.115	0.09	0.12	10.15	8.46	0.17	0.22	3.315	7.09	0.145
140726	LPS	F	n/a	0.2	0.88	2.36	0.09	0.12	29.69	160.17	5.93	0.22	64.51	29.41	19.04
134097-3	RML	M	0	0.28	0.15	0.14	0.14	0.15	0.3	0.58	0.3	0.29	4.015	0.44	ND
			1	0.29	0.155	0.145	0.13	0.15	0.305	0.59	0.305	0.285	3.3	0.46	0.145
			20	0.29	0.155	0.145	0.13	0.15	0.305	0.59	0.305	0.285	3.3	0.46	0.145
			40	0.205	0.045	0.115	0.09	0.12	2.64	0.44	0.17	0.23	3.51	0.32	0.29
			60	0.205	0.79	0.115	0.085	0.12	0.21	0.425	0.17	0.22	3.58	0.32	0.165
			80	0.205	0.04	0.115	0.085	0.12	0.21	0.425	0.17	0.22	3.58	0.32	0.165
			Term	0.205	0.04	0.115	0.085	0.12	0.21	0.425	0.17	0.22	3.58	0.32	0.165
134097-4	RML	M	0	0.28	0.15	0.14	0.72	0.15	0.3	0.58	0.3	0.29	4.015	0.44	ND
			1	0.29	0.155	0.145	6.31	0.15	0.305	0.59	0.305	0.285	3.3	0.46	0.145
			20	0.29	0.155	0.145	21.63	0.15	0.305	0.59	0.305	0.285	3.3	0.46	0.145
			40	0.205	0.045	0.115	19.29	0.12	0.22	0.44	0.17	0.23	3.51	0.32	0.29
			60	0.205	0.04	0.115	16.55	0.12	0.21	0.425	0.17	0.22	3.58	0.32	0.165
			80	0.205	0.04	0.115	13.93	0.12	0.21	0.425	0.17	0.22	3.58	0.32	0.165
			Term	0.205	0.04	0.115	0.085	0.12	0.21	0.425	0.17	0.22	3.58	0.32	0.165
136539-1	RML	M	0	0.18	0.045	0.11	0.08	0.12	0.21	0.445	0.175	0.215	2.885	0.315	0.155
			1	0.18	0.045	0.11	0.08	0.12	4.44	0.445	0.175	0.215	2.885	0.315	0.155
			20	0.18	0.045	0.11	11.69	0.12	2.49	0.445	0.175	0.215	2.885	0.315	0.155
			40	0.18	0.045	0.11	3.29	0.12	3.62	0.445	0.175	0.215	2.885	0.315	0.155
			60	0.2	0.05	0.115	7.24	0.12	5.77	0.44	0.17	0.22	56.75	0.32	0.145
			80	0.2	0.05	0.115	8.89	0.12	4.76	0.44	0.17	0.22	30.19	0.32	0.145
			Term	4.08	0.05	2.04	3.61	0.12	4.76	0.44	0.17	0.22	102.32	0.32	0.145
136539-2	RML	M	0	0.18	0.045	0.11	1.9	0.12	3.06	0.445	0.175	0.215	2.885	0.315	0.155
			1	0.18	0.045	0.11	7.83	0.12	3.06	0.445	0.175	0.215	2.885	0.315	0.155
			20	0.18	0.045	0.11	8.67	0.12	0.21	0.445	0.175	0.215	2.885	0.315	0.155
			40	0.18	0.045	0.11	3.52	0.12	0.21	0.445	0.175	0.215	2.885	0.315	0.155
136539-3	RML	M	0	0.18	0.045	0.11	41.03	0.12	6.55	0.445	0.175	0.215	79.39	0.315	0.155
			1	0.18	0.045	0.11	17.59	0.12	0.21	0.445	0.175	0.215	2.885	0.315	0.155
			20	0.18	0.045	0.11	36.28	0.12	3.89	0.445	0.175	0.215	49.63	0.315	0.155
			40	0.18	0.045	0.11	23	0.12	0.21	0.445	0.175	0.215	34.64	0.315	0.155

						Cytokine Data (Serum)									
Animal ID	TX Grp	M/F	DPI	GM-CSF	IFN-ϒ	IL-1β	IL-2	IL-4	IL-5	IL-6	IL-12p70	IL-13	IL-18	TNF-α	IL-10
141158	LPS	M	n/a	0.2	0.05	0.115	0.09	0.12	10.15	8.46	0.17	0.22	3.315	7.09	0.145
140726	LPS	F	n/a	0.2	0.88	2.36	0.09	0.12	29.69	160.17	5.93	0.22	64.51	29.41	19.04
134908-1	RML	F	0	0.28	0.15	0.14	0.92	0.15	0.3	0.58	0.3	0.29	4.015	0.44	ND
			1	0.29	0.155	0.145	28.46	0.15	0.305	0.59	0.305	0.285	3.3	0.46	0.145
			20	0.29	0.155	0.145	63.95	0.15	7.74	0.59	0.305	0.285	3.3	0.46	0.145
			40	0.205	0.045	0.115	37.15	0.12	10.97	0.44	0.17	0.23	3.51	0.32	0.29
			60	0.205	0.04	0.115	24.24	0.12	4.18	0.425	0.17	0.22	3.58	0.32	0.165
			80	0.205	0.04	0.115	25.99	0.12	3.37	0.425	0.17	0.22	3.58	0.32	0.165
134098-2	RML	F	0	0.28	0.88	0.14	0.14	0.15	1.52	0.58	0.3	0.29	4.015	0.44	ND
			1	0.29	0.155	0.145	0.13	0.15	0.305	0.59	0.305	0.285	3.3	0.46	0.145
			20	0.205	0.045	0.115	4.25	0.12	20.73	0.44	0.17	0.23	42.15	0.32	25.06
			40	0.205	10.05	0.115	4.46	0.12	22.77	10.77	0.17	0.23	3.51	0.32	28.07
			60	0.205	8.54	0.115	6.92	0.12	16.65	0.425	0.17	0.22	42.96	0.32	0.165
			80	0.205	7.32	0.115	6.35	0.12	10.17	0.425	0.17	0.22	3.58	0.32	3.53
			Term	0.18	10.41	0.11	17.46	0.12	13.23	0.445	0.175	0.215	2.885	0.315	0.155
134098-3	RML	F	0	0.28	0.15	0.14	0.14	0.15	1.44	0.58	0.3	0.29	4.015	0.44	ND
			1	0.29	0.155	0.145	0.13	0.15	0.305	0.59	0.305	0.285	3.3	0.46	0.145
			20	0.205	0.045	0.115	0.09	0.12	0.22	0.44	0.17	0.23	3.51	0.32	0.29
			40	0.205	0.045	0.115	0.09	0.12	2.64	0.44	0.17	0.23	3.51	0.32	0.29
			60	0.205	0.04	0.115	0.085	0.12	7.14	0.425	0.17	0.22	3.58	0.32	0.165
			80	0.205	1.13	0.115	0.085	0.12	7.14	0.425	0.17	0.22	3.58	0.32	0.165
			Term	0.205	0.04	0.115	0.085	0.12	0.21	0.425	0.17	0.22	3.58	0.32	0.165
134098-4	RML	F	0	0.28	0.15	0.14	0.14	0.15	1.4	0.58	0.3	0.29	4.015	2.09	ND
			1	0.29	0.155	0.145	31.07	0.15	12.8	0.59	0.305	0.285	3.3	0.46	0.145
			20	0.205	0.045	0.115	16.96	0.12	5.21	0.44	0.17	0.23	3.51	0.32	0.29
			40	0.205	0.045	0.115	25.2	0.12	6.28	0.44	0.17	0.23	3.51	0.32	0.29
			60	0.205	0.04	0.115	20.77	0.12	6.94	0.425	0.17	0.22	3.58	0.32	0.165
			80	0.205	0.04	0.115	28.79	0.12	0.21	0.425	0.17	0.22	3.58	0.32	0.165
			Term	0.18	0.045	0.11	0.08	0.12	0.21	0.445	0.175	0.215	2.885	0.315	0.155

						Cytokine Data (Serum)									
Animal ID	TX Grp	M/F	DPI	GM-CSF	IFN-ϒ	IL-1β	IL-2	IL-4	IL-5	IL-6	IL-12p70	IL-13	IL-18	TNF-α	IL-10
141158	LPS	M	n/a	0.2	0.05	0.115	0.09	0.12	10.15	8.46	0.17	0.22	3.315	7.09	0.145
140726	LPS	F	n/a	0.2	0.88	2.36	0.09	0.12	29.69	160.17	5.93	0.22	64.51	29.41	19.04
134098-5	RML	F	0	0.28	0.15	0.14	0.14	0.15	0.3	0.58	0.3	0.29	21.84	0.44	ND
			1	0.29	0.155	0.145	16.45	0.15	6.01	0.59	0.305	0.285	95.94	0.46	0.145
			20	0.205	0.045	0.115	24.16	0.12	7.44	0.44	0.17	0.23	116.19	0.32	7.84
			40	0.205	0.045	0.115	13.91	0.12	6.37	0.44	0.17	0.23	75.79	0.32	0.29
			60	0.205	0.04	0.115	9.23	0.12	3.37	0.425	0.17	0.22	48.65	0.32	0.165
			80	0.205	0.04	0.115	23.3	0.12	6.56	0.425	0.17	0.22	3.58	0.32	0.165
			Term	0.18	0.045	0.11	0.08	0.12	7.19	17.82	0.175	0.215	2.885	0.315	0.155
135588-2	RML	F	0	0.28	0.15	0.14	1.24	0.15	1.68	0.58	0.3	0.29	4.015	0.44	ND
			1	0.29	0.155	0.145	12.15	0.15	0.305	0.59	0.305	0.285	3.3	0.46	0.145
			20	0.205	0.045	0.115	20.65	0.12	5.69	0.44	0.17	0.23	3.51	0.32	0.29
			40	0.205	0.045	0.115	18.35	0.12	5.21	0.44	0.17	0.23	3.51	0.32	0.29
			60	0.205	0.04	0.115	17.58	0.12	2.95	0.425	0.17	0.22	3.58	0.32	0.165
135588-4	RML	F	0	0.28	0.15	0.14	0.8	0.15	2.39	0.58	0.3	0.29	18.06	2.09	ND
			20	0.205	0.045	0.115	2.61	0.12	0.22	0.44	0.17	0.23	3.51	0.32	0.29
			40	0.205	0.045	0.115	1.08	0.12	11.07	0.44	0.17	0.23	53.61	0.32	0.29
			60	0.205	0.04	0.115	0.085	0.12	5.38	0.425	0.17	0.22	42.96	0.32	0.165
			80	0.205	0.79	0.115	0.085	0.12	0.21	0.425	0.17	0.22	3.58	0.32	0.165
136550-1	RML	F	0	0.18	0.045	0.11	18.68	0.12	0.21	0.445	0.175	0.215	2.885	0.315	0.155
			1	0.18	0.045	0.11	13.14	0.12	7.32	0.445	0.175	0.215	2.885	0.315	0.155
			20	0.18	0.045	0.11	22.88	0.12	16.54	0.445	0.175	0.215	2.885	0.315	0.155
			40	0.18	0.045	0.11	9.23	0.12	4.97	0.445	0.175	0.215	60.89	0.315	0.155
			60	0.2	0.05	0.115	10.3	0.12	5.77	0.44	0.17	0.22	56.75	0.32	0.145
136550-2	RML	F	0	0.18	0.045	0.11	9.31	0.12	7.19	0.445	0.175	0.215	2.885	0.315	0.155
			1	0.18	0.045	0.11	11.02	0.12	4.17	0.445	0.175	0.215	2.885	0.315	0.155
			20	0.18	0.045	0.11	10.02	0.12	4.97	0.445	0.175	0.215	2.885	0.315	0.155
			40	0.18	0.045	0.11	14.74	0.12	2.49	0.445	0.175	0.215	2.885	0.315	0.155
			60	0.2	0.05	0.115	5.19	0.12	2.67	0.44	0.17	0.22	3.315	0.32	0.145
			80	0.2	0.05	0.115	10.22	0.12	4.5	0.44	0.17	0.22	3.315	0.32	0.145
136550-3	RML	F	0	0.18	0.045	0.11	7.57	0.12	0.21	0.445	0.175	0.215	2.885	0.315	0.155
			1	0.18	0.045	0.11	6.38	0.12	3.06	0.445	0.175	0.215	2.885	0.315	0.155
			20	0.18	0.045	0.11	12.53	0.12	4.71	0.445	0.175	0.215	2.885	0.315	0.155
			40	0.2	0.05	0.115	6.81	0.12	7.25	0.44	0.17	0.22	44.26	0.32	0.145
136550-4	RML	F	0	0.18	0.045	0.11	15.02	0.12	3.62	0.445	0.175	0.215	2.885	0.315	0.155
			1	0.18	0.045	0.11	7.14	0.12	0.21	0.445	0.175	0.215	2.885	0.315	0.155
			20	0.18	0.045	0.11	12.46	0.12	0.21	0.445	0.175	0.215	2.885	0.315	0.155
			40	0.2	0.05	0.115	20.87	0.12	8.71	0.44	0.17	0.22	117.75	0.32	0.145

Table 1 (sB): Cytokine Trends - Brain

						Cytokine Data (Brain)									
Animal ID	TX Grp	M/F	DPI	GM-CSF	IFN-Y	IL-1β	IL-2	IL-4	IL-5	IL-6	IL-12p70	IL-13	IL-18	TNF-α	IL-10
141158	LPS	M	n/a	0.2	0.05	**4.28**	**3.36**	0.12	0.22	0.44	0.17	0.22	421.18	0.32	**47.62**
140726	LPS	F	n/a	0.2	0.05	**4.79**	**2.71**	0.12	0.22	0.44	0.17	0.22	335.1	0.32	**33.17**
133157-5	NBH	M	40	0.2	0.05	0.115	0.09	0.12	0.22	0.44	0.17	0.22	504.64	0.32	**44.87**
133157-4	NBH	M	60	0.2	0.05	0.115	0.09	0.12	0.22	0.44	0.17	0.22	3.315	0.32	0.145
133157-3	NBH	M	80	0.2	0.05	0.115	0.09	0.12	0.22	0.44	0.17	0.22	3.315	0.32	0.145
133157-1	NBH	M	158	0.2	0.05	0.115	0.09	0.12	0.22	0.44	0.17	0.22	3.315	0.32	0.145
133157-2	NBH	M	158	0.2	0.05	0.115	0.09	0.12	0.22	0.44	0.17	0.22	3.315	0.32	0.145
136540-1	NBH	F	40	0.2	0.05	0.115	0.09	0.12	0.22	0.44	0.17	0.22	3.315	0.32	0.145
136540-2	NBH	F	60	0.2	0.05	0.115	0.09	0.12	0.22	0.44	0.17	0.22	3.315	0.32	0.145
133158-5	NBH	F	80	0.2	0.05	0.115	0.09	0.12	0.22	0.44	0.17	0.22	3.315	0.32	0.145
133158-1	NBH	F	158	0.2	0.05	0.115	0.09	0.12	0.22	0.44	0.17	0.22	3.315	0.32	0.145
133158-3	NBH	F	158	0.2	0.05	0.115	0.09	0.12	0.22	0.44	0.17	0.22	3.315	0.32	0.145
136539-2/136539-3	RML	M	40	0.2	0.05	0.115	0.09	0.12	0.22	0.44	0.17	0.22	3.315	0.32	0.145
133707-4/134097-1	RML	M	60	0.2	0.05	0.115	0.09	0.12	0.22	0.44	0.17	0.22	3.315	0.32	0.145
133707-1/133707-2	RML	M	80	0.2	0.05	0.115	0.09	0.12	0.22	0.44	0.17	0.22	3.315	0.32	0.145
134097-2	RML	M	120	0.2	0.05	0.115	0.09	0.12	0.22	0.44	0.17	0.22	3.315	0.32	0.145
136539-1	RML	M	121	0.2	**1.71**	0.115	**6.36**	0.12	0.22	0.44	0.17	**4.81**	**478.03**	0.32	**44.87**
134097-4	RML	M	128	0.2	0.05	0.115	0.09	0.12	0.22	0.44	0.17	0.22	3.315	0.32	0.145
134907-3	RML	M	144	0.2	0.05	0.115	0.09	0.12	0.22	0.44	0.17	0.22	3.315	0.32	0.145
136550-3/136550-4	RML	F	40	0.2	0.05	0.115	0.09	0.12	0.22	0.44	0.17	0.22	3.315	0.32	0.145
135588-2/136550-1	RML	F	60	0.2	0.05	0.115	0.09	0.12	0.22	0.44	0.17	0.22	3.315	0.32	0.145
135588-4/136550-2	RML	F	80	0.2	0.05	0.115	0.09	0.12	0.22	0.44	0.17	0.22	3.315	0.32	0.145
134908-3	RML	F	100	0.2	0.05	0.115	0.09	0.12	0.22	0.44	0.17	0.22	3.315	0.32	0.145
134098-5	RML	F	100	0.2	0.05	0.115	0.09	0.12	0.22	0.44	0.17	0.22	3.315	0.32	0.145
134098-4	RML	F	111	0.2	0.05	0.115	0.09	0.12	0.22	0.44	0.17	0.22	3.315	0.32	0.145

Histopathology:

A. 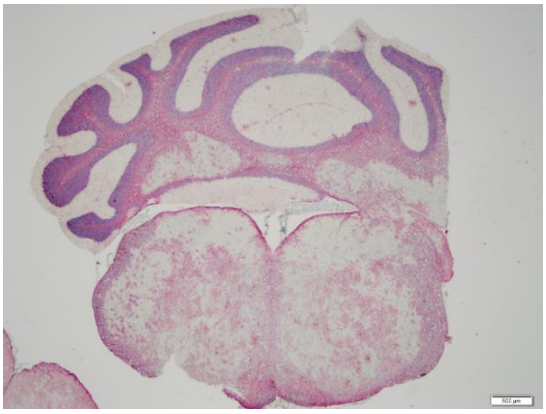 B. 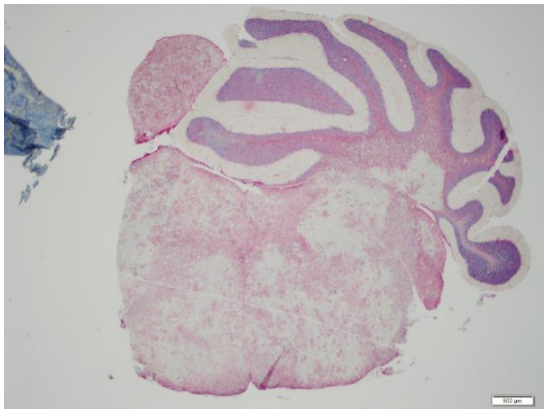

C. 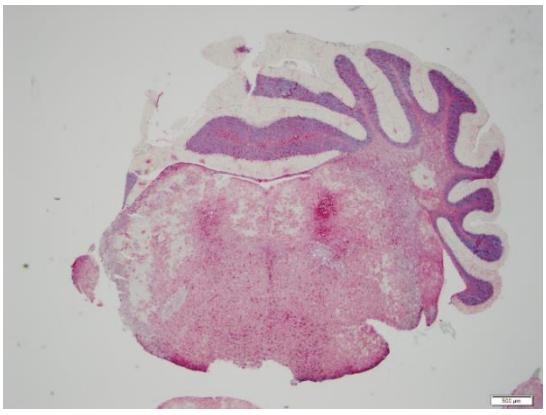 D. 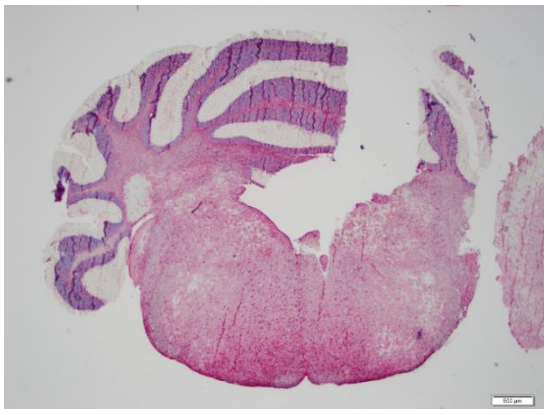

(Figure 16—Supplementary): GFAP—Low Magnification Images

Same images and mice as Figure 16 viewed here at low-power magnification to illustrate GFAP staining in the medulla at the level of the cerebellar peduncles. Intensity of GFAP staining is less in NBH-inoculated mice (A & B) compared with what was observed in RML-inoculated mice (C & D).